Aalto University
School of Chemical
Technology

School of Chemical Technology
Degree Programme of Materials Science and Engineering

Essi Puustinen

ENHANCING THE MECHANICAL PROPERTIES OF SOLID SOLUTION STRENGTHENED FERRITIC SPHEROIDAL GRAPHITE CAST IRON WITH AUSTEMPERING HEAT TREATMENT

Master's thesis for the degree of Master of Science in Technology submitted for inspection, Espoo, 10 January, 2015.

Supervisor **Professor Seppo Louhenkilpi**

Instructor **M.Sc. Tony Pitkänen**
Lic.Tech. Tapio Rantala
Professor Seppo Kivivuori

Aalto University
School of Chemical
Technology

Aalto University, P.O. BOX 11000, 00076 AALTO
www.aalto.fi

Abstract of Master's Thesis

Author Essi Puustinen

Title of thesis Enhancing the mechanical properties of solid solution strengthened ferritic spheroidal graphite cast iron with austempering heat treatment

Department Materials Science and Engineering

Professorship Metallurgy **Code of professorship** MT-37

Thesis supervisor Professor Seppo Louhenkilpi

Thesis advisors M.Sc. Tony Pitkänen, Lic.Tech. Tapio Rantala, Professor Seppo Kivivuori

Date 10.01.2015 **Number of pages** 102 **Language** English

Abstract

This thesis studies the mechanical properties of solid solution strengthened spheroidal graphite cast iron after austempering heat treatment. Austempering heat treatment consists of three stages: austenitising, quenching and austempering. In the end the microstructure should consist of austenite and ferrite needles, generally called ausferrite. This unique material is called austempered ductile iron (ADI). With successful heat treatment the casting gains better mechanical properties.

Aim in the experimental part of this thesis is to find a suitable combination of austenitising and austempering processes to improve the mechanical properties of the used samples with less alloying or even to develop a new austempered material. Inspected samples are solid solution strengthened irons with a silicon content that is 1–1.8% higher than usual. Silicon changes the phase boundaries and therefore samples require tailored heat treatment. Different parameters of heat treatment are tested, with starting values based on existing literature. Methods used to test the resulting material include Vickers and Brinell hardness tests, microstructure analysis and tensile test.

The properties of solid solution strengthened ductile iron grades GJS-500-14 and GJS-600-10 are investigated and grade GJS-500-7 is used as a reference material. First, different austenitising temperatures were tested, and the microstructure and hardness of the samples are analysed to select the austenitising temperature. Second, components were austenitised in the selected temperature and then austempered for different times and at different temperatures in molten salt bath. Finally, the optimised combination of heat treatments is tested with tension test bars.

The austenitising tests showed 950°C to be a good austenitising temperature for the solid solution strengthened materials due to higher silicon content. For reference grade GJS-500-7 normal temperature 860°C was used. In the second stage, austempering temperature 310°C with one hour austempering time was selected for further investigations.

Tensile strength tests show that with this tailored heat treatment GJS-500-14 gained approximately 30% better yield and tensile strength compared to GJS-500-7, but elongation was 13% lower. Heat-treated GJS-600-10 gained 22% better yield strength and 30% better tensile strength with 25% lower elongation. Hardness increased 20% in both materials compared to GJS-500-7. When comparing the studied solid solution strengthened grades to standardised ADI, the elongation was doubled with the same strength values. Combining these grades with the proposed heat treatment creates a material, which has potential for a novel austempered grade with example values GJS-1300-950-7.

Keywords austempered ductile iron, austempering, solid solution strengthening, silicon

Tekijä Essi Puustinen

Työn nimi Liuoslujitetun pallografiittivaluraudan mekaanisten ominaisuuksien parantaminen austemperoimalla

Laitos Materiaalitekniikka

Professuuri Metallurgia **Professuurikoodi** MT-37

Työn valvoja Professori Seppo Louhenkilpi

Työn ohjaajat DI Tony Pitkänen, TkL Tapio Rantala, Professori Seppo Kivivuori

Päivämäärä 10.01.2015 **Sivumäärä** 102 **Kieli** Englanti

Tiivistelmä

Tämän diplomityön tarkoituksena oli liuoslujitetun pallografiittivaluraudan mekaanisten ominaisuuksien tutkiminen austemperoinnin jälkeen. Tähän lämpökäsittelyyn kuuluu kolme vaihetta: austenitointi, sammutus ja austemperointi. Käsittelyssä mikrorakenne muuttuu austeniitiksi ja ferriittineulasiksi, mitä kutsutaan ausferriitiksi ja itse materiaalia ADI:ksi (Austempered Ductile Iron). Onnistuneen lämpökäsittelyn tuloksena valutuotteen mekaaniset ominaisuudet paranevat.

Kokeellisen osuuden tavoitteena on löytää sopivin austenoinnin ja austemperoinnin yhdistelmä ja saavuttaa samat mekaaniset ominaisuudet niukemmalla seostuksella, tai jopa löytää uusi austemperoitu materiaali. Tässä työssä tutkitaan liuoslujitettua pallografiittirautaa, jonka piipitoisuus on 1–1,8 % normaalia suurempi. Pii muuttaa faasirajoja ja edellyttää lämpökäsittelyn räätälöimistä. Testattavat lämpötilat ja ajat lämpökäsittelyihin valitaan kirjallisuuden perusteella. Materiaalia tutkitaan Vickers ja Brinell kovuuskokeilla sekä mikrorakennekuvien ja vetokokeen avulla.

Liuoslujitetuttujen rautalaatujen GJS-500-14 ja GJS-600-10 ominaisuuksia halutaan tutkia, ja GJS-500-7 toimii vertailukohteena. Ensin testataan eri austenitoinnin lämpötiloja ja sen jälkeen austemperoinnin eri aikoja ja lämpötiloja suolakylvyssä. Lopuksi, näiden lämpökäsittelyiden parasta yhdistelmää testataan vetosauvoilla.

Austenitointitestit osoittivat, että liuoslujitetuille korkeamman piipitoisuuden materiaaleille sopiva lämpötila on 950°C, mutta GJS-500-7 kannattaa austenitoida normaalissa 860°C:n lämpötilassa. Toisessa vaiheessa valittiin seuraavia austemperointeja varten lämpötilaksi 310°C ja ajaksi yksi tunti.

Vetotulokset osoittavat että räätälöidyn lämpökäsittelyn avulla materiaalin GJS-500-14 myötö- ja murtolujuus paranevat noin 30% verrattuna materiaaliin GJS-500-7, mutta venymä pienenee 13%. Lämpökäsitelty GJS-600-10 puolestaan saavuttaa 22% paremman myötölujuuden ja 30% paremman murtolujuuden sekä 25% pienemmän venymän kuin GJS-500-7. Molempien liuoslujitettujen materiaalien kovuus oli 20% suurempi referenssimateriaaliin nähden. Verrattaessa lämpökäsiteltyjä liuoslujitettuja materiaaleja standardoituihin ADI-laatuihin venymä on jopa kaksi kertaa parempi samoilla lujuuden arvoilla. Lämpökäsittelemällä liuoslujitettua valurautaa saadaan materiaali, joka on potentiaalinen uusi ADI-laatu esimerkiksi ominaisuusarvoilla GJS-1300-950-7.

Avainsanat austemperoitu pallografiittivalurauta, austemperointi, liuoslujittuminen, pii

PREFACE

To begin with, I would like to thank Componenta for giving me the opportunity to write my thesis of this topic, which was also part of FIMECC's Breakthrough steels and applications project and sub project Novel Cast Materials. This project has given me insight into the metallurgy behind complex casting process.

Special thanks belong to my instructor Tony Pitkänen, who has guided me through the challenging topics and gave me valuable comments whenever I needed. I would also like to express my gratitude to supervisor Seppo Louhenkilpi for giving me encouragement and instructors Tapio Rantala and Seppo Kivivuori for all their support during the process. For valuable proofreading, I am grateful to my friend Juulia Suvilehto. In addition, I will never forget the help of Karkkila foundry's workers with the experimental part and Käpylä office's warm and fun atmosphere, especially among my trainee group.

Throughout my studies, I have been lucky to meet such a variety of people and get to know awesome individuals, whom I can these days call my best friends. I am happy for the adventures which studies and student activities have brought to my life since the first day as a freshman in Otaniemi. With the words of my favourite teekkari-song, I wish "*livet är härligt*" also after graduation and I can continue growing as a person with all of you.

Last but not least, I want to thank my family and relatives for all their support during my life. Also mummi who does not understand what I just wrote!

Remember to enjoy your life and smile as long as you live!

Espoo, January 2015

Essi Puustinen

TABLE OF CONTENTS

Preface IV
Table of contents V
Abbreviations and notations VII

1 INTRODUCTION 1

2 INTRODUCTION TO DUCTILE CAST IRONS 4
2.1 As-cast ductile irons 4
2.1.1 World's cast iron production 4
2.1.2 Foundry process 6
2.1.3 Nodularising treatment 9
2.1.4 Forms of graphite and nodularity 12
2.1.5 Metallography and microstructures of ductile iron 13
2.1.6 Production control and alloying of ductile cast iron 16
2.1.7 Properties of ductile cast iron 20
2.1.8 Solid solution strengthened ferritic grade and its properties 21
2.2 Austempered ductile iron 25
2.2.1 Introduction to ADI 25
2.2.2 Microstructure of ADI 27
2.2.3 Chemical composition and their effect on ADI 29
2.2.4 Properties of ADI 32
2.2.5 Effect of silicon 38

3 HEAT TREATMENT PROCESS OF ADI 41
3.1 Introduction to ADI heat treatment 41
3.2 Austenitising 45
3.2.1 Austenitising Time 45
3.2.2 Austenitising Temperature 46
3.3 Quenching 47
3.4 Austempering 48
3.4.1 Austempering temperature 49
3.4.2 Austempering time 50

4 RESEARCH METHODS 55
4.1 Introduction 55
4.2 Test plan 55
4.2.1 Austenitising tests 55
4.2.2 Austempering tests 56
4.2.3 Testing the full austempering process with tensile bars 56
4.3 Manufacturing of the test materials 57
4.3.1 Sample preparation 57
4.3.2 Chemical compositions of the test materials 58
4.4 Test procedures and equipment used 60
4.4.1 Furnace and salt bath 60
4.4.2 Microstructure analysis with optical microscope 60
4.4.3 Hardness tests 63
4.4.4 Tensile test 65

5 RESULTS AND DISCUSSION 67
5.1 Results of austenitisation tests 67
5.1.1 Microstructures 67
5.1.2 Hardness tests 70
5.2 Results of austempering tests 73
5.2.1 Microstructures 73
5.2.2 Hardness tests 78
5.3 Results of full austempering process 82
5.3.1 Microstructures 82
5.3.2 Hardness tests 84
5.3.3 Tensile strength test 86
5.3.4 Discussion and comparison of the results 88
5.4 Reliability of the results 92
5.4.1 Before and during the heat treatment 92
5.4.2 Microstructures 93
5.4.2 Hardness tests 93
5.4.3 Tensile test 94

6 CONCLUSION 95
References 97
Appendices 100

ABBREVIATIONS AND NOTATIONS

A	elongation (%)
A_1	temperature at which austenite begins to form on heating
ADI	austempered ductile iron
CE	carbon equivalent
GJL	grey cast iron
GJS	ductile cast iron
HB	Brinell hardness
HV	Vickers hardness
M_s	martensite start temperature
$R_{po,2}$	yield strength (MPa)
R_m	tensile strength (MPa)
SSF	solid solution strengthened ferritic ductile iron
UCT	upper critical temperature
α	ferrite
γ	austenite

1 INTRODUCTION

Ductile iron is a great way to produce various kinds of casting products. More improved version was developed in the middle of 20th century when ductile iron was heat treated in a special way after casting and therefore the strength and ductility of the end product increased. Nowadays, solid solution strengthened grades are also involved and even better materials are developed through combining quality ductile iron, heat treatment and strengthening the alloy with solid solution.

Ductile iron is an alloy, which consists mainly of iron, silicon and carbon. In this matrix, carbon exists as graphite nodules due to nodularisation treatment, which makes the iron more ductile. The special heat treated version of this is called Austempered Ductile Iron (ADI), austempering being the heat treatment employed to improve properties. Austempering process consists of three stages as shown in Figure 1. First the heated component is held at target temperature, i.e. austenitised, to transform the matrix into austenite. Second stage is called quenching, where the casting is rapidly cooled to a lower temperature. Thirdly, in this austempering temperature matrix transforms into ausferrite, combination of austenite and needle-shaped ferrite. Austempering is an isothermal heat treatment, where temperature is kept constant for the chosen duration. Convenient time depends on the amount of alloying and the desired properties in the end. Lastly, the component is moved to room temperature to cool down slowly. With successful heat treatment the casting gains better mechanical properties.

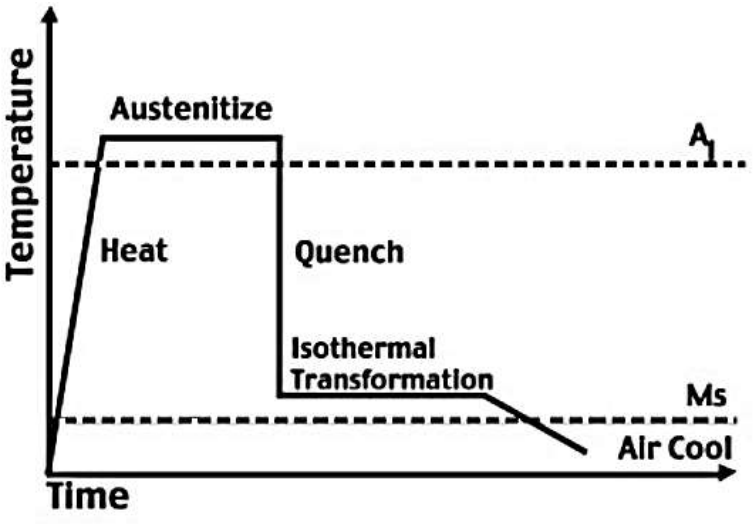

Figure 1 Austempering process. [1]

In this thesis, instead of heat treating conventional ductile iron, new solid solution strengthened grades are used as samples and finally a new ADI material will be developed. Solid solution strengthening means that atoms of an alloying element are added to the structure, these atoms diffuse into the matrix and together they form a solid solution with more strength. Three new solid solution strengthened ferritic spheroidal graphite cast iron (SSF) grades were standardised in 2012 at standard EN1563 and two of these are selected to this research [2, 3]. The added strengthening component is silicon, which alters the phase boundaries and requires tailored heat treatment.

Heat treatment process can be used to tailor properties and microstructure of the material. It is essential to carefully control the thermodynamics and kinetics to reach the desired microstructure. [4] The aim in the present study is to figure out how the properties of solid solution strengthened ductile iron change through tailored ADI heat treatment. The test materials are standard grades from the foundry process with less alloying. The intention is to get properties that are superior, or at least equal to those in conventional ADI material. An additional target is to develop new material, which exceeds the current demands for ductile iron and which could be used to produce new kinds of products.

This thesis includes a practical part in which various austempering heat treatments are conducted to the samples. Two different types of iron with unusually large silicon content (GJS-500-14 and GJS-600-10) are subjected to heat treatments and compared with reference material (GJS-500-7) to find out whether silicon has enhancing effect on the properties. First, the different austenitising temperatures are tested and based on the results, the optimal temperature is selected for the austempering tests. In the second stage, components are austempered for different times and at different temperatures in molten salt bath. Finally, the optimal combination of heat treatments is tested with tension test bars. Tensile strength test are conducted in addition to hardness tests and optical microstructure analysis. Optimising these parameters is considered the main research question in this study.

This thesis starts with a literature review on ductile iron and ADI in Chapter 2. The structure of the austempering part follows the logical order of the heat treatment: Chapter 3 first explains the austenitising stage, then quenching and lastly austempering. This is followed by research methods in Chapter 4 and the results are presented with discussion in Chapter 5.

2 INTRODUCTION TO DUCTILE CAST IRONS

Cast iron can be defined as an alloy of iron and carbon containing more than 1.7% of carbon. Generally the amount of carbon ranges between 2.4% and 4%. Other common alloys are silicon, manganese, sulphur and phosphorus. Iron carbon alloys with less carbon are called steels. In cast irons carbon exists as graphite crystals, which also divide cast iron to five main groups: flake graphite cast iron, ductile cast iron, vermicular graphite cast iron, white cast iron (all graphite in sementite) and malleable cast iron. [5]

This thesis focuses on austempered ductile iron (ADI), which is a heat-treated version of ductile cast iron. Here we are interested in ADI with a higher silicon content than is normal, therefore also solid solution strengthening is introduced. This chapter covers the main properties of ductile cast iron and with more details on the special characteristics of austempered ductile iron.

2.1 As-cast ductile irons

This chapter starts with an overview of cast iron production. It is followed by an explanation of foundry and nodularising processes to give insight into the whole production process. Then are described the graphite nodules, the beauty of metallurgy and the effects of important chemical components more in detail. These all affect the properties of ductile iron which are introduced in the end, before the insight into solid solution strengthened ductile iron.

2.1.1 World's cast iron production

Casting is one of the most energy efficient and dimensionally flexible ways of producing metal components that is also reasonably fast. The mass of the product can weigh anything between a few grams to a few hundred tons and material loss is minimized because components will be casted to near net shape and wall thickness. Also the material selection is wide. [6] Two main groups are flake graphite iron, also called grey iron, and nodular graphite cast iron, which is also known as ductile or spheroidal graphite cast iron. The standardised properties and guidance values for ductile iron can be found from standard EN-

1563: Founding – Spheroidal graphite cast iron, which also served as guideline in this thesis. [2]

World's cast production grew 2.3% during year 2012 and reached a total of 100.8 million tons, which was divided among different materials as seen in Figure 2. This was the highest production rate ever in history, even though in Finland production continued to decline. Total cast production in Finland in 2012 was 85 507 tons and in 2013 only 77 054 tons, of which iron castings covers 68 484 tons. The distribution is illustrated in detail in Figure 3. This is the lowest number in 40 years. There are around 51 000 foundries in the world and out of which 39 are located in Finland. [7]

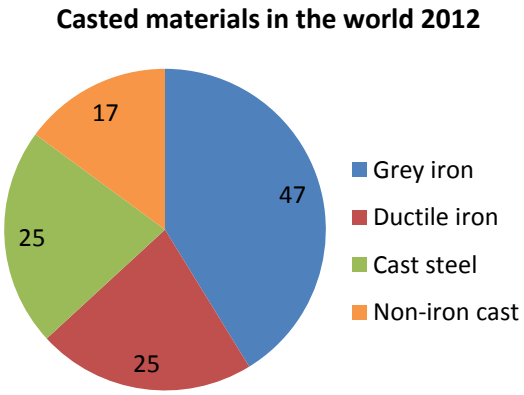

Figure 2 Casted materials in the world divided into four groups. Numbers represent both million tons and percentage of year 2012 production, since total production was 100 million tons. [8]

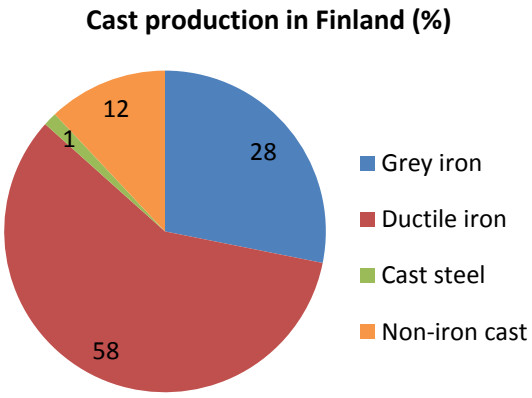

Figure 3 Cast production in Finland in year 2013 divided by materials. Numbers represent the percentage of 77 054 tons production. [7]

According to the definition stated in the beginning of this chapter, cast iron refers to family of materials whose major constituent is iron with important amount of carbon and silicon. Their properties are determined by their microstructure and phases formed during solidification and heat treatment. For example, the shape and distribution of graphite greatly influences the mechanical and physical properties of the cast iron. [1] Next the production processes are explained in more detail.

2.1.2 Foundry process

Casting means that liquid metal is poured into a mould, which contains the frame of the desired shape as a hollow cavity. After the alloy has cooled and solidified, it is broken out of the mould. Basic production process for a casted component has five separate larger stages: moulding, melting, casting, demoulding and after-treatment. Heat treatments are a part of the fourth stage. In the next sections the stages are discussed in detail.

MOULDING

Pattern is used to replicate the shape of the desired final product and can be made of wood, plastic or metal. Pattern is enveloped by frames in which the moulding sand is then fed and hardened with the help of specific compounds depending on the type of sand and pressure. The pattern is removed and the hollow cavity of the final product remains in the mould. In addition, cores can be added when assembling the different parts of the mould to create hollow areas in the mould. Refractory dressing is added to the surface of the cores and mould to both protect the parts but also to decrease the amount of casting defects. Feeders are essential for supplying additional metal to the mould as the metal changes its volume when cooling down, and filters are used to avoid impurities flowing to the mould. Overall picture of a mould is presented in Figure 4.

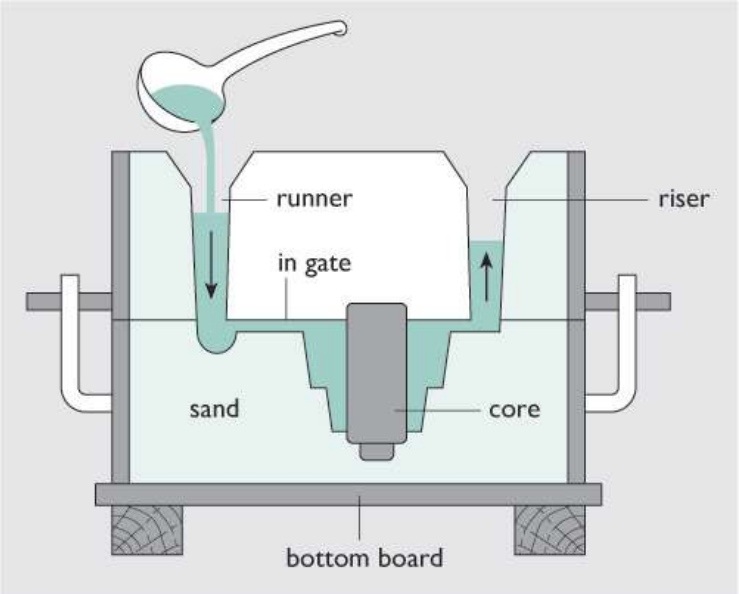

Figure 4 Cross-sectional view of the casting process. [9]

MELTING

Metal has to be melted in order to achieve liquid phase. Pure iron melts in 1535°C, but because of the other alloys affecting the melting point, the temperatures vary at the foundry. Purchased steel, pig iron, foundry returns and alloying elements are heated in a furnace up to 1530°C. Before moving to the next stage in the process, carbon equivalent ($CE=C\%+{}^{1}/_{3}(Si\% + P\%)$) must be calculated to find out whether the contents of carbon, silicon and phosphorus are in balance. If CE is higher than 4.3, primary graphite nodules can occur, especially with thick wall sections. This value is a useful guide to foundry behaviour and also a diagram, like in Figure 5, can provide guidance on an optimum range of composition. [10]

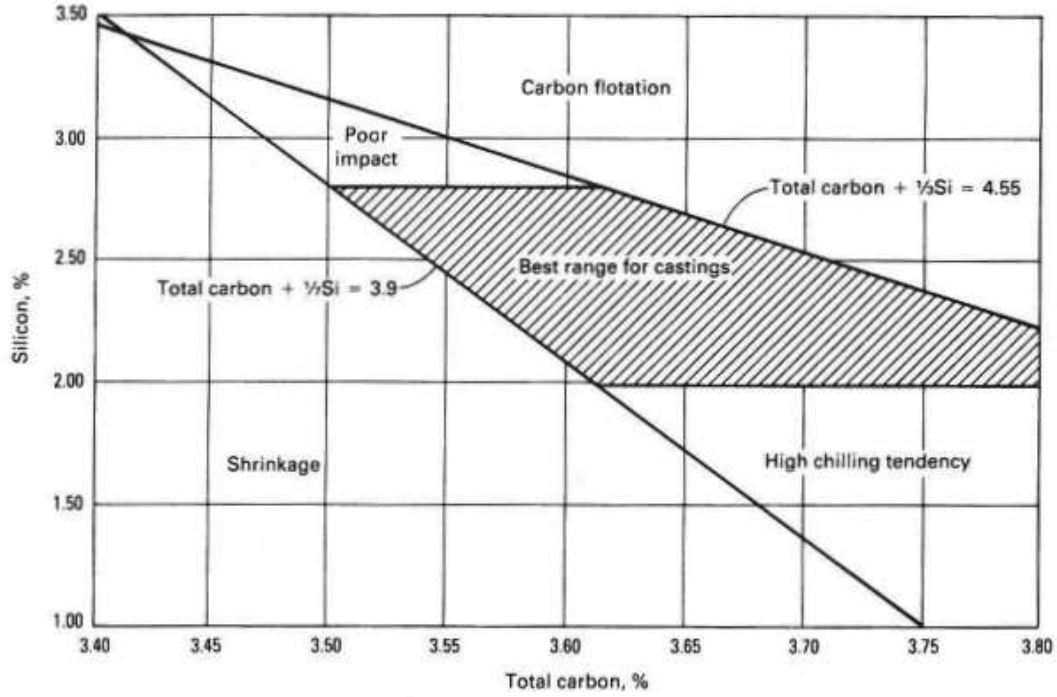

Figure 5 Typical carbon and silicon ranges for ductile iron castings. [10]

AFTER MELTING AND CASTING

Nodularising treatments of graphite, called spheroidising, happens at this stage. A detailed description is presented in section 2.1.3. After nodularising, melt is poured into a transport vessel and slag is skimmed. Slag is non-metallic liquid floating on the batch and it contains all kinds of impurities which must be removed before casting. Finally, the melt is poured into moulds at casting temperature 1300–1400°C and solidification begins with cooling. [5, 11]

DEMOULDING

After component has cooled, the next step is to remove the sand mould around the component by shake-out. Then attached runners, gates and feeders must be removed with cutting tools. When the actual demoulding has been done, the component must be shot-blasted to remove the attached sand from the surface. This means mechanically cleaning the surface with hard steel granules, which are propelled against the casting. After shot-blasting heat treatments, one described in Chapter 3, can be done.

AFTER-TREATMENT

For a casted component last stage at the foundry includes inspections, additional cleaning and sanding, and sometimes painting and machining. In the end, components are packed and shipped to the customer.

2.1.3 Nodularising treatment

In order to get spheroidal shaped graphite, specific agents must be added to the molten alloy before casting. Nodularising treatment, also called as spheroidising, consist of three stages: desulphurisation, magnesium treatment and inoculation. [12]

Desulphurisation starts the process. Sulphur is the key element which can deteriorate the nodularising effect of magnesium, because of its tendency to form manganese sulphide. Sulphur content must be less than 0.02% and therefore additional sulphur is removed, for example with calcium carbide CaC_2. [12] Depending on the quality of the molten iron, desulphurisation might not be needed.

In the second stage, magnesium is added to form the spheroids. Usual magnesium content in the end of the casting is 0.025–0.04% depending on wall thickness. [11] Magnesium cannot be inserted directly into the melt, because it has low density and low boiling point, and therefore it usually is added as an alloy of magnesium ferrosilicon (MgFeSi) or with other metals. By alloying magnesium with silicon, the forming of carbides is more moderate [13]. Usually the MgFeSi amount added is 1.0–1.5% of the volume of the melt. Magnesium treatment can be successful only if the chamber size, pouring rate and amounts of added alloys are in balance with each other. [12]

Finally, inoculation is carried out, which means that particles are added to molten metal. These added particles modify the structure and thereby change the mechanical and physical properties [5]. In this case, ferrosilicon inoculant containing calcium and barium is added to increase the nucleation points,

which also helps in obtaining the required matrix with the desired properties. [12, 13]

During these three steps, spheroidising occurs. Figure 6 illustrates the microstructural evolution during casting for ductile cast iron with CE>4,3%. Four stages during solidification (dashed line) starts with temperature dropping below liquidus temperature (A) allowing graphite nodules to nucleate (1) and grow (2). Second change happens when solidus temperature T_G is passed and graphite is enclosed in an austenite shell (3) with austenite dendrites nucleating simultaneously. In fourth stage (4) carbon is in the liquid next to dendrites hereby providing conditions for new nucleations of graphite inside the austenite. [14]

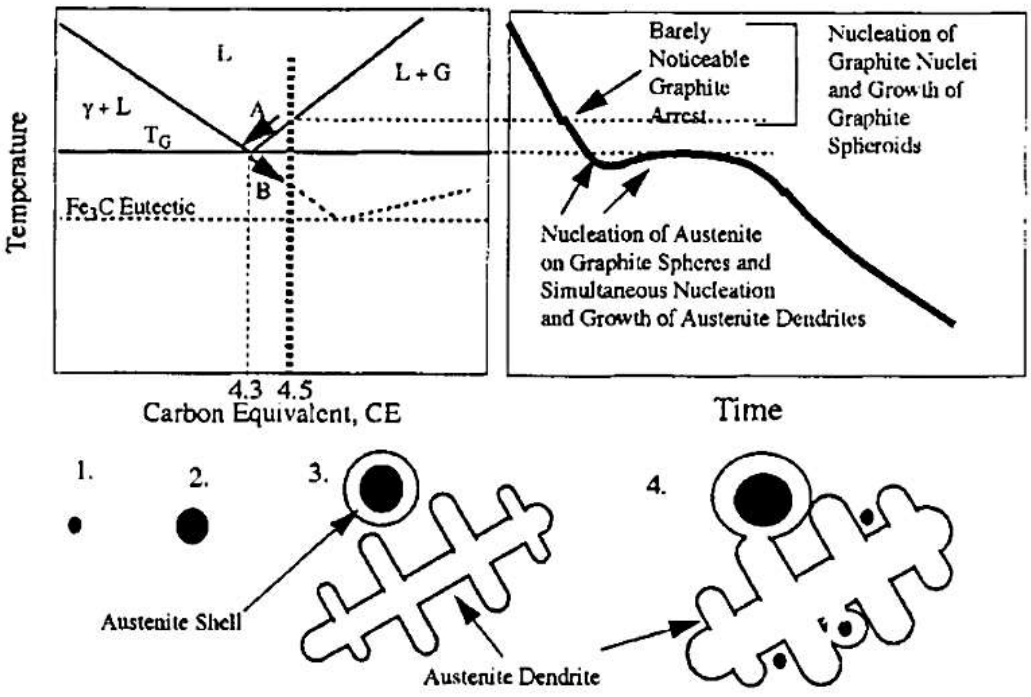

Figure 6 Phase diagram, cooling curve and solidification steps 1. Graphite nodules nucleate 2. Graphite nodules start growing 3. Graphite is enclosed in an austenite shell 4. New graphite nodules nucleate. [14]

The final chemical composition, inoculation method and the remaining magnesium concentration all affect the outcome of the nodularising treatment. Nevertheless, the solidification rate of the melt and wall thickness also have

significant influence. [2] If the cooling rate of the melt is too fast, there is no time for graphite nodules to grow. Also if there are not enough nucleation points, carbides can form in thin walls which decreases ductility. In addition, the presence of rare earth metals can cause the graphite nodules to explode (Figure 7) or form chunky graphite (Figure 8), if their content is too high. [13] All in all, careful spheroidising is the key to reach the properties which spheroidal graphite cast iron has.

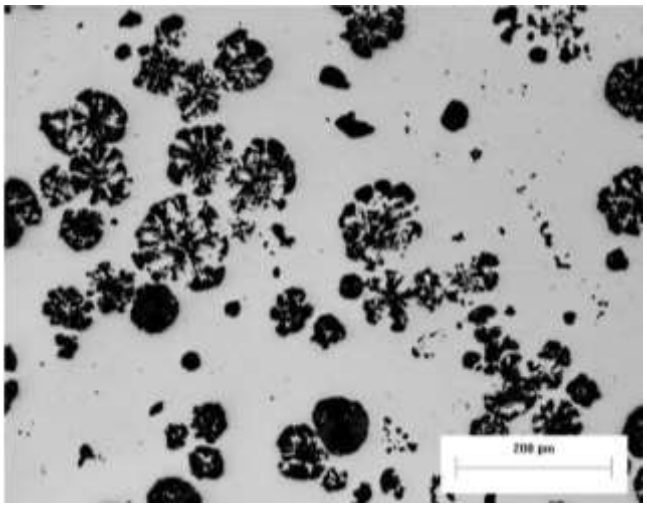

Figure 7 Sample with exploded graphite present due to excess concentration of rare earth metals. [15]

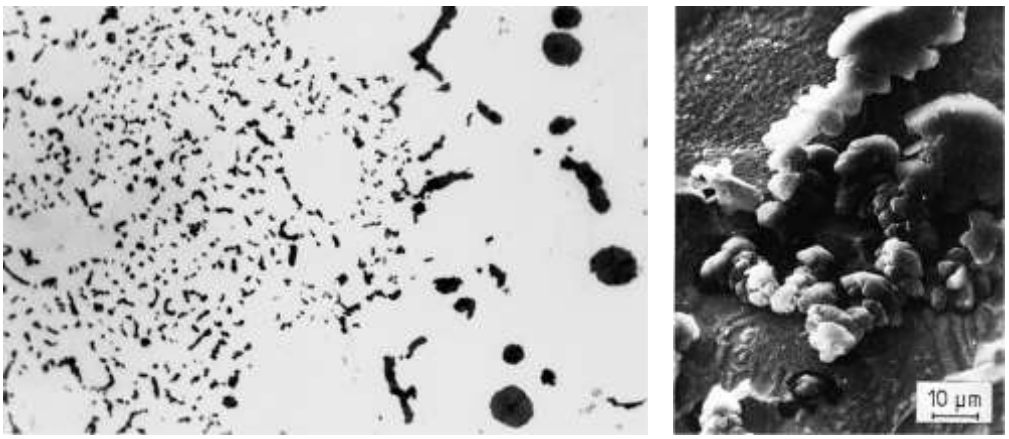

Figure 8 Samples with chunky graphite. On the left, magnification to 100:1 and on the right, scale shown in picture. [12]

2.1.4 Forms of graphite and nodularity

In cast irons carbon (C) exists as graphite crystals. The forms of graphite have great impact on the mechanical properties. [16] In the standard ISO 945-1:2008/Cor 1:2010, the forms of graphite in cast irons are classified to six different forms: I) Lamellar (flake) graphite, II) Crab graphite, III) Compacted (vermicular) graphite, IV) Temper carbon, V) Slightly irregular spheroidal graphite and VI) Spheroidal graphite. These are also presented in Figure 9. [17]

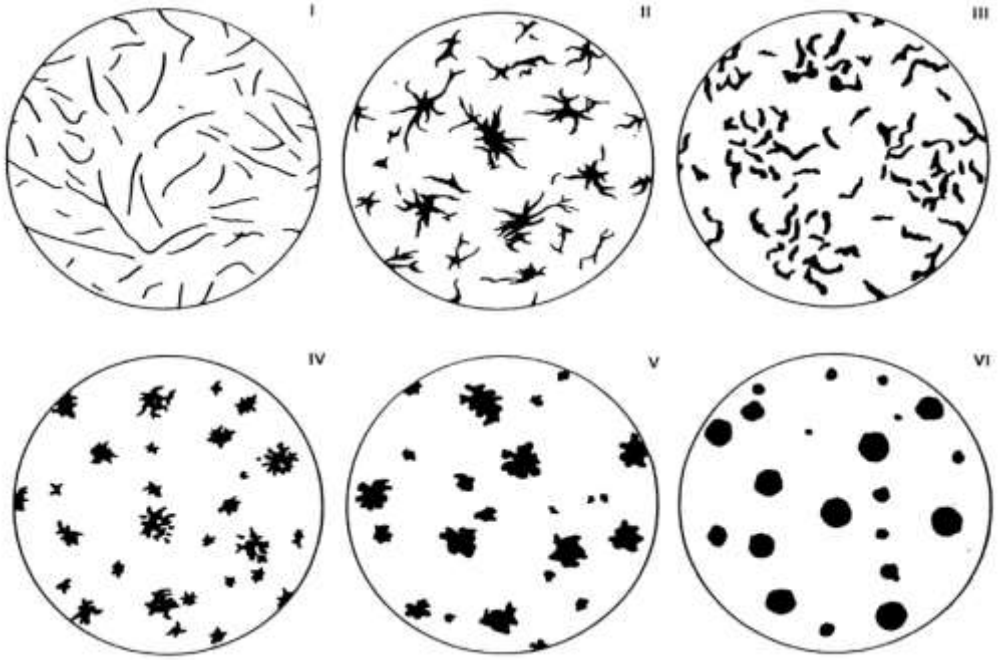

Figure 9 Graphite types in cast iron. [17]

Form I, flake graphite, has interconnected particles within eutectic cells. This lamellar graphite has sharp ends and the matrix is austenitic. It represents the principal form in grey cast iron. Picture of the form is presented in Figure 10a.
Form II is an aggregate of graphite flakes and form III has even more compacted graphite. These resemble worms with rounded ends and can occur in spheroidal cast iron. Form IV is the principal form in malleable cast irons and it is easy to recognise from irregular isolated spheroidal graphite. Last two forms (V and VI) are counted as acceptable forms in spheroidal graphite cast irons. Form V has slightly irregular spheroids but form VI has the desired appearance with clearly isolated particles. This form is presented also in Figure 10b. [17]

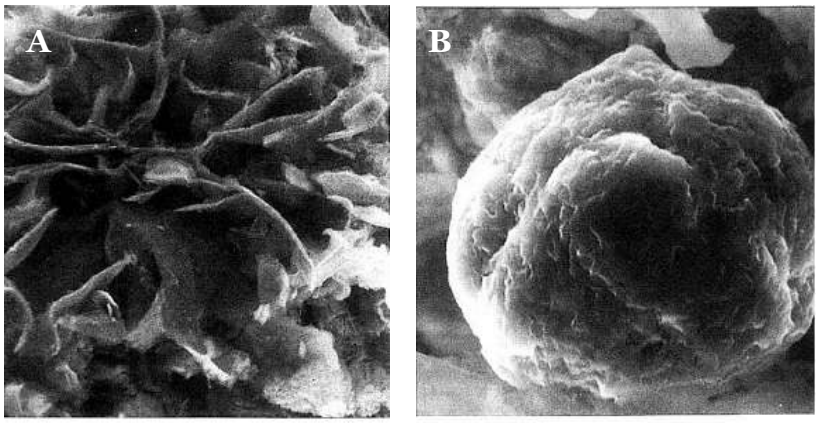

**Figure 10 Pictures of the graphite forms, 500:1.
a) flake graphite b) nodular graphite. [12]**

Shape of the nodules is only one aspect affecting the quality of the material. The number and uniform distribution of the nodules are also relevant. Nodularity can be defined as percentage of graphite particles that are spheroidal or nodular in shape (form V and VI of EN ISO 945-1) [2]. Nodularity of 80% usually ensures the minimum tensile properties if also the nodule count, i.e. the amount of nodules in the area, is high enough (100/mm^2). [2, 12, 15, 18]

2.1.5 Metallography and microstructures of ductile iron

The cast irons consist of base metal iron (Fe) with more than 2% of carbon (C), which exists mainly in the form of graphite. The combination of these two elements can form different microstuctural arrangements, called matrices. These phases are illustrated in Fe-C phase diagram (Figure 11), which tells when each phase can occur at equilibrium.

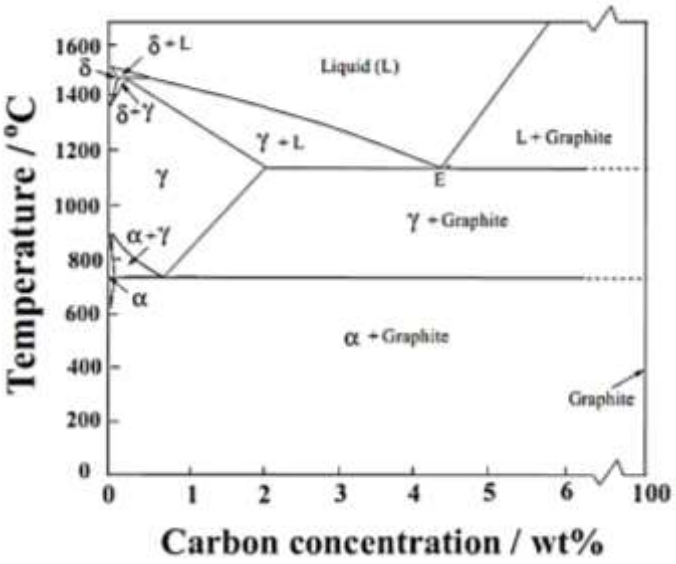

Figure 11 Iron carbon diagram. [1]

Ductile iron castings have mostly a ferritic, ferritic-pearlitic, or pearlitic matrix. [18] **Ferritic** matrix (α) is tight body-centred cubic crystal structure, which solutes only 0.02% of carbon [19]. Therefore it is called the purest iron phase in a cast iron [15]. Ferritic iron acts as the solvent and the structure is shown in Figure 12a [12, 19]. Ferrite gives ductile iron high ductility and toughness, but produces lower strength and hardness [15]. This matrix is result from slow furnace cooling with low alloying elements [19].

Then, **pearlite** ($\alpha+Fe_3C$) is the combination of ferrite and cementite Fe_3C (Figure 12b). There are separate cementite lamels in the ferrite matrix, where the size and distance of lamellar pearlite determines the properties. [5, 15] Pearlite provides higher strength, moderate ductility and good wear resistance [15]. This microstructure can be gained by alloying with pearlite promotive copper (Cu), tin (Sn) or manganese (Mn). Then there is the combination **ferritic-pearlitic** structure (Figure 12c), which is the most common grade of ductile iron and its as-cast form. Its properties are a combination of ferritic and pearlitic grades which results in good machinability and low production costs. [15]

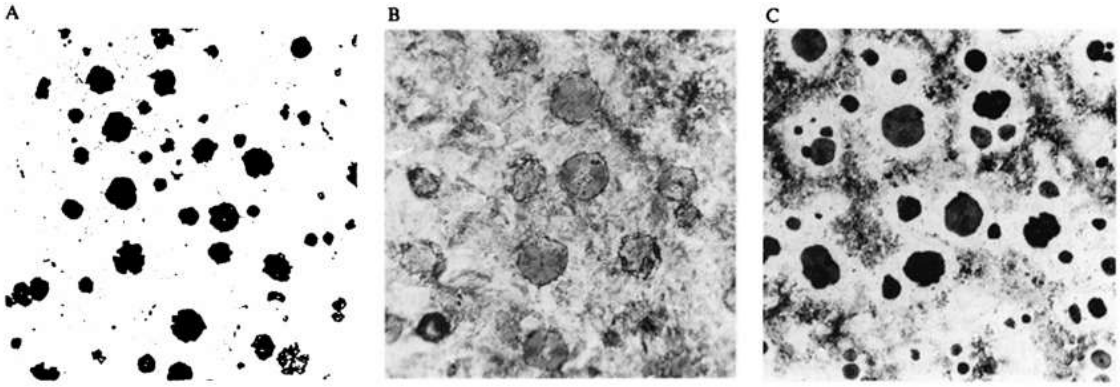

Figure 12 Microstructures of ductile iron, nital 100x. A) Ferritic B) Pearlitic and C) Ferritic-pearlitic structure. [11]

In addition to these as-cast phases, there are also others, non-equilibrium phases, which occur as a result of alloying or heat treatment. The high temperature phase is called austenite and hard phase is martensite (Figure 13). **Austenite** (γ) normally exists at high temperatures (over 720°C), but also at room temperature with suitable treatment or alloying [5, 13, 15]. Carbon is dissolved in austenite (maximum of 2%) and structure is face centred cubic crystal. [5, 15] In austempered irons, austenite provides good toughness and ductility [15]. Instead, **martensite** forms upon rapid cooling (quenching) from austenite, without diffusion and carbon has no time to form pearlite. This oversaturated carbon is distorted tetragonally in ferrite, as interstitial atom, and gives hard and brittle properties for the material. [5, 12, 15] With heat treatment the properties can be controlled to good combination of high strength and wear resistance [15]

Figure 13 Micrograph of martensitic quenched ductile iron. ~880x [19]

Moreover, there is **bainite**, which consists of ferrite and carbide (Figure 14). Structure is the same as pearlite, but it is not lamellar. It is not a desired structure due to its poor properties caused by extremely hard and brittle carbide. These compounds of carbon (Fe_3C) increase wear resistance but decrease machinability. [15]

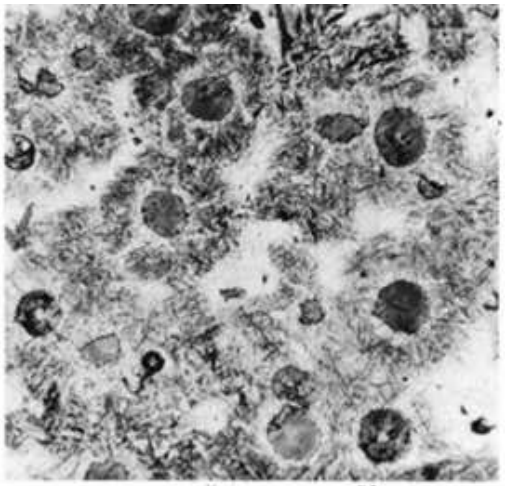

Figure 14 Bainitic microstructure of ductile iron, nital 100x. [11]

2.1.6 Production control and alloying of ductile cast iron

The production control must be precise in order to reach the specific and sensitive properties of ductile cast iron. Casted material should possess more than 80% nodularity and have minimum of 100/mm² nodule count as already mentioned in section 2.1.4. The material should also have consistent chemical composition without carbides, inclusions or porosity. [15]

In order to reach these goals, cooperation must be continuous between all the workers handling the product. But even they cannot correct the situation if the alloying has gone badly wrong. Main element of ductile iron is naturally iron (Fe) reaching more than 90% of the composition. The other elements must be selected carefully, because each will impact the final properties. All elements which negatively effect these must be limited, and only then the upgrading components can be selected. Table 1 summarises the effects of carbon, silicon and other important elements for ductile iron. [15]

Table 1 Primary elements of ductile iron with their effects on the properties.

Carbon, C	Graphite is a soft form of carbon, but in spheroidal form it increases mechanical properties in ductile iron when acting like "crackarrester" in the matrix [1, 15]. When there is 3 to 4% of carbon, the tensile strength increases but hardness and elongation values do not deteriorate remarkably. [1] Usually the amount of carbon is within the range 3.4% to 3.8% [6]. The thinner the wall of casted component is, the higher the carbon content should be [6].
Silicon, Si	Silicon is a graphitiser, which promotes graphite and ferrite formation. [11] Usually the content of silicon must be higher when walls of the casting are thinner [6]. By conventional standards, the silicon should be within the range 1.8–2.8% [6]. The effects of Si are described in more detail in section 2.2.5.
Magnesium, Mg	Magnesium is used to produce spheroidal graphite [6, 20]. Magnesium content in final casting is usually 0.025 to 0.04%. If magnesium content is too low or iron has high content of elements which obstruct graphite formation, graphite can be vermicular or even lamellar. [11] Too large amount of magnesium can create hard carbides [13]. More detailed information about magnesium can be found in section 2.1.3, nodularising treatment.
Sulphur, S	Amount of sulphur must be as low as possible, because it makes spheroidising/ nodularising treatment harder. Magnesium first attempts to remove sulphur and only after starts nodularising the graphite. Content should not exceed 0.02%. [6, 11, 20]

Nickel, copper and molybdenum are the main alloying elements of ductile iron. [11] Alloying elements can be divided into two main groups based on their segregation tendency during solidification: a) graphitisers and b) carbide formers. [21] Main role for graphitisers is to adjust the processing window when spheroids are formed. [1] Graphitisers generally reduce the carbon solubility in austenite, since they segregate near nodules while forming a carbon diffusion barrier. This slows down the diffusion between graphite nodules and the matrix. [21] In cast iron silicon, copper and nickel are graphitising elements, but silicon acts somwhat differently because it does not segregate near nodules. [21, 22]

Unlike graphitisers, carbide formers segregate as far from the nodules as they can, i.e. at the cell boundary. [21, 22] This increases the carbon content locally and with high amounts of carbide formers undesired sementite Fe_3C appears. [11, 21] Common carbide formers are molybdenum and manganese, which tend to increase hardness [22]. A schematic picture of segregation is presented in Figure 15 and more detailed properties of the common alloying elements can be found in the Table 2 on page 19.

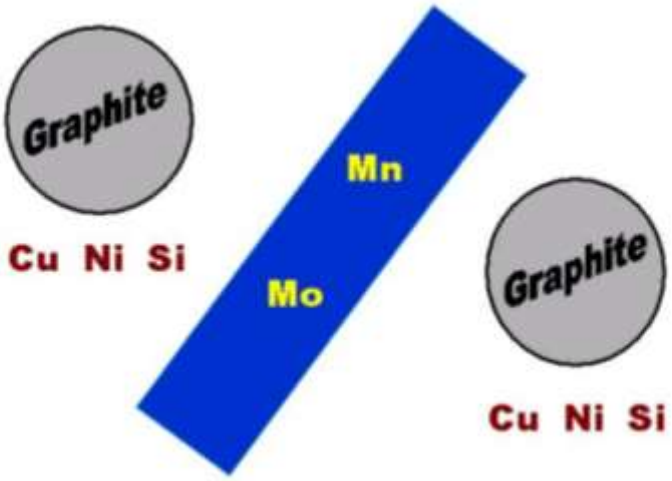

Figure 15 A schematic showing the segregation of alloying elements in ductile iron during solidification. [23]

In addition to main elements and alloys, there are some gases and ingredients which are not purposely added to iron but still exist there because removing them is challenging. These include lead (Pb), bismuth (Bi), antimony (Sb), aluminum (Al), titanium (Ti), selenium (Se) and tellurium (Te). These residual elements can be harmful in the nodularising process, but luckily adding 0.01 to 0.02% of cerium (Ce) usually eliminates the effect. [11] In conclusion, even if some of the effects of the individual elements are known, it is more difficult to determine their impact when combined. [11, 21]

Table 2 Typical alloying elements of ductile iron with their effects on the properties.

Nickel, Ni	Nickel is an expensive alloy. In ferritic ductile iron it increases strength, yield strength, hardness and corrosion resistance, but diminishes elongation. [11] In pearlitic ductile iron nickel stabilises pearlite but does not form carbides. [15]
Copper, Cu	Copper is disturbing element in ferritic ductile iron, since it favours pearlite. In pearlitic grades it can be added up to 0.7%, since it creates fine structured pearlite and increases both strength and hardness. Additional copper might negatively influence nodularisation and segregate after heat treatment. [11]
Molybdenum, Mo	Molybdenum is the most powerful alloy to increase the hardness of ductile iron and especially suitable for materials used at high temperatures. [11] Usually ductile iron contains 0.02% to 0.3% of molybdenum [13].
Manganese, Mn	Manganese content range should be between 0.1–0.25% with ferritic alloys and 0.5–0.8% with more strength demanding materials [6]. Manganese can be both beneficial and harmful element [1]. Manganese favours pearlite, which increases the hardness of the material [6, 13, 21] but too high content creates carbides during solidification when it segregates to cell boundaries [1, 21]. It is not needed to fix sulphur like with flake-graphite cast iron [6].
Phosphorus, P	Content of phosphorus should not be above 0.05% because it highly diminishes the elongation, impact strength and raises the transition temperature [6, 11]. Decent amount of phosphorus increases creep, but too high amount makes material hard [13]. Phosphorus is seen as impurity element, since it has a strong embrittling effect. [15]
Chromium, Cr	Usage of steel scrap brings chromium to the alloy, even when it is not added intentionally. [21] Chromium causes lower rotating fatigue strength, if the content is higher than 0.2%. Like manganese, chromium also segregates to cell boundaries. [21]

2.1.7 Properties of ductile cast iron

There are certain kinds of properties which define how metallic material reacts to certain types of external forces. Usually these mechanical properties, like tensile strength, elongation, ductility, hardness and toughness, are used as starting point for designing a product. Ductile cast iron has good properties which originate in the existence of nodular graphite.

Tensile strength is defined as maximum force that a material can withstand before fracturing and it is reported in terms of force per unit of area (N/mm^2=MPa). **Elongation** means length at breaking point expressed as percentage of its original length. Ductile cast iron has standardized grades based on the properties they have. [24] GJS means ductile cast iron (spheroidal graphite) and GJL means flake graphite. Typical standardized grade is for example GJS-500-7. After the definition of the graphite type, there are stated tensile strength (R_m, MPa) and elongation (A, %) as numbers.

Tensile strength and elongation give estimation also about other properties. The higher the elongation, the higher the **ductility** too. Bendability and crushability are synonyms for ductility, and they all indicate how the material withstands plastic deformation without rupture. Spheroidal graphite cast iron shows large deformation before fracture and therefore it is also called as ductile iron. When compared to flake graphite cast iron, spheroidal has much better ability to stand plastic deformation, but compared to steels the elongation is at the same level.

In addition to the properties stated in the standardized grade name, spheroidal graphite cast iron has also good **hardness**. It means resistance of a material to a plastic local and superficial deformation. In Table 3, there are the guidance values for Brinell hardness of main ductile irons. It can be seen that ductile iron defeats grey cast irons easily.[2] As a rule of thumb, higher tensile strength means lower elongation and higher hardness.

Table 3 Guidance values for Brinell hardness of ductile iron. t = relevant wall thickness [2]

Material	Brinell hardness range (HB)	
	t ≤ 60mm	60mm< t ≤ 200mm
GJS-350-22	less than 160	less than 160
GJS-400-18	130-175	130-175
GJS-400-15	135-180	135-180
GJS-450-10	160-210	160-210
GJS-500-7	170-230	150-230
GJS-600-3	190-270	180-270
GJS-700-2	225-305	210-305
GJS-800-2	245-335	240-335
GJS-900-2	270-360	270-360

All these properties originate from the graphite nodules. The shape interrupts the continuity of the matrix much less than a graphite flake and this results in higher toughness and strength. **Toughness** means ability to absorb considerably energy before fracture and resistance to crack formation. The graphite nodules stop the cracks growing when flakes itself act like harmful cracks. [1, 15]

Limitations for using nodular graphite iron are only few. Properties are not as suitable for joint welding as steel's and the production is more complex than with flake graphite irons. Therefore the price is also a little higher compared to flake graphite irons, but not as high as steel's. [6]

2.1.8 Solid solution strengthened ferritic grade and its properties

Solid solution strengthening is one way to alter the mechanical properties of ductile iron, in addition to altering the metallic phases. The idea is to add atoms of alloying element to crystalline lattice of the base metal. In this case silicon

acts as alloying element, and when it diffuses into the matrix, together these two form solid solution. In this crystalline system the elements can be arranged as substitutional solid solution or an interstitial solid solution depending on the size of the alloying element [5]. Figure 16a presents a substitutional solid solution, where the alloying atom is large enough to replace the original atoms of the lattice. To be more precise, Hume-Rothery rules states that the size of the atoms must not differ more than 15% in order to form this type of solution. [25, 26]

Also, the interstitial solid solution is essential when dealing with Fe-C systems. Here the additional atom can be equal to or smaller than the original atom, and then it can find its place in between atoms, interstitially, in the base matrix. This is illustrated in Figure 16b. Carbon in iron is one good example of this solid solution. Both of these solutions exist, because base matrix needs to be strengthened. In interstitial solution it is caused by the interstitial atoms which make bonds of the original atoms to compress and thus deform. Both types cause strengthening basically by local stress and tension, which then restricts the movement of dislocations and strengthens the material. [25, 26] In this thesis solid solution strengthening is important, since there is more silicon present which affects the structure and properties even more than with normal alloys.

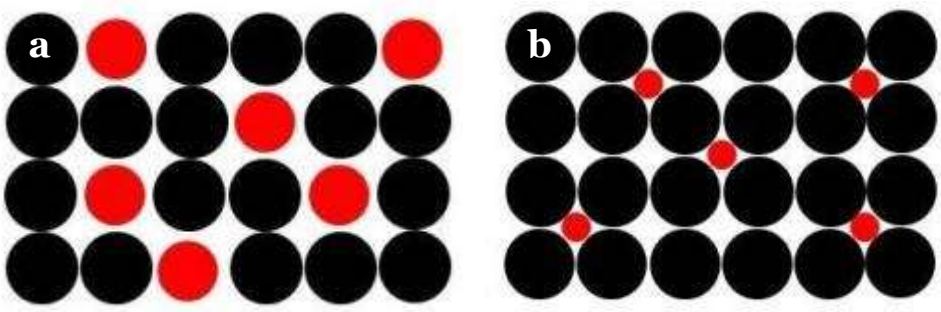

Figure 16 a) Substitutional solid solution and b) interstitial solid solution with black original atoms and red alloying atoms. [26]

It is recommended to strengthen ferritic structure by silicon [2]. Then spheroidal cast iron becomes solid solution strengthened ferritic spheroidal graphite cast iron (SSF). The enhanced properties and compositions are already

standardised within the EN1563 for spheroidal graphite cast iron. The accepted SSF grades include GJS-450-18, GJS-500-14 and GJS-600-10, which each have constant alloying level of silicon independent of casting size and geometry [2, 3]. Table 4 shows the guidance values for chemical composition of SSF grades. It must be remembered that silicon content may be lower due to other alloying element, and with lower manganese content (e.g. 0.30 %) elongation and machinability will be improved. [2]

Table 4 Guidance values for chemical composition of solid solution strengthened ferritic grades. [2]

Material	Silicon % (approx.)	Phosphorus % (max.)	Manganese % (max.)
GJS-450-18	3.20	0.05	0.50
GJS-500-14	3.80	0.05	0.50
GJS-600-10	4.30	0.05	0.50

Table 5 presents the main mechanical properties of these SSF grades and illustrative stress-strain curves are presented in Figure 17. With increasing silicon percentage yield strength increases faster than tensile strength, which means higher bearing strength before plastic deformation. This allows designing components with thinner wall thickness, which automatically causes 1.5% weight savings. Still it must be remembered that adding silicon does not enhance the properties endlessly and above 4.3% of silicon elongation drops suddenly and material becomes brittle. Until this limit, there is linear relation between silicon and tensile and yield strength, but also elongation is surprisingly high. [3] It has been argued that the increase in strength by solid solution strengthening can be much more effective than the strengthening achieved by grain refinement or forming. [12]

Table 5 Mechanical properties for solid solution strengthened ferritic grades with relevant wall thickness of ≤30mm (except HB with ≤60mm). The test pieces are machined from cast samples. [2]

Material	Minimum yield strength $R_{0.2}$ (MPa)	Minimum tensile strength R_m (MPa)	Minimum elongation A (%)	Brinell hardness range (HB)
GJS-450-18	340-350	430-450	14-18	179-200
GJS-500-14	390-400	480-500	12-14	185-215
GJS-600-10	450-470	580-600	8-10	200-230

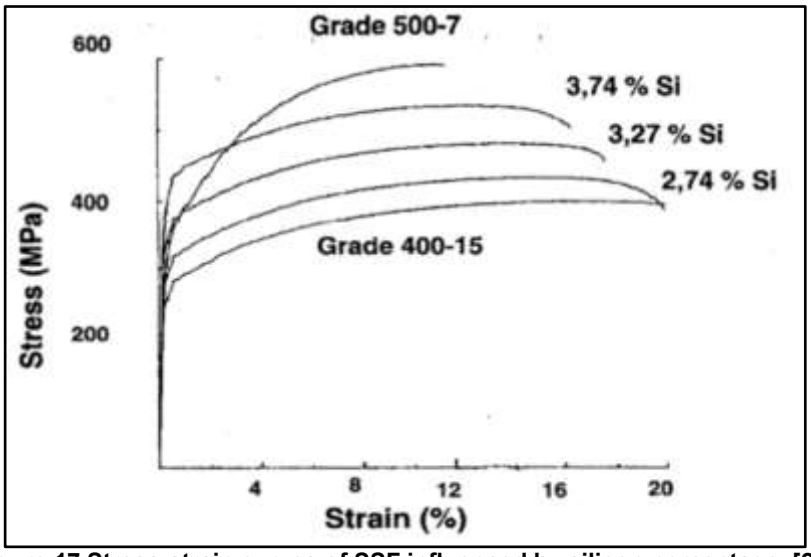

Figure 17 Stress-strain curves of SSF influenced by silicon percentage. [27]

These properties change at different temperatures, which is demonstrated in Figure 18. In this figure solid solution strengthened alloys with 3.94% and 4.03% silicon are set as examples. The figure shows that properties remain unchanged up to 400°C, but at higher temperatures elongation increases and tensile strength decreases. Contraction in the figure means necking, reduction in area, during tensile test. [28] Other concerns with SSF cast irons are a slightly higher tendency for porosities and also for chunky graphite. The undesired graphite shape originates from the increased silicon percentage and affects especially thickest wall areas, but luckily the properties of SSF grades are less dependent on nodularity. [3]

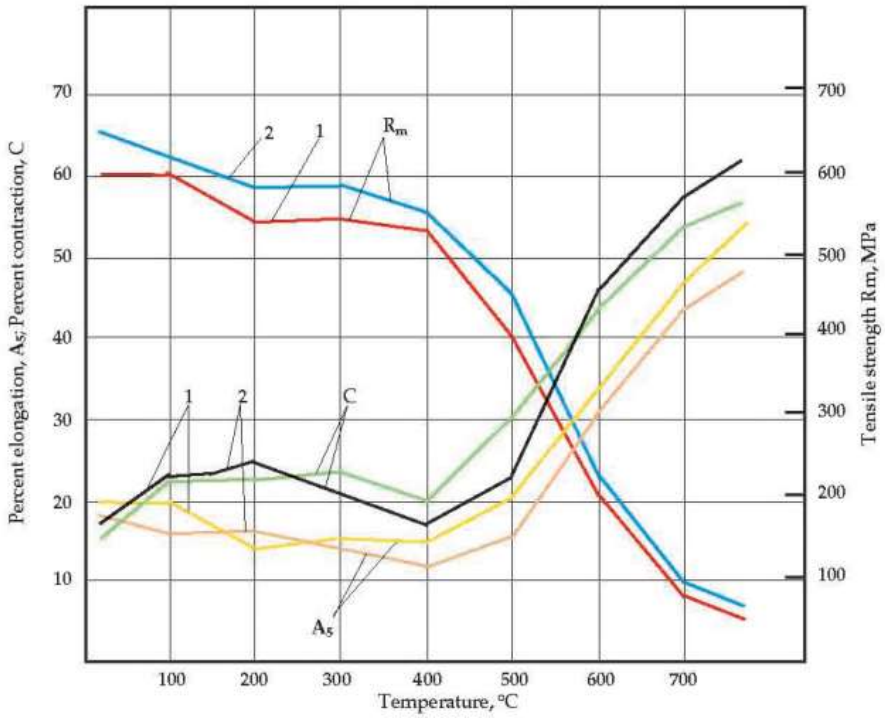

Figure 18 The influence of the temperature on the tensile strength (R_m), elongation (A%) and contraction (C) of middle silicon ductile iron containing Si-3.94% (curve 1) and Si-4.03% (curve 2). [28]

2.2 Austempered ductile iron

This section covers introduction, microstructure, alloying and properties of Austempered Ductile Iron (ADI). In the end the effects of silicon on ductile iron are examined in detail. The austempering heat treatment is presented in Chapter 3.

2.2.1 Introduction to ADI

ADI was developed at the Högfors foundry in Finland and in 1972 a patent was granted [6]. The austempering process has been in use for wrought and cast steels since 1930's [15], but using the same heat treatment for ductile iron was a new invention. Commercial world-wide production of ADI started slowly due to missing international standard, but still in year 1998 world-wide production approached 100 000 tonnes annually [3, 5, 15]. ADI grades were standardised in 1997 by EN 1564 Founding - Austempered ductile cast irons.

According to the standard, austempered ductile cast irons are spheroidal graphite cast irons which combine higher toughness and strength properties as a result of a special heat treatment. The matrix is ausferritic and has spheroidal graphite particles in it. Mechanical properties are a result of the appropriate composition and selected processing. [24] ADI grades are standardised both in Europe (EN1564) and in the United States (ASTM897). The properties of these grades are presented in Table 6 and Table 7.

Table 6 European standard grades according to EN 1564 with relevant wall thickness of ≤30mm. [24]

ADI Grade	Min. Tensile Strength (MPa)	Min. Yield Strength (MPa)	Elongation (%)	Hardness (HB)
GJS-800-10	800	500	10	250-310
GJS-900-8	900	600	8	280-340
GJS-1050-6	1050	700	6	320-380
GJS-1200-3	1200	850	3	340-420
GJS-1400-1	1400	1100	1	380-480

Table 7 US standard grades according to ASTM A897/A897M-03. [29]

ADI Grade	Min. Tensile Strength (MPa)	Min. Yield Strength (MPa)	Elongation (%)	Hardness (HB)
1	900	650	9	269-341
2	1000	750	7	301-375
3	1200	850	4	341-444
4	1400	1100	2	388-477
5	1600	1300	1	402-512

2.2.2 Microstructure of ADI

While conventional ductile iron has a mixture of pearlite and ferrite in its metal matrix, ADI consists of ferrite and stabilized austenite, generally called ausferrite. [12, 30] Ferrite exists as needles, in acicular form and austenite is stabilised by carbon, therefore it is also referred to as high carbon austenite. [22] This ausferritic structure is gained during a special austempering heat treatment. [12]

There are two main reasons why ADI gains the kind of matrix it has. Firstly, during the heat treatment, the lattice transforms from cubic face-centred austenite into cubic body-centred ferrite. These two lattices are shown in Figure 19. The second reason for the formation of ausferrite matrix is the insolubility of carbon in ferrite, which allows carbon to precipitate in the form of graphite and iron carbide. [12]

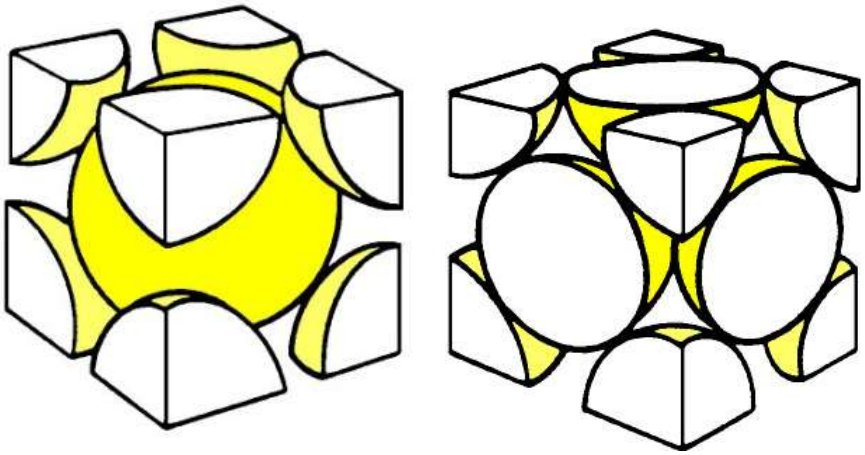

Figure 19 Body centred cubic ferrite matrix of conventional ductile cast iron (left) and face centred cubic matrix of austenite (right). [31]

When cast iron is austempered below temperature of 400°C, short-term diffusion occurs and carbon will be displaced from the ferrite while accumulating in the austenite. This reaction allows carbon content in austenite increase up to 2%, which stabilises the austenite. The fine acicular ferrite in austenite matrix provides improved strength and toughness. The microstructure can be seen in Figure 20. [12]

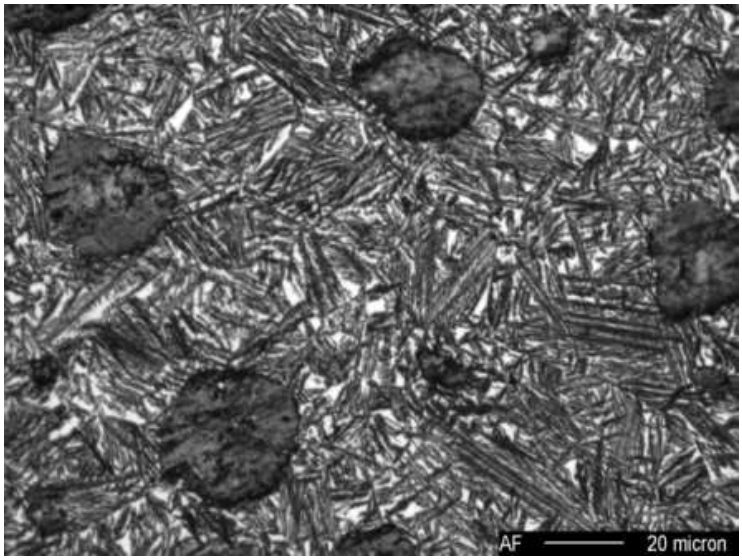

Figure 20 Ausferritic matrix of nodular graphite cast iron, etched. [12]

The properties of ADI are also affected by the type of austenite that is formed during the heat treatment. Since the carbon content of austenite increases, the cooling to room temperature does not result in martensite formation and the resulting structure is called high carbon austenite, reacted austenite or thermally stable austenite. If the elements in the matrix are distributed heterogenically, carbon content in the austenite remains low and is likely to be thermally unstable. This means that it can transform into martensite during cooling to room temperature or if stressed. As the austenite carbon content increases also the stability of austenite increases, which plays an important role in the ductility of ADI component. [22]

ADI is sometimes referred to as bainitic ductile iron, which is based on a misconception. In fact, correctly heat treated ADI contains hardly any bainite, which consists of acicular (plate-like) ferrite and carbide. Still the two matrixes resemble each other metallographically and steel has bainitic structure after certain heat treatment, which makes the structures easy to mix. Over tempering is the only way an ausferrite matrix to convert to bainite. [15] Clarifying chart in Figure 21 [32].

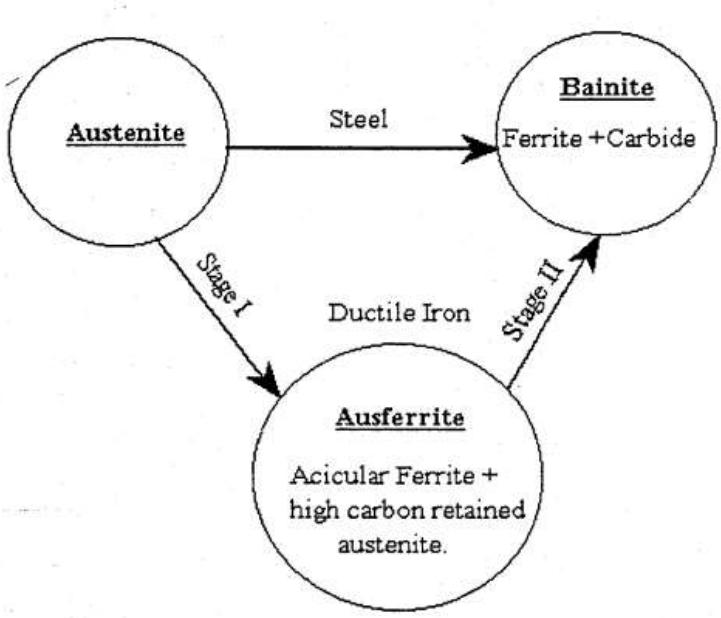

Figure 21 Schematic representation of austempering reaction in steel and ductile iron. Stage II must be avoided and casting cooled slowly when ausferrite structure is reached. [32]

2.2.3 Chemical composition and their effect on ADI

Ausferrite is the result of a specific kind of a heat treatment and all of the ingredients can alter the final outcome in their own way. Before the steps of heat treatment are explained in detail in Chapter 3, the effect of each important primary element is listed in Table 8.

Table 8 Primary elements and their effect on the properties of ADI.

Carbon, C	Shape of the graphite nodules cannot be changed by heat treatment; only the primary microstructure can be modified [19]. Still, the carbon in the matrix changes properties by infusion from one matrix to another [4]. Carbon content mainly influences the thermal and mechanical stability of the austenite [22].
Silicon, Si	Silicon is the source of graphite formation, but it also decreases the solubility of carbon in austenite, inhibits the formation of bainitic carbide and increases the eutectoid temperature. With proper amount of silicon the impact strength increases but a surplus causes the ductile-brittle transition temperature to lower. [15] In this thesis the content is higher than traditionally and therefore effects are described in detail in section 2.2.5.

Manganese, Mn	Manganese increases hardenability, but it also tends to segregate. This affects the carbon distribution and it might cause non-uniform austempering reaction, if the content is too high. At cell boundary area, where manganese and carbon concentration is high, austempering reaction is slow, while at the graphite/matrix interface the concentration is low and the reaction is rapid. This might cause a situation, where at some areas austempering reaction has not even started, while at other areas reaction has reached already the stage when it starts to form bainite. Segregation is a bigger problem in larger castings, where concentration should be limited to 0.3 % whereas with smaller (less than 60 mm) the limit is 0.5 %. With large castings, also the increased nodule count and decreased cell size also help. [21] In addition to that, manganese also slows down carbon diffusion in austenite and the ferrite growth in austempering reaction. Yield and tensile strengths might be lower due to manganese, while it also sometimes increases the impact energy. [21] Austenitising reaction is also affected, when manganese lowers the upper critical temperature by about 25°C per percent manganese.

Main purpose of adding copper, nickel or molybdenum to ADI is to increase the hardenability [15, 23]. Hardenability of metal alloy means the depth up to which a material is hardened after heat treatment process. It is measured as length and it indicates how deep into the material certain hardness can be achieved. [19] Detailed description of the effects of copper, nickel and molybdenum can be found in Table 9. For austenitising, hardenability is an important parameter, since with increased austenitising temperature the carbon content in austenite also increases and this influences greatly the material's hardenability. By adding these components, also formation of pearlite is avoided during the austempering process. [15] Since the austempering process determines the final mechanical properties, these elements have only marginal effect on them. For cost saving reason and possible difficulties with quality, only the minimum amount of alloying elemetns should be added. Typical control ranges are listed in Table 10. [15]

Table 9 Components increasing hardenability of ADI.

Copper, Cu	Copper increases hardenability of ADI and also ductility if austempering temperatures is below 350°C. It has no significant effect on tensile properties. [15] Copper can be added up to 0.8%, since it segregates at the graphite/matrix interface and forms a carbon diffusion barrier. This extends the saturation time and adds to the costs of the heat treatment. [15, 21, 23]
Nickel, Ni	Up to 2% nickel may be added to increase hardenability, impact energy and fatigue strength. Nickel increases fracture toughness and ductility, but reduces tensile strength at austempering temperature below 350°C. [15, 21] It does not significantly segregate nor affect the process variables. Disadvantage of using nickel is the often fluctuating price and higher cost compared to copper. [21]
Molybdenum, Mo	The most powerful component increasing hardenability is molybdenum, but at the same time it decreases both strength and ductility. This happens because molybdenum segregates to cell boundaries and carbides are formed, if the content exceeds 0.3%. [15, 21, 23] Also upper critical temperature (A_1) is affected and components are not as easy to machine, since properties vary in the casting and un-reacted metastable austenite might exist. [21] Molybdenum is also used to prevent formation of pearlite in thick parts of the casting. [15]

Table 10 Typical composition and control range of alloys in ADI.
***Carbon and silicon should be controlled within the desired carbon equivalent range. [15]**

Alloy	Composition	Control range
Carbon*	3.7%	± 0.2%
Silicon*	2.5%	± 0.2%
Manganese	0.28%	± 0.03%
Copper	as required	± 0.05% up to 0.8% maximum
Nickel	as required	± 0.10% up to 2.0% maximum
Molybdenum	only if required	± 0.03% up to 0.25% maximum

All these chemical components are mentioned here because they will provide an industrially successful ADI composition. Still, these will not guarantee ADI properties nor are they mandatory. Everything can go wrong already at casting, as seen in Figure 22. There the nodule count is low, which leads to larger spacing between nodules and larger regions of segregation. The heavy segregation is not only caused by alloying but also originates from nodularising treatment. The combination of controlled chemistry and heat treatment are the keys for a desired outcome.

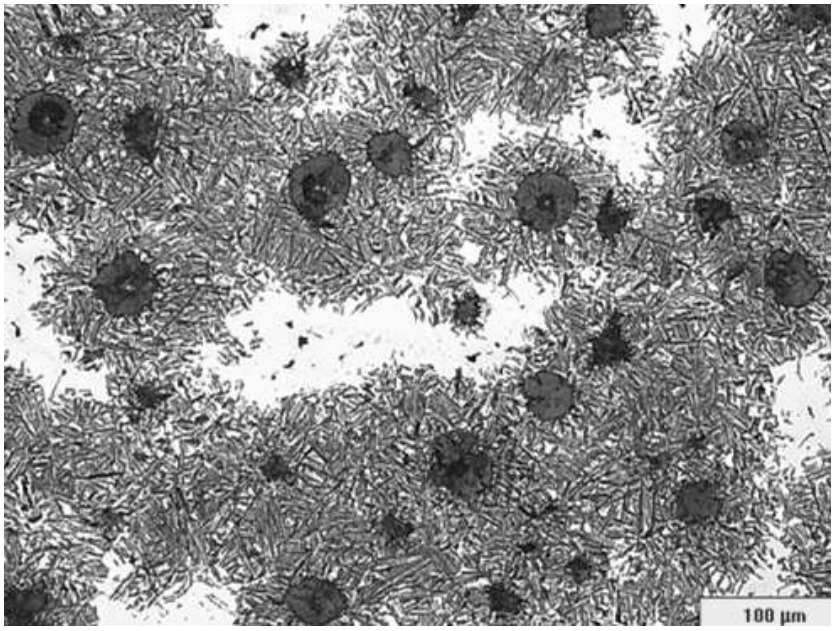

Figure 22 Microstructure of ADI. White segregated regions with high manganese. [23]

2.2.4 Properties of ADI

Compared to as-cast irons, Austempered Ductile Iron (ADI) has superior mechanical properties [4, 15]. After casting it is subjected to an austempering process, which enhances the mechanical properties remarkably.

To begin with, ADI has up to 100% better **strength** compared to as-cast irons. [23] Figure 23 provides comparison between yield strength of steels and ductile irons. ADI can easily beat as-cast iron but steel has higher elongation both in the higher and lower strength regions. Figure 24 illustrates relative weight per unit of yield strength, and it shows that ADI is comparable to heat treated steel. It

can also be seen that ADI weights less than cast or forged aluminium, when the yield strength is taken into account. Figure 25 shows the tensile strength versus elongation of ductile iron. ADI has higher tensile strength than conventional grades of ductile iron, but it cannot reach as high elongation rates as low strength ferrite and ferrite-pearlite. [15]

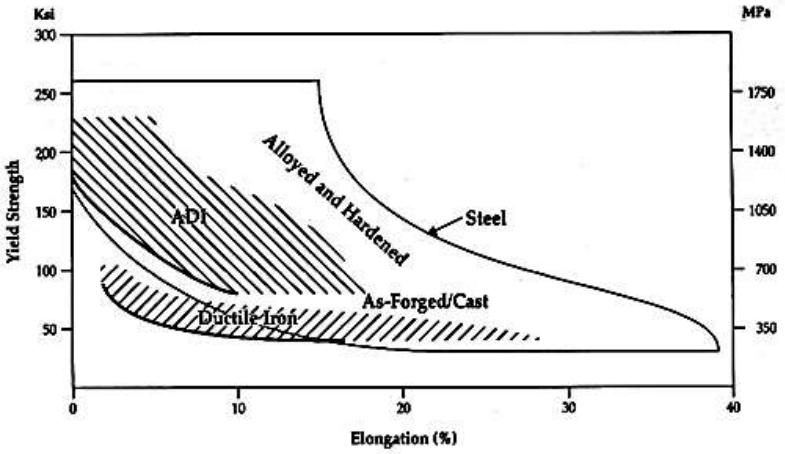

Figure 23 Comparing strength of steel and ductile iron. [15]

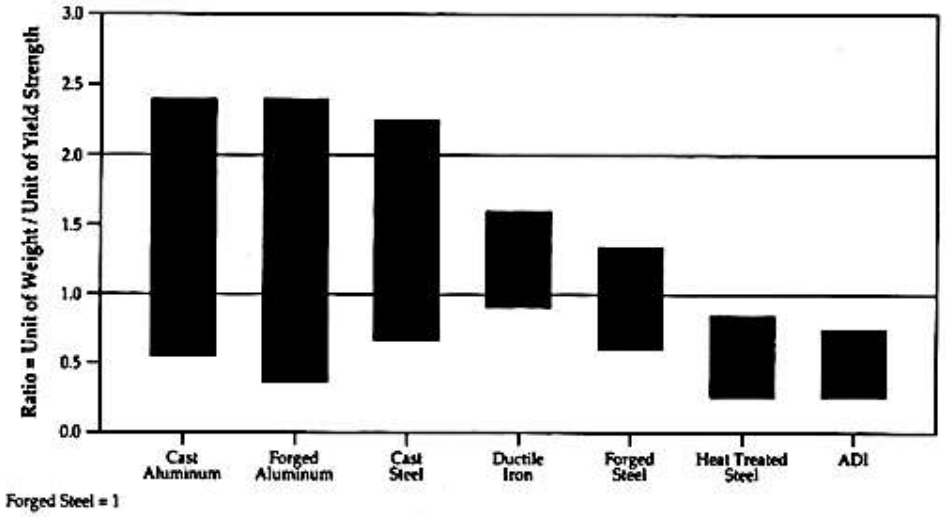

Figure 24 Relative unit weight of yield strength. [15]

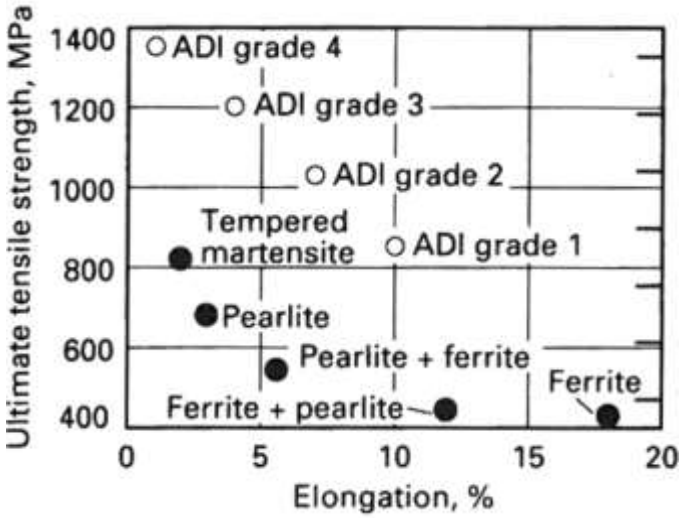

Figure 25 Tensile strength versus elongation of ductile iron. Minimum values of austempered ductile iron grades specified in ASTM897. [10]

ADI has also remarkable **wear resistance** (Figure 26)**,** which means that the surface does not erode or deform remarkably when two surfaces interact. This originates from the properties of carbon enriched austenite which can undergo a strain-induced transformation into martensite when exposed to high forces. With most metallic materials this is called work hardening, which means that hardness and stress tolerance will increase, but for ADI impact is greater: localised increase in volume is produced by the transformation which leads to high compressive stresses and inhibiting crack formation and growth. This improves **fatigue properties** (Figure 27)**,** weakening of a material caused by repeatedly applied loads, and therefore the material bears machining and surface treatments better. [15]

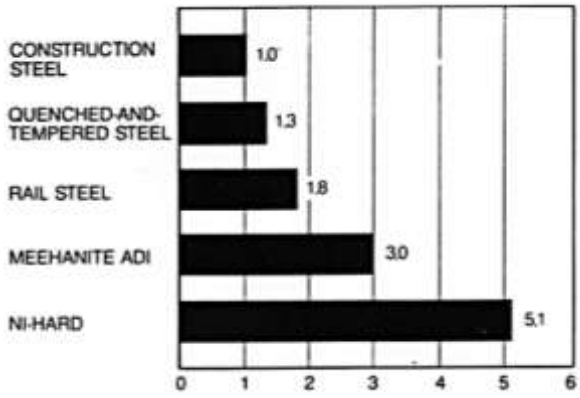

Figure 26 Abrasive wear resistance of ADI compared to other materials. Meehanite is nickname for ADI. [33]

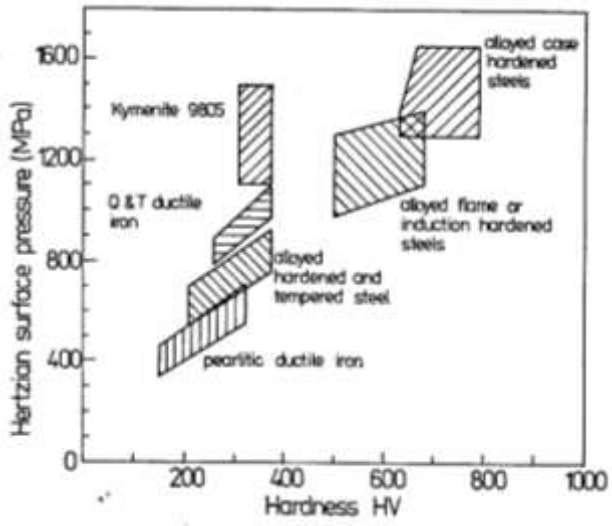

Figure 27 Fatigue strength for various materials under Hertzian contact stress. Kymenite 9805 is nickname for ADI. [18]

In addition to strength, wear resistance and better fatigue properties, also **fracture toughness** is very good. Fracture toughness describes how well the material can resist crack propagation. ADI's toughness is much greater than conventional ductile iron has, and it even reaches easily the level of cast and forged steels. Like most of the other properties, also toughness is strongly dependent on the grade and microstructure of ADI. Figure 28 shows that the ADI toughness increases strongly with increasing austempering temperature. The fracture toughness for ADIs ranges from 55 to 105 MPa at room temperature, which compares favourably with fracture toughness of 22 to 33 MPa for carburized and hardened 8620 steel. [15]

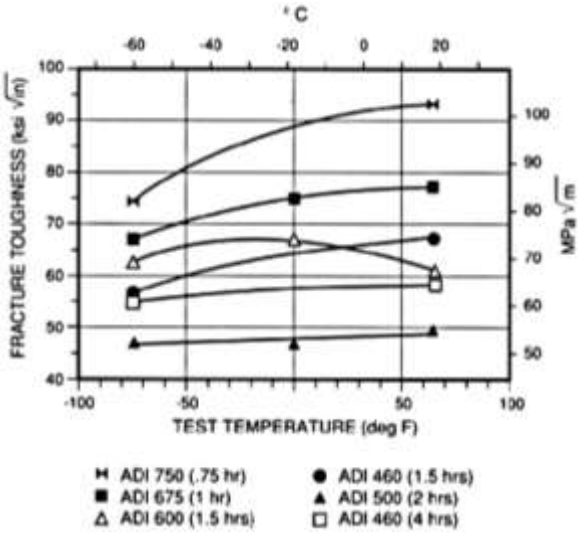

Figure 28 Effect of heat treatment and test temperature on fracture toughness of ADI. [15]

Brinell hardness of ADI grades are in Table 11. It can be seen that the values are double to the conventional ductile iron grades, still the material is not too hard to be machined.

Table 11 Guidance for ADI's Brinell hardness. [24]

Material designation	Brinell hardness range HBW
EN-GJS-800-10, EN-GJS-800-10-RT	250 to 310
EN-GJS-900-8	280 to 340
EN-GJS-1050-6	320 to 380
EN-GJS-1200-3	340 to 420
EN-GJS-1400-1	380 to 480

One of the major advantages of ductile iron is **machinability** but for ADI it is at the acceptable level**.** Machinability means ability to be shaped with stock removal using a cutting tool in order to gain the desired geometrical dimensions. Compared to low alloy steel (AISI 4140), ADI has better strength and wear resistance, but still machinability is equal or better (Figure 29). Usually parts can be machined in the as-cast state before the heat treatment, because dimensional growth of ADI during the handling is only 0.4%, which is generally within the tolerance. By using increased feed rate and reduced surface speed the metal removal rate is best for ADI and work hardening is minimal. [15]

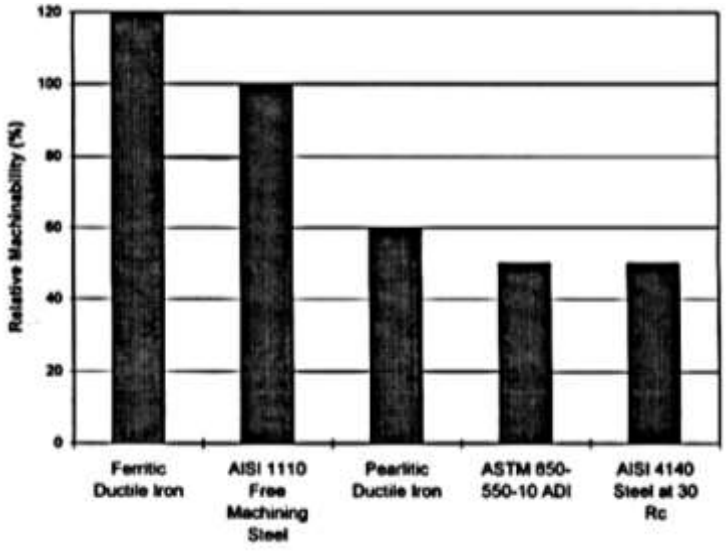

Figure 29 Relative machinability of several ferrous materials. [15]

All of the aforementioned mechanical properties vary based on the selected heat treatment. With a high austempering temperature (400°C) ADI becomes highly ductile, has yield strength in the range of 500 MPa, good fatigue and impact strength and it also responds well to the surface strains transformation, which increases bending fatigue strength. On the other hand, lower austempering temperature (260°C) gives ADI high hardness, excellent wear resistance, very high yield strength (1400 MPa) and high contact fatigue strength. [15]

The last improved property involves **costs**. Naturally, when employing a more complex heat treatment, the production costs increaese but on the other hand, a more useful combination of properties is gained [18]. ADI has 2.3 times larger Young's modulus than aluminium and weighs only 2.4 times more. The density is also 10% lower when compared to steel. The economic advantages of ADI become apparent, when comparing both the cost of unit weight and cost-per-unit-strength: ADI costs 20% less than steel and half that of aluminium. Figure 30 shows the cost efficiency relative to the strength. [15] Nevertheless, ADI can beat aluminium only with thin wall castings, but steel is the main competing material.

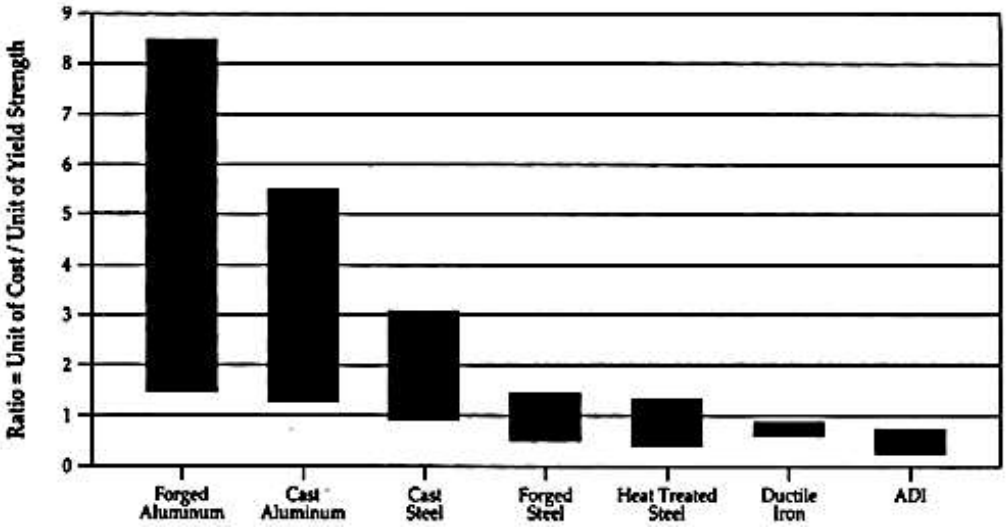

Figure 30 Relative cost per unit of yield strength. [15]

2.2.5 Effect of silicon

Silicon (Si) is an important element in ductile iron. With conventional ductile iron the silicon content is usually 1.8-2.8% [6]. The experimental part of this thesis uses ductile iron with higher silicon content, due to solid solution strengthening. This affects the properties, but also the way the casting process and especially heat treatments must be planned.

Figure 31 is Fe-Fe_3C phase diagram and illustrates how different content of silicon influences the phase boundaries. In Figure 31a silicon content is 2.4% and in the other 4.8%. [19] The basic structure in this picture is naturally quite the same but small differences are visible. With higher silicon content, the upper critical temperature has risen from 800°C to nearly 900°C, and also the lower critical temperature has slightly increased too. Additionally, the area of pure austenite is clearly smaller and it affects the carbon content of final ausferritic structure. The shapes and sizes of phase line above 1200°C have changed, but this thesis uses a heat treatment that occurs in temperatures under 1000°C and therefore these areas are not discussed further.

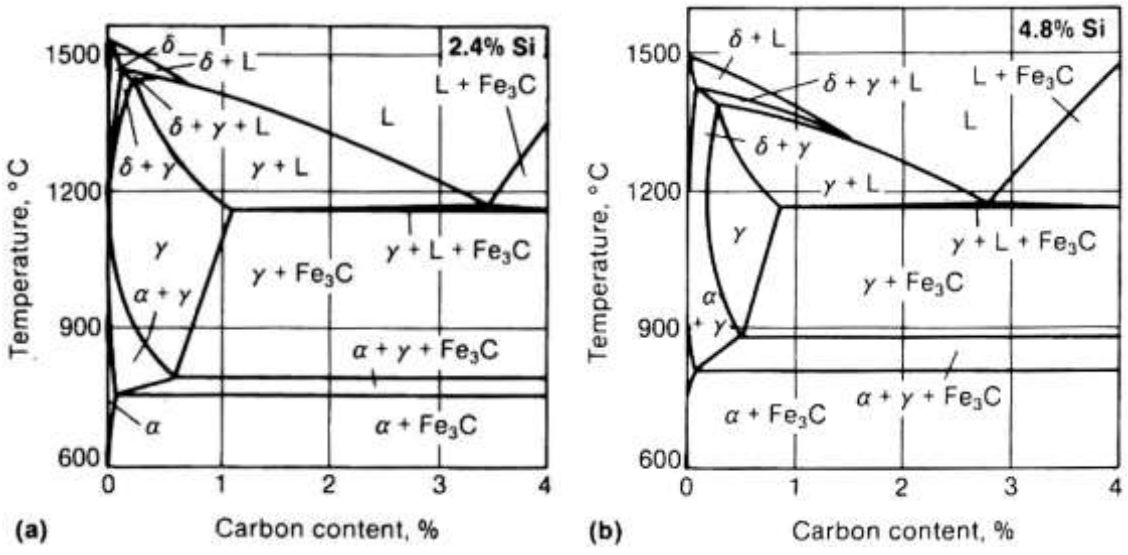

Figure 31 Influence of silicon content on the solubility lines and equilibrium temperatures of the Fe-Fe_3C system. a) Si-2.4% and b) Si-4.8% [19]

There is indication that silicon raises upper critical temperature 50°C for each percent of silicon [21]. For average ductile iron this means 125°C and with amounts used in this thesis even 150°C. This must definitely be taken into account when evaluating the optimal austenitising temperature. If the temperature is not high enough, ADI casting will contain pro-eutectoid ferrite, which lowers the strength properties. [21]

Even if the austenitising temperature has been selected correctly, higher silicon content influences the properties of cast iron. Figure 32 presents the effect of silicon to heat treated ferritic ductile iron. With higher silicon the tensile and yield strengths as well as hardness increase substantially, but at the same time elongation deteriorates steadily. [11] It depends on the final product which properties are more important and whether the higher silicon content really improves the structure. If the level of silicon is reduced, some other strengthening element must be added to meet the strength requirements [15].

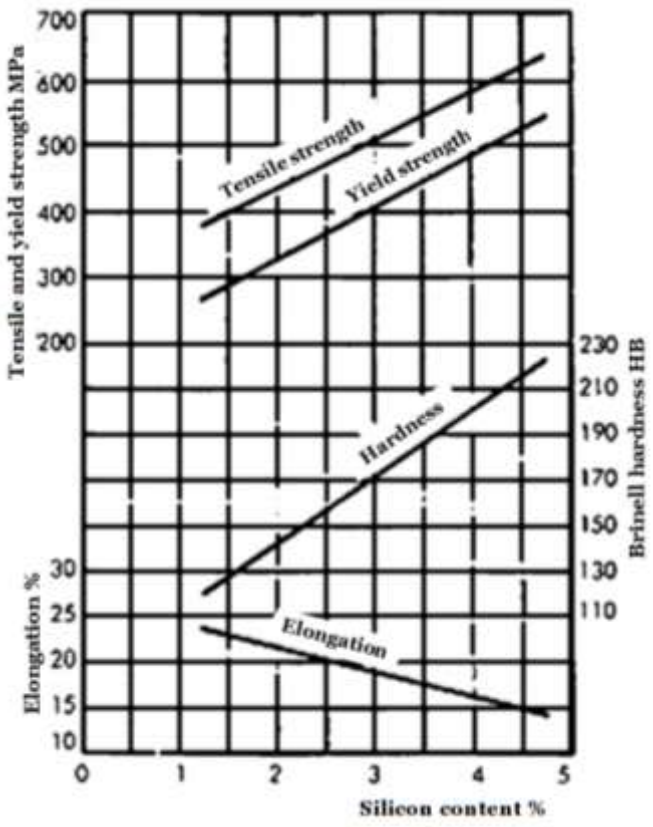

Figure 32 Silicon effects on the properties of heat treated ductile iron. [11]

When it comes to ADI, there has been a lot of debate and misconceptions on the effects of silicon. First misunderstanding is that ductile iron becomes brittle due to a higher silicon content. In fact, silicon alone is not to blame, since in these pioneering austempering trials the content of manganese was also higher than recommended and therefore it was probably also responsible for low ductility. [34] Second misconception involves chunky graphite, which is not allowed in nodular cast iron due to reduced mechanical properties. Higher silicon levels are blamed for forming chunky graphite, but the main reason apparently is locally low oxygen content in the melt during solidification or presence of some strong rare earth oxide formers. Apparently chunky graphite is sometimes a problem with ADI, but it could be prevented with high nodule count, by using chills, avoiding large risers and controlling Ce + Sb balance. [34]

When it comes to silicon, it should be remembered that the compositions used in this thesis could be classified as ”middle silicon” ductile irons. These need to be separated from the category of high silicon cast irons, since those commonly contain approximately 15% silicon by standard ASTM A518. Chromium is added to improve performance and carbon amount is only 0.65–1.15%. High silicon ductile iron is used in severe corrosive environments like offshore structures, buried cables and underground pipelines, because the material is corrosion-resistant and provides cathodic protection. [35]

3 HEAT TREATMENT PROCESS OF ADI

Heat treatments are used to create structures and mechanical properties, which are not gained during casting. Most used ones for cast iron are stress relieving, annealing, normalizing and hardening, but in this thesis only austempering is covered. [19] This chapter aims to deepen the knowledge of austempering by first outlining the basic steps of the heat treatment. Then each step is explained in detail from the viewpoints of temperature and time. Also the effect of silicon in solid solution strengthened matrix can be found in the chapters.

3.1 Introduction to ADI heat treatment

> *"Today is difficult to distinguish whether ADI is a process or a product. It is the result of a unique co-operative effort on the part of widely diverse industries as well as the scientific and educational communities in many different countries. Many of us believe that ours was the unique contribution; however, we are all proud to have been, and continue to be, a part of this emerging technology"*

This was said by J. A. Lincoln at ADI conference in 1984 [36]. It describes well how proud the community was of the new invention, but also the difficulty of defining it as a process or a product. In a way, it is a product since the material has totally new properties, but also a process since everything lies in the unique heat treatment process.

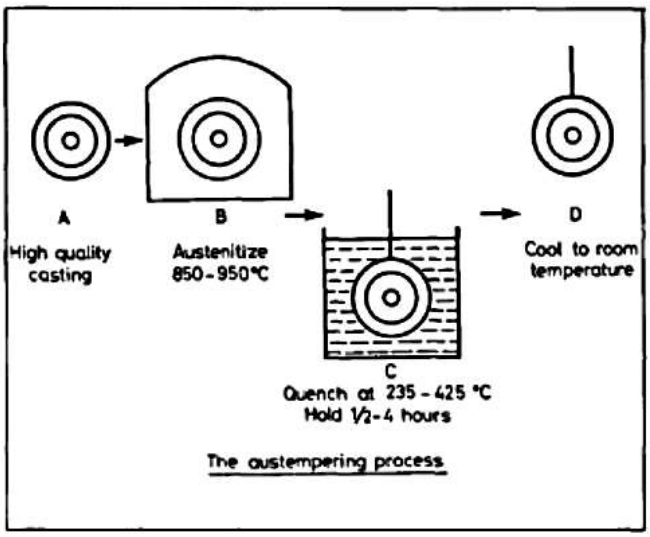

Figure 33 Illustration of austempering process. [1]

Figure 33 above shows that the basic austempering process includes austenitising, quench and cooling. More in detail austempering process consists of five stages as seen in Figure 34. In the beginning, the casting is heated up to the austenitising temperature 800–950°C (A-B) and held there for sufficient time to allow carbon dissolve in austenite (B-C). Then, rapid cooling called quenching is done to austempering temperature above the martensite start temperature (M_s) (C-D). By quenching quickly the formation of pearlite can be avoided. After that, actual austempering happens at temperature range of 240–400°C in molten salt and continues until the isothermal transformation to acicular ferrite and carbon enriched austenite, ausferrite, has occurred (D-E). In the end, components are left to room temperature to cool down (E-F). [1, 37]

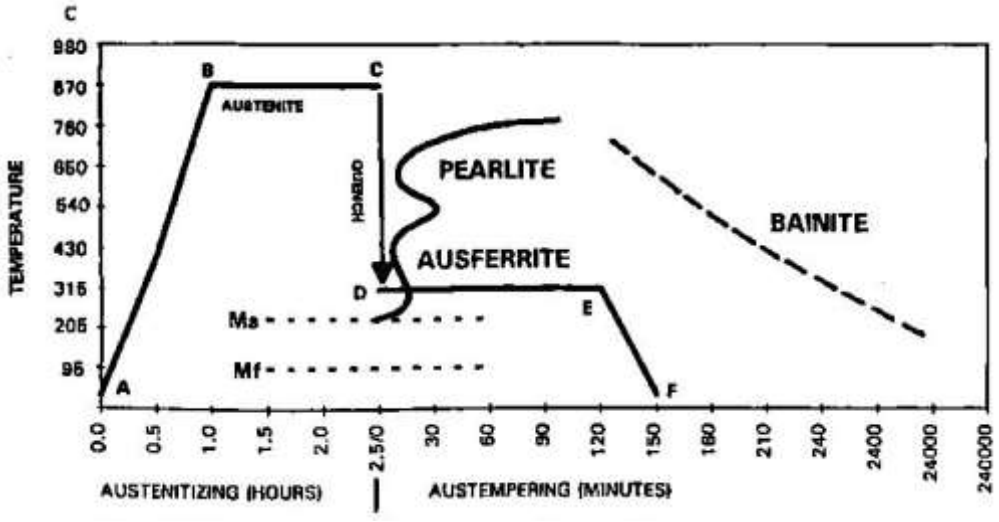

Figure 34 Austempering process for cast irons. [37]

Important in this heat treatment process is the route that has just been described, since it ensures the targeted ausferritic properties. Firstly, the austenitisation temperature must be tailored above upper critical temperature (UCT in Figure 35), in order to reach the austenitic lattice. Secondly, quench must not drop to martensite start line (M_s) to avoid the martensitic structure, but also the pearlite nose should be passed. In the end, the austempering time should not exceed the bainitic line to keep its ausferritic properties. Even so, the cooling rate to room temperature has no effect on the final microstructure, because carbon content is high enough and therefore it lowers martensite start temperature significantly below room temperature [23].

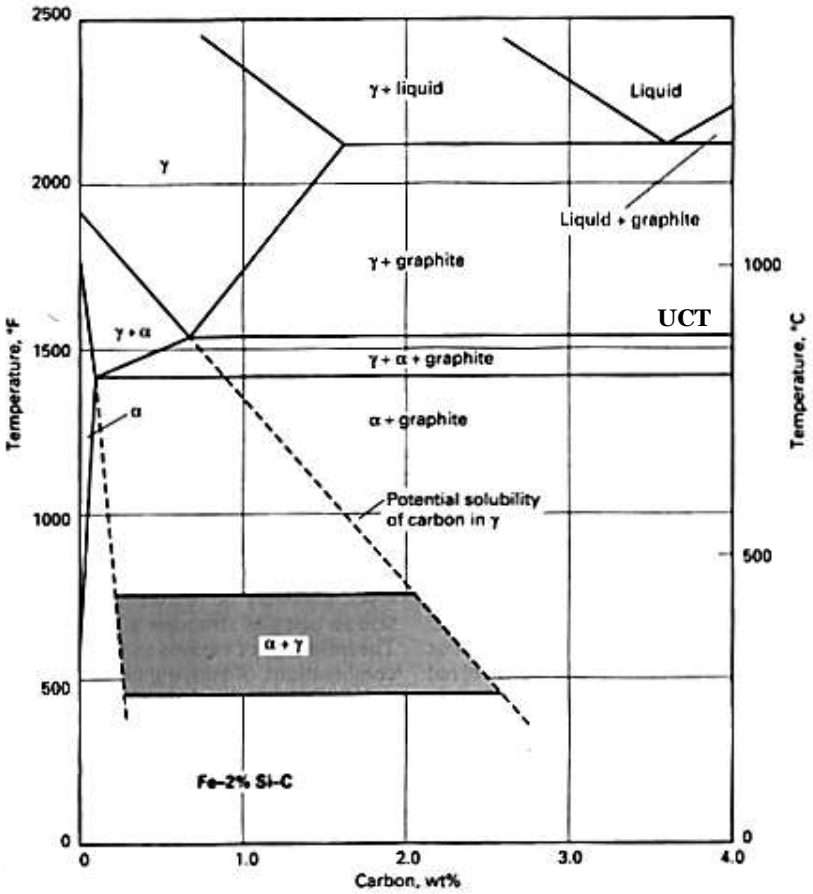

Figure 35 Section of the Fe-C-2% Si equilibrium phase diagram showing a metastable projection of the α+γ two-phase field. [19]

In the Figure 36 is presented the whole heat treatment in modified Fe-C phase diagram. With the program FactSage, the sample's chemical compositions were used to calculate more precise equilibria. FactSage is a database computing system for chemical thermodynamics and it calculates conditions for multiphase and multicomponent equilibria [M]. The used chemical composition included iron, carbon, 3.42% of silicon and 0.35% of manganese. In addition to default phase lines also metastable γ/α+γ phase boundary and with equation 1 calculated M_s line are added to the picture [22]. Then the red line is drawn to illustrate the transformations of the cast sample through the casting to the final cooling after heat treatment.

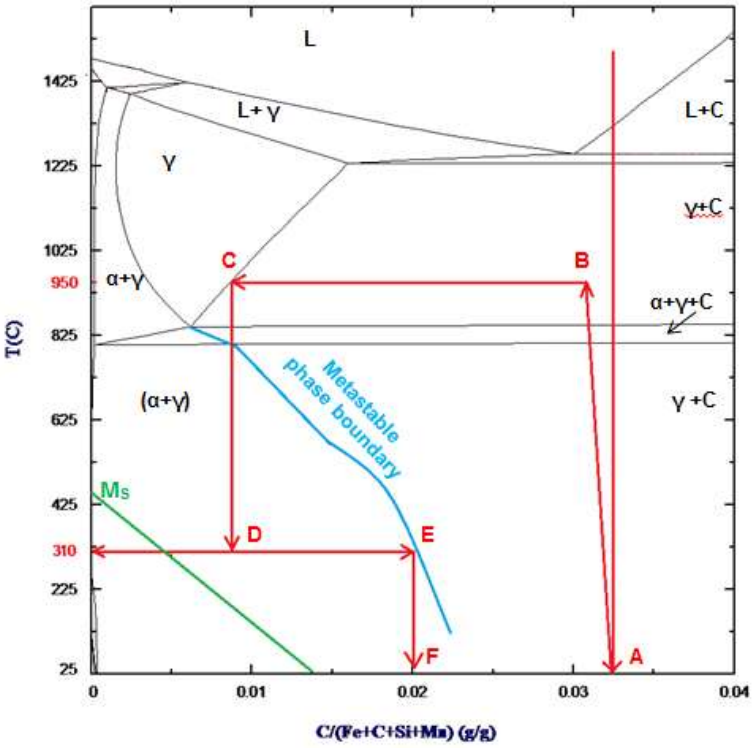

Figure 36 Modified Fe-C phase diagram with Si-3.42% and Mn-0.35%. L=liquid, γ=austenite, α=ferrite, C=cementite

$$M_s(°F) = 930 - 540\text{C} - 60\text{Mn} - 40\text{Cr} - 30\text{Ni} - 20\text{Si} - 20\text{Mo} \qquad \text{(eq. 1)}$$

Here are the transformations listed according to the letters in Figure 36 above:

A) After casting, the part cools down slowly to point A and consists of ferrite, pearlite and graphite nodules.

B) When it is heated to austenitising temperature B and held there until reach C, it crosses phase boundary, where microstructure transforms from body centred cubic ferrite to face centred cubic austenite. This requires time.

C) Quenching from C to D to salt bath must be fast. If it is not fast enough, as-cast structure will appear.

D) At point D the austenite will decompose to α-ferrite with tiny amount of carbon and austenite with more carbon. If austempering occurs at too low temperature (below M_s), martensite will form to the structure.

E) If the austempering continues too long, point E is crossed and some carbide might appear.

F) Cooling in air to room temperature will end the route in between the metaphase boundary and M_s line, and the structure is ausferritic.

During the whole heat treatment process, it must be remembered that austempering is not a cure for poor quality iron. Instead, tiny defects can result in larger mechanical problems due to austempering. [23] There are designated stages of the austempering process and each has their own critical limits for time and temperature. Next these are examined in detail, and also how the silicon influences the process.

3.2 Austenitising

Austenitising is a heat treatment to produce austenite from a ferrous alloy. [5] It is also an essential part of austempering heat treatment, because matrix must be austenite before it can transform into ausferrite. Austenitising also defines the final carbon content which affects the properties.

3.2.1 Austenitising Time

First notable thing about austenitising time is that the heating rate does not affect the final properties of ADI. However, the temperature and the time duration have significant effect on the properties. [21] The time must be sufficient to accomplish two aspects: 1) Entire matrix must transform into cubic face-centred austenite and 2) Austenite must be saturated with carbon. [21] The equilibrium level of carbon is typically about 1.1–1.3%. [15] If the minimum austenitising time is exceeded, the properties are no longer affected and holding the component in a furnace is just waste of energy. [21] For unalloyed ductile iron, complete austenitisation can be reached in 60 minutes but heavily alloyed material takes more time to austenitise [23, 32]. Naturally casting size and type, composition, austenitising temperature and nodule count are all affecting the optimal austenitising time for a specific casting. [15]

3.2.2 Austenitising Temperature

Austempering temperature affects the properties of the final product. This originates from the fact that austenitising temperature controls the carbon content of austenite, which alters the structure and properties of the casting. [15] When austenitising temperature is high, the carbon content of austenite increases and thus hardenability increases. On the other hand, transformation during austempering becomes more problematic because longer transformation time is required, and mechanical properties might deteriorate. [15, 21, 22] Usually the carbon content after austenitising varies between 0.6–1.1% depending on the austempering temperature and iron composition. [22]

Austenitising temperature should be as low as possible to produce desired structure, but then the silicon content must be precisely controlled. Reason for this is silicon's significant effect on the upper critical temperature of ductile iron. [15] Theory says that the critical transformation temperature for iron can be calculated with equation 2. [19]

$$Critical\ temperature\ (°C) = 730 + 28(\%Si) - 25(\%Mn) \qquad \text{(eq. 2)}$$

This was proved also by calculating multicomponent equilibria with program FactSage. In the Figure 37 there is equilibrium of a material with iron, C-2.82%, Mn-0.32% and silicon is on the x-axis up to 0.06%. It can be clearly seen that when silicon amount increases, also the austenitisation temperature must be higher. This is the reason why in the experimental part the iron with lower silicon content (GJS-500-7, Si-2.09%) will be austenitised at lower temperature (860°C) and the two others with higher silicon content (GJS-500-14, Si-3.42% and GJS-600-10, Si-4.09%) needs to be austenitised at higher temperature (950°C).

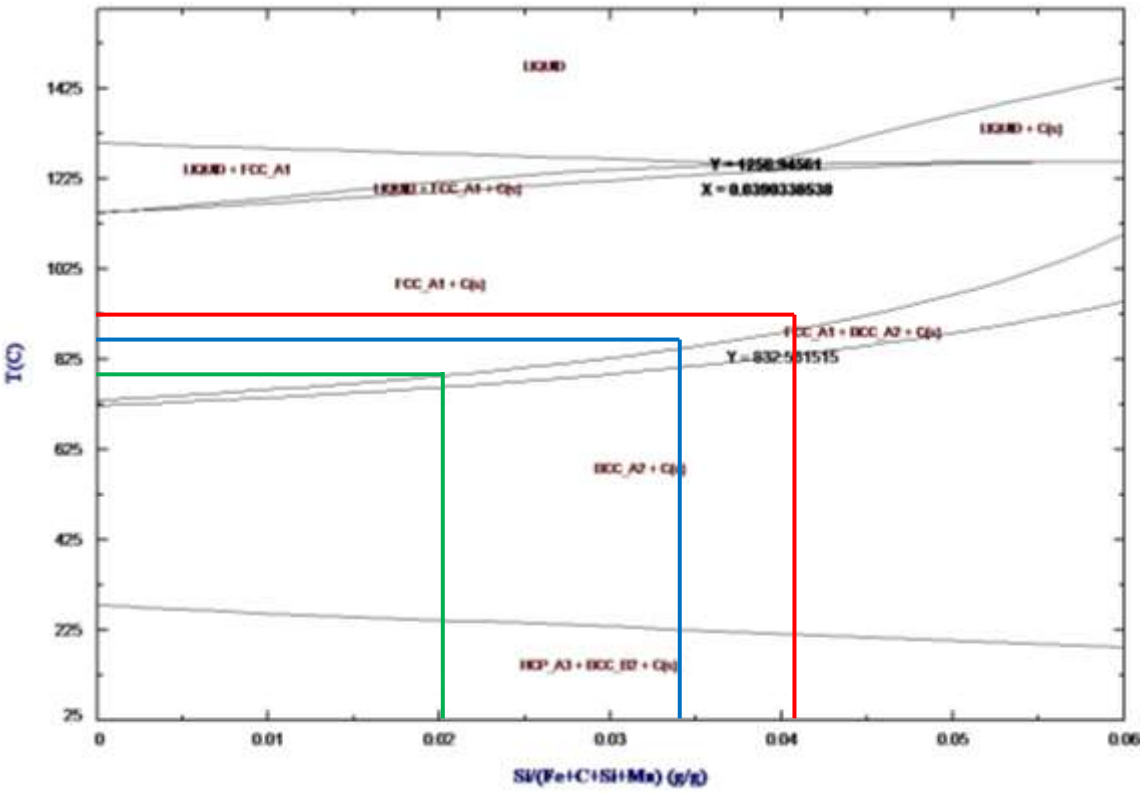

Figure 37 Multicomponent equilibria of Fe-C-Si-Mn. Green line refers to silicon content of GJS-500-7, blue to GJS-500-14 and red to GJS-600-10.

3.3 Quenching

Quenching can be defined as rapid cooling after heating the component, and is used to increase hardness and prevent formation of martensite and pearlite [5, 21]. Casting must be quenched to the austempering temperature with fast enough cooling rate to reach the desired temperature in the casting before the austempering reaction begins [21]. In the Figure 38 all three cooling curves avoided pearlite zone but only with curve 3 the right temperature was reached in time. With cooling curves 1 and 2 the matrix has mixed structures and mechanical properties are lower. The chemical composition also determines the effective cooling rate and the maximum cross section size of the casting that can be fully austempered. [21]

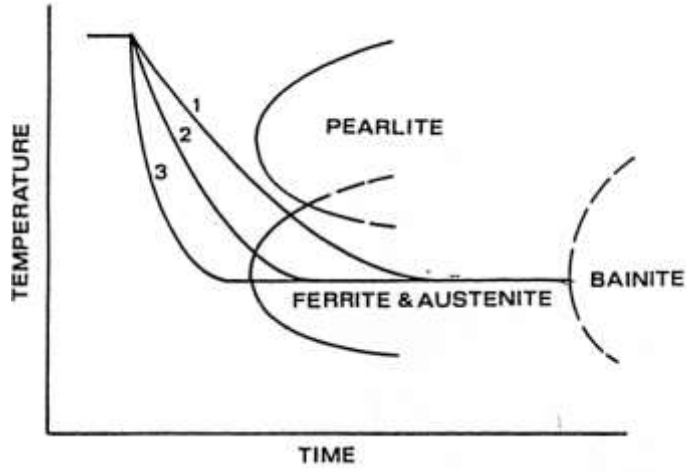

Figure 38 Three different cooling curves affecting the ADI structure. [21]

The critical characteristics with quenching involve four aspects: First, the transfer time from austenitising environment to austempering environment and secondly, the quench severity of austempering bath. Thirdly, the size and type of casting, especially the hardenability and lastly, the mass of the load relative to the quench bath size. [15] When all these are optimised, the combination itself minimizes hardenability requirements and this brings savings for alloying costs. [15]

In this thesis salt bath quench was used. Molten salt is the most used quenching medium in austempering, because it transfers heat rapidly, its viscosity is uniform at different temperatures and it stays stable at the operating temperature. For example water would not be suitable, because iron has relatively high hardenability, and therefore this medium is used only in surface hardening. [19]

3.4 Austempering

Austempering can be defined as a heat treatment process where castings are heated above AC1 temperature and held there for sufficient time to increase the carbon content of the austenite. This is followed by cooling which occurs at the rate when pearlite cannot form but matrix structure transforms into ausferrite,

microstructure consisting of ferrite and austenite. Cooling must happen above martensite start temperature and continue sufficient amount of time to produce desired properties. [24]

3.4.1 Austempering temperature

With austempering, the temperature is the factor that must be selected first, because it widely determinates the mechanical properties of ADI castings [15]. When the austempering temperature is higher (350–400°C), ADI has lower strength but higher fracture toughness and elongation [15, 21]. This originates from matrix with coarse ausferrite and higher amounts of carbon stabilised austenite, like in Figure 39 (left). When going to extremes, also formation of un-reacted or metastabile reacted austenite might occur, like inFigure 39 (right).

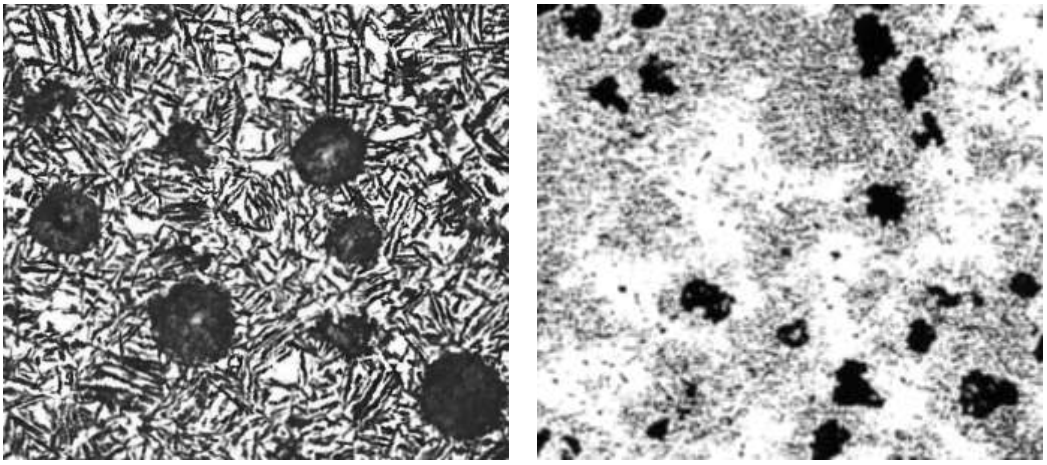

Figure 39 Microstructures of high austempering temperature. On the left, coarse acicular structure austempered at 370°C. On the right, metastable unreacted austenite. [19, 21]

Instead, selecting lower austempering temperature (below 350°C) produces ADI with greater strength and wear resistance, and fine acicular structure. This can be seen in Figure 40 (left), which is the same ductile iron as in Figure 39 (left), just austempered at different temperature [19]. But when the temperature is too low, strength properties are lowered because pro-eutectoid ferrite forms. This structure is shown in Figure 40 (right). [21] Right temperature depends on the chemical composition, which determines the upper critical temperature. [21] Also the desired ADI grade affects the selection of temperature, while lower

grades (1 and 2, Table 7) require higher and other grades (3, 4, 5) prefer lower temperature [23].

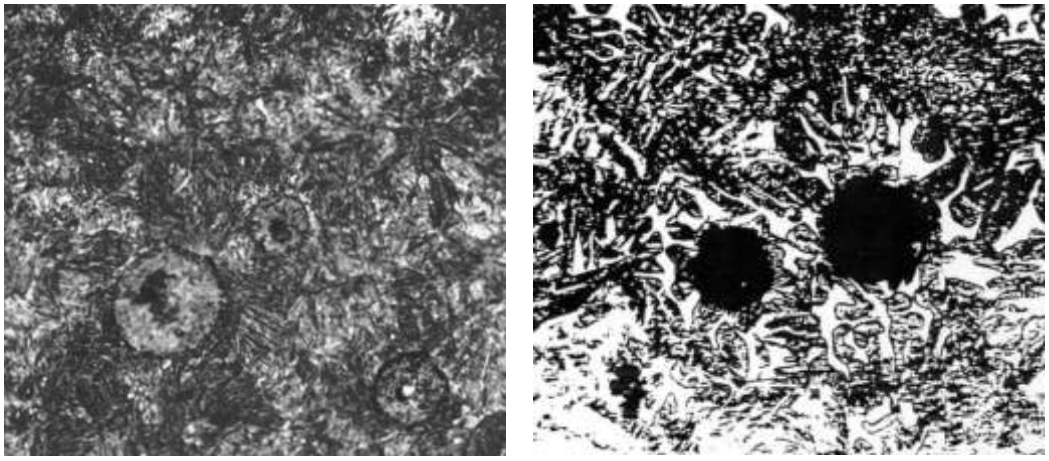

Figure 40 Microstructure of low austempering temperature. On the left, fine acicular structure austempered at 260C. On the right, pro-eutectoid ferrite. [19, 21]

Austempering itself happens when the component is bathing in molten salt. This substance was selected while it has right kind of quench severity and also other properties suitable for cast iron. Naturally the austempering temperature must be selected also based on the type of bath.

3.4.2 Austempering time

Once the austempering temperature and the substance are selected, it is time to optimise the austempering time and therefore also the final properties of casting. [15] As already described in the section 3.1, the optimal time is when ausferrite has formed, austenite has stabilised and bainite boundary approaches. [15, 21] Austempering time can range in between 30 minutes to several hours, depending greatly on the temperature [15, 23]. Figure 41 shows the typical austempering cycles for different grades and resulting Brinell hardness values. [15]

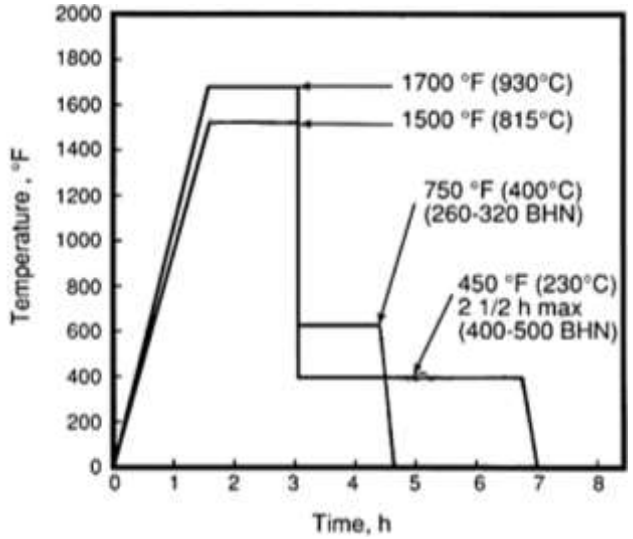

Figure 41 Typical austempering cycles for different grades of ADI. NB: temperature axis is Fahrenheit scale and BHN stands for Brinell hardness number. [15]

Both too short and too long austempering times must be avoided: Short time might cause insufficient diffusion of carbon to austenite which normally stabilises it. Therefore martensite can form during cooling to room temperature and material would have high hardness but lower fracture toughness and ductility. This kind of microstructure is in Figure 42, which shows how ausferrite formation starts close to the graphite nodules where driving force is highest [22, 34]. Then again, too long time causes ausferrite to decompose into bainite, which has lower strength, fracture toughness and ductility. [15] Volume changes of each structure (ferrite, austenite, retained austenite) within austempering time is shown in Figure 43. When the amount of ferrite and retained austenite increases, the volume of austenite decreases.

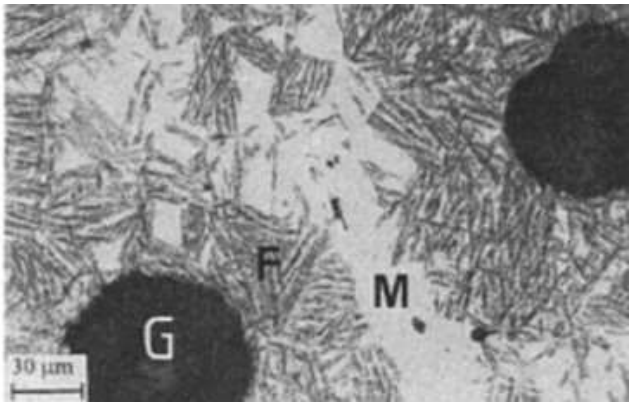

Figure 42 Ausferrite formation around the graphite nodule for ADI (Si-2,64%). Austenitised 920°C/2h and austempered at 400°C/15min. Etched with Nital 2%. G=graphite, F=ferritic plates and M=martensite. [22]

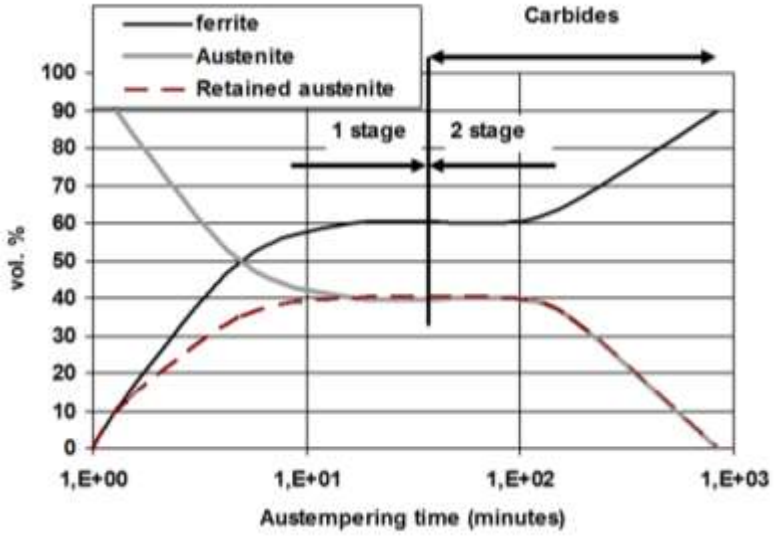

Figure 43 Effect of austempering time on structure. [39]

If examined the effect of silicon, three interconnected impacts can be identified. Firstly, higher content of silicon affects the austempering heat treatment itself by increasing the thermodynamic activity of carbon and reducing the free enthalpies of the transforming phases. This results in an increased nucleus size for the phase being formed and therefore the grains in the end matrix are smaller. [18] Second major character of silicon is related to carbon in austenite: Silicon accelerates carbon diffusion in austenite, but reduces carbon solubility in it. This means that the diffusion is faster, but the amount of carbon in the crystal structure will remain lower. [18, 21]

Thirdly, silicon influences the austempering time by altering the phase lines, like in the isothermal transformation diagram in Figure 44. There Stage I shows the area where transformation to desired ausferrite occurs and austenite is enriched with carbon. This area is sometimes referred to as process window. Instead, Stage II is already the undesired bainite and the casting should be moved to room temperature for cooling before it happens. Silicon plays important and helpful role in this, while it promotes ferrite nucleation and accelerates ferrite growth during austempering. [21] This decreases austempering time and makes Stage I area wider. At the same time silicon pushes Stage II further and delays formation of bainite by preventing the

formation of iron carbide (Fe3C). At the end, ausferritic structure is reached faster and there is smaller concern of bainite formation. [19, 21]

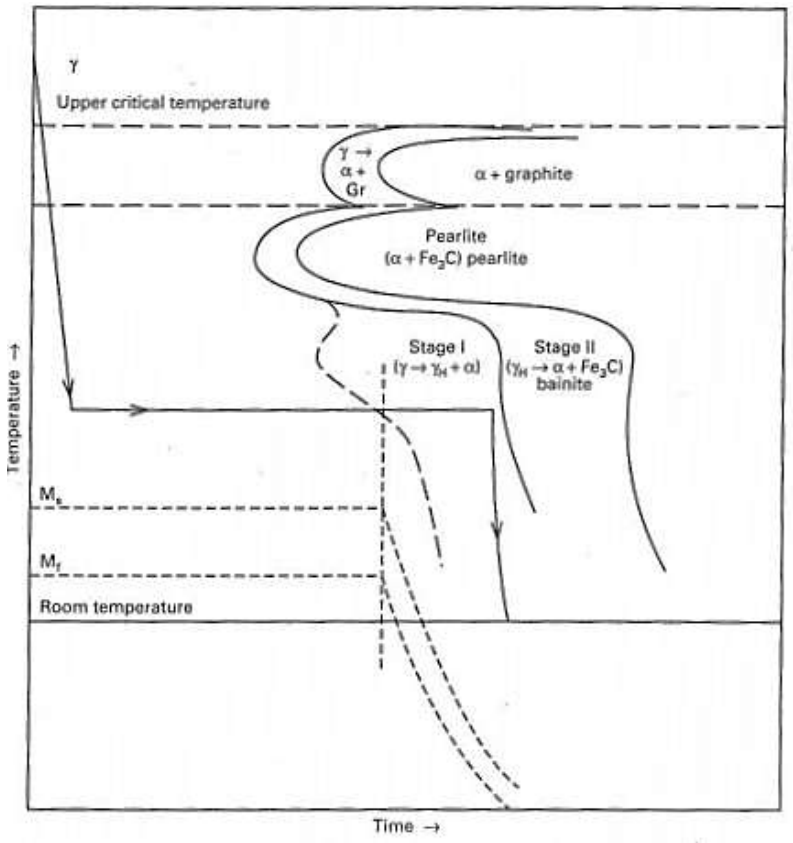

Figure 44 Isothermal transformation diagram of austempering with M_s and M_f decreasing as the γ is enriched with carbon during stage I. [19]

Figure 45 illustrates graphically the microstructure during austempering reaction. At point E the ferrite nucleation begins and when reaching point F, matrix starts to transform to ausferrite, acicular ferrite with high carbon austenite. This metastable austenite has about 1.2–1.5 % carbon and may transform to martensite if it is cooled to low temperature (below M_s) or under stress. [21, 22] Between points F and G, the existing ferrite grains continue to grow and simultaneously austenite is enriched with carbon. By reaching finally content of 1.8–2.2%, austenite becomes both mechanically and thermally stable. Austempering should be continued close, but not beyond, to the bainite boundary to reach better machinability properties. If the point G is passed, austenite decomposes to harmful bainite, consisting of bainitic ferrite and carbide. [21, 22]

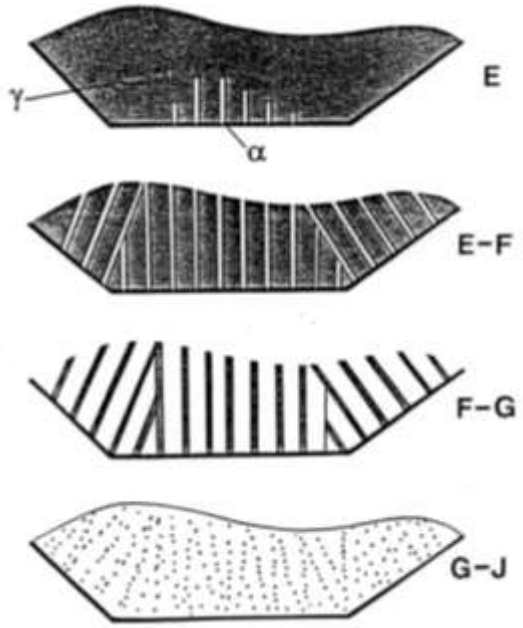

Figure 45 Graphic illustration of the austempering reaction. [21]

Right timing depends greatly on the wall thickness of the casting, since the surface and middle part of the castings might be on the opposite ends of ausferrite forming reaction: surface has already turned into ausferrite but the middle has just started. Also the alloying elements might cause uneven carbon solubility and thus segregate elements, which cause non-uniform ausferrite reaction and more mechanically unstable austenite [22]. Therefore the process window must be controlled with alloying but also too thick castings should be avoided before the reaction is known better.

4 RESEARCH METHODS

4.1 Introduction

Aim of the research is to find the optimal combination of heat treatments for the selected cast iron. Firstly, the austenitising tests were conducted to find out the limits for this heat treatment. Secondly, the austempering was tested in salt bath. Finally, the selected combination of these two gave the parameters for the last full heat treatment test with tension test bars.

The study concentrates on solution strengthened spheroidal graphite cast iron (SSF), which is tested with one wall thickness but with two different silicon concentrations. The sample materials were manufactured in Componenta foundries Karkkila, Pori and Suomivalimo in Finland. This chapter covers practicalities the experimental part, including test plan, manufacturing the samples, testing methods and equipment used.

4.2 Test plan

4.2.1 Austenitising tests

In order to find out the right austenitising temperature, all materials were tested with different temperatures, as shown in Table 12. Samples were 25mm thick and altogether three materials were tested. A furnace was heated to the right temperature and then samples were treated for 1.5 hours before moving them to a bucket of cold water. After cooling, the samples were examined to discover the properties.

Table 12 Test plan for austenitising.

Name of the sample	Original shape of the cast	Austenitising temperatures	Time in furnace
GJS-500-7/2.09	sample bar	860°C, 920°C	1.5h
GJS-500-14/3.42	sample bar	920°C, 950°C, 980°C	1.5h
GJS-600-10/4.09	y-shaped block	920°C, 950°C, 980°C	1.5h

4.2.2 Austempering tests

As already explained in the heat treatment section 3.4, austempering is a salt bath heat treatment which is implemented after austenitising. The process starts same way as austenitising. The samples were 25mm thick and made of two different alloys with different Si-content. Two pieces, GJS-500-14 and GJS 600-10, were put in the 950°C furnace simultaneously. After 90 minutes, two samples were moved quickly to 350°C degree salt bath in an open cage. The salt bath was heated during the night in order to stabilize the temperature. After a sufficient amount of time in the bath (0.5-2 hours), samples were lifted to room temperature to another cage and left there to cool down. This procedure was repeated in two different salt bath temperatures, 290°C and 310°C, and for four different durations (0.5h, 1h, 1.5h, 2h) with each temperature. These tests were repeated with two sample materials and the reference material GJS-500-7, which was austenitised in 860°C. All austempering samples are listed in Table 13.

Table 13 Austempered samples. All samples were austenitised for 1.5h and austempered for four different times (o.5h, 1h, 1.5h, 2h).

Sample name	Original shape of the cast	Austenitising temperature	Salt bath temperature
GJS-500-7 /2.09	sample bar	860°C	290°C, 310°C
GJS-500-14 /3.80	y-shaped block	950°C	290°C, 310°C, 350°C
GJS-600-10/4.09	y-shaped block	950°C	290°C, 310°C, 350°C
GJS-600-10 /4.32	y-shaped block	950°C	290°C, 310°C, 350°C

4.2.3 Testing the full austempering process with tensile bars

For testing the ADI process, samples were cut and machined as preforms of the tensile bars. The GJS-500-7 was already in bar shape, but GJS-500-4 and GJS-600-10 bars were machined from one 50mm Y-block. Heat treatments were conducted one by one due to the small size of the salt bath container. Altogether three bars of GJS-500-7 were austenitised in 860°C for 1.5 hours and the same amount of GJS-500-14 and GJS-600-10 in 950°C for 1.5 hours. Temperature of

the salt bath was 310°C and bars were there for one hour, then bars cooled to room temperature. Test plan for tensile bars is shown in Table 14.

Table 14 Tensile bar samples, which were austenitised for 1.5 hours.

Name of the sample	Original shape of the cast	Austenitising temperature	Salt bath temperature	Time in salt bath
GJS-500-7/2.33	sample bar	860°C	310°C	1h
GJS-500-14/3.80	sample bar	950°C	310°C	1h
GJS-600-10/4.32	y-shaped block	950°C	310°C	1h

4.3 Manufacturing of the test materials

4.3.1 Sample preparation

All samples were casted by professionals at Componenta's iron foundries Karkkila, Suomivalimo and Pori. Most of the samples were casted to Y-shaped mould, which is commonly used for material testing. The shaded part in Figure 46 was chosen for the samples and it was sawed down to 25mm thick cubes as directed in standard EN 1563. Later the tensile bars were also machined from the sample. Bar of 25mm diameter was another shape which was used and it also was cut to 25mm pieces (Figure 47). All austenitising and austempering tests were carried out with 25mm thick pieces in order to see the effect of the heat treatment with this specific wall thickness (Figure 48).

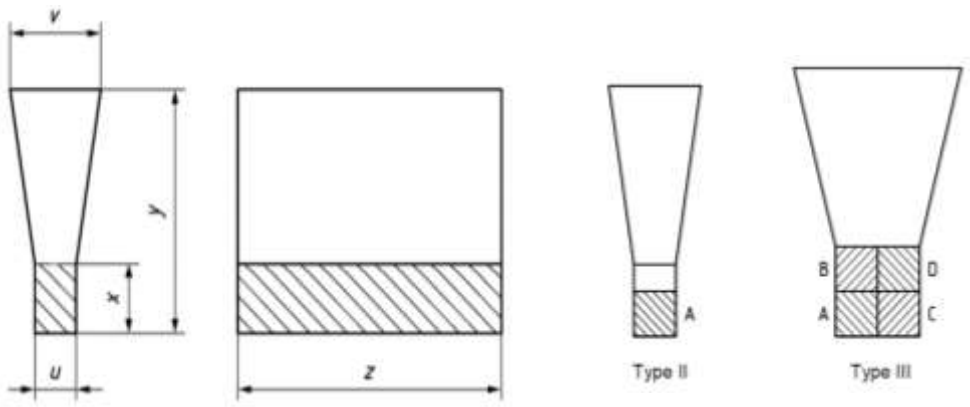

Figure 46 Y-shaped cast samples. The ideal dimensions are u=25, v=55, x=40 and y=140 for 25mm block (Type II) and u=50, v=100, x=50 and y=150 for 50mm block (Type III). Sectioning procedure is on the right. [24]

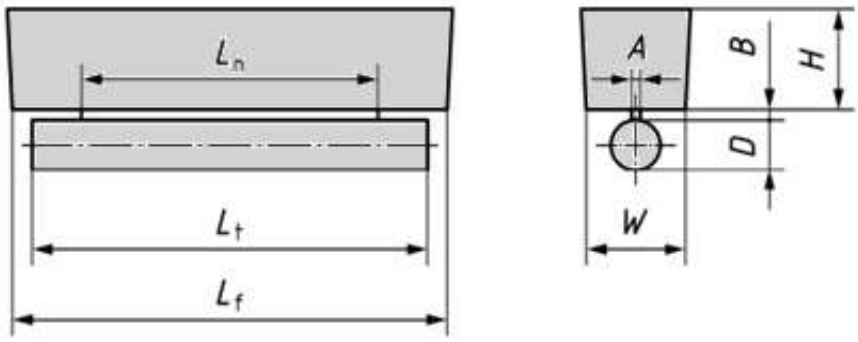

Figure 47 Sample bar casting instruction. [2]

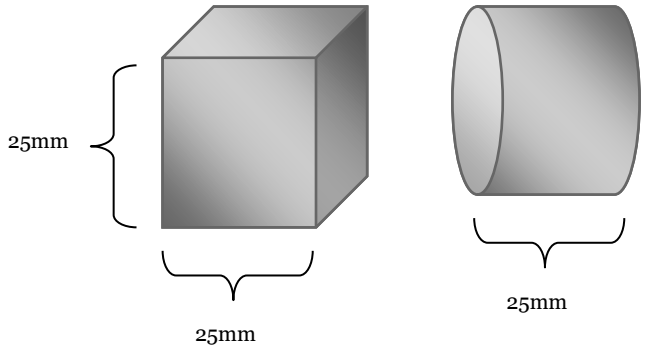

Figure 48 Illustration of the samples before entering the furnace.

4.3.2 Chemical compositions of the test materials

The chemical compositions of all test materials were analysed with Optical Emission Spectrometer. Slightly different alloyings are used at the foundries and therefore compositions differ even with the same iron grade. Compositions used for austenitising, austempering and tension bar tests are presented in Table 15. Some original properties before heat treatments are presented in Table 16, where HB indicates Brinell hardness, R_m tensile strength, $R_{0.2}$ yield strength and A% elongation.

Table 15 Chemical compositions of the casted test materials, and information in which tests those were used. Silicon content is added to the name of the material.

	GJS-500-7 /2.09	GJS-500-7 /2.33	GJS-500-14 / 3.42	GJS-500-14 /3.80	GJS-600-10/4.09	GJS-600-10 /4.32
C	3.60	3.69	3.24	3.434	2.82	3.20
Si	2.089	2.33	3.42	3.799	4.09	4.32
Mg	0.042	0.04	0.047	0.046	0.047	0.05
Cu	0.3031	0.15	0.07	0.091	0.07	0.08
P	0.0221	0.037	0.003	0.031	0.03	0.04
Mn	0.260	0.40	0.35	0.388	0.32	0.35
S	0.0079	0.012	0.008	0.008	0.012	0.01
Ni	0.020	0.03	0.03	0.043	0.03	0.11
Cr	0.027	0.06	0.04	0.038	0.04	0.04
Al	0.0095	0.016	0.016	0.012	0.014	0.01
Ti	0.0099	0.012	0.008	0.017	0.01	0.02
Sn	0.0044	0.011	0.007	0.008	0.007	0.01
V	0.004	0.007	0.007	0.006	0.006	0.01
Mo		0.01	0.01	0.018		0.02
Austenitising	X		X		X	
Austempering	X			X	X	X
Tensile tests		X		X		X

Table 16 Original properties of the test materials.

	GJS-500-7 /2.09	GJS-500-7 /2.33	GJS-500-14 / 3.42	GJS-500-14 /3.80	GJS-600-10/4.09	GJS-600-10 /4.32
HB	202	197	187	207	206	229
R_m	692.3	626	532	557	604	620
$R_{po.2}$	363.0	380	416	453	505	517
A %	6.98	8.1	15.3	15	9.9	19.2
Nodularity	89.59	70.61	85.54	77.38	82.46	75.17
Nodule count	236.04	146.79	112.51	172.37	209.64	210.36

4.4 Test procedures and equipment used

During the experimental part of this thesis, several pieces of equipment had to be used in order to execute all the tests needed. All tests were done according to the valid standards. In this chapter the main practices and procedures are elaborated.

4.4.1 Furnace and salt bath

Heat treatments were conducted at Aalto University in Otaniemi. The equipment used was a smaller version of the ones used in real life. Austenitising furnace in Otaniemi was five litres in volume and called Nabertherm (Figure 49). Amount of molten salt in Otaniemi was seven and half litres consisting equally of sodium nitrite ($NaNo_2$) and potassium nitrate (KNO_3). Samples were sawed down from the casted Y-shaped blocks and bars with different sawing machines.

Figure 49 A Furnace in Otaniemi.

4.4.2 Microstructure analysis with optical microscope

After the heat treatment, samples' microstructure was analysed with optical microscope GWB Olympus PME3. Three steps were carried out before taking the pictures: sawing, hot mounting and grinding. First, the pieces were cut to half in order to find out how the heat affected the middle mass centre of the

sample. Manual cross-cutting saw Struers Labotom 3 was used with low foaming additive Struers Corrozip, which cooled the surface during cutting. [40]

Secondly, the samples were hot mounted with Struers Labopress-3 machine. Black and transparent epoxies surrounded the sample tightly. It was heated to 180°C degrees and epoxy melted around the sample in cylinder form. Mounting helps to achieve better attachment to the grinding machine and therefore better polishing quality. Figure 50 shows mounted tensile bar samples.

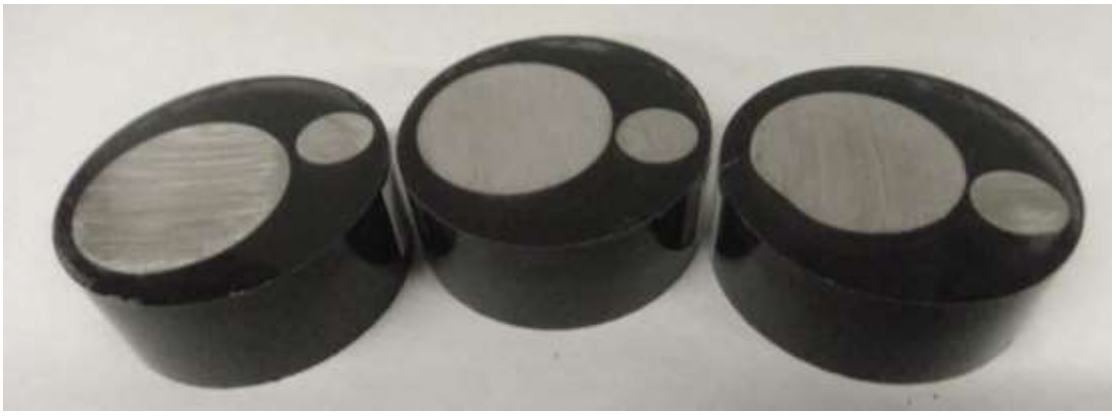

Figure 50 With black and transparent epoxy mounted samples.

The third step before examining the surface with microscope was grinding and polishing. With this mechanical preparation the cut surface was abraded and polished in order to get a representative picture with the optical microscope. With Strueres Roto Pol-31 machine it was possible to handle up to six mounted samples at the same time. Five different grinding discs were used for two minutes with the force of 40N gradually decreasing over grinding.

At the beginning, samples were grinded with MD-System grinding discs (MD Piano 120 and MD Piano 220) with water to cool the surface and to remove material gently from it. After the plane grinding, diamond paste was used as abrasive. With fine grinding cloths (MD-Allegro and MD-Largo) the 9µm and 3µm size diamond pastes were added during the process with lubricating liquid (DP-Lubricant Blue). Fine grinding removes the deformation formed during plane grinding and prepares the surface for polishing. Also the last spins were

polished with diamonds and woven wool was used as the material for the polishing cloth (MD-Mol). [40]

When the required polishing result was reached, pictures were taken from different places/points of the sample with inverted microscope Olympus PME3. All magnifications from 2,5x to 50x were used to scan the surface of the sample. The scale was half-automatically added to the pictures which were later used to analyse nodularity of the sample. After the first pictures, samples were etched with 4% Nital and new pictures of the surface were taken. Nital contains 96–98 mL ethanol, 2–4mL nitric acid (HNO_3) and it is the most common etchant for iron, because it reveals alpha grain boundaries and constituents. With the picture of etched surface it was easier to analyse the microstructure since features were optically enhanced.

Nodularity of the samples was calculated with program ImageJ. It is a Java-based image processing program and has features to help counting the nodules of the microstructure picture [41]. Unetched pictures of each sample were selected to the examination. With the program all complete nodules above the size of 22µm within the area were counted and incomplete ones were left out. Good nodules with circularity (0.55–1) were compared to total number of graphite particles, and the ratio is called nodularity, equation 3 [30]. Also the amount of nodules in the area was calculated which was used to count the nodule count (pcs/mm^2), equation 4.

$$\%Nodularity = \frac{Acceptable\ particles}{Acceptable\ particles + unacceptable\ particles} \cdot 100 \qquad \text{(eq. 3)}$$

$$Nodule\ count = \frac{Acceptable\ particles}{Area\ of\ the\ picture} \qquad \text{(eq. 4)}$$

4.4.3 Hardness tests

Hardness of metals is tested by applying force to the surface of the material through specific intender. The greater the hardness of the metal, the better it resists the deformation and the smaller the indentation. Two types of hardness tests were used because they bring slightly different angle on the properties of the material. Brinell hardness makes larger indentation compared to Vickers and therefore it tells more about overall hardness of the material. Intender of the Vickers can hit in between the graphite nodules and therefore values can vary more, but tells more about the hardness of that precise location. [5, 42]

Brinell hardness (HB) is standardised in EN ISO 6506-1 [42]. It was invented in Sweden by Dr. J. A. Brinell in 1900 and thus it is the oldest still utilized hardness test method for castings and forgings. Ball shaped hard metal intender is pressed with force and maintained for a specific dwell time 10–15 seconds (Figure 51). Then the load is removed and two diagonals of the round indentation are measured. Area of the curved surface is calculated from the mean diameter d, when the indentation is considered as segment of a sphere of diameter D. This allows calculating the Brinell hardness which is the load F (41) divided by surface area of indentation (mm^2), the specific equation presented in equation 5.

$$HB = \frac{F}{S} = \frac{2F}{\pi D(D-\sqrt{D^2+d^2})} \qquad \text{(eq. 5)}$$

In this thesis 10mm intender ball was used with 3000N force pressing for 10 seconds, since these values are commonly used for cast iron. Even when the sample preparation time is slow and diameters must be optically measured, Brinell test is widely usable for metals due to the wide selection of test forces and ball sizes. [5, 42]

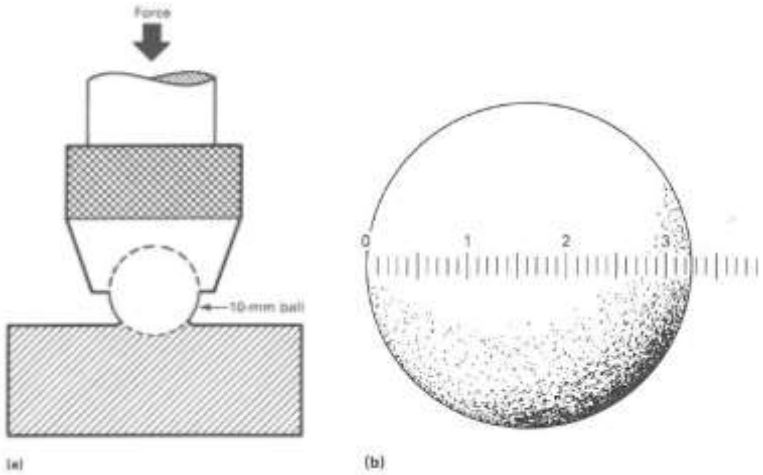

Figure 51 Brinell indentation process. a) Schematic of the principle of the Brinell indentation process. b) Brinell indentation with measuring scale in millimetres. [43]

Vickers hardness test was also conducted according to its standard, ISO 6507-1:2005. [44] This time, the intender is a shape of a pyramid, has square base and angle of 136° between opposite faces, as seen in Figure 52. Material is under the load of F and after it is removed, the diagonals *d1* and *d2* are measured and then arithmetical mean *d* is calculated. Vickers hardness HV is then the load F in newtons divided by the surface area of the indentation in millimetres, approximately presented in equation 6. [5]

$$HV = 0{,}189 \cdot \frac{F}{d^2} \qquad \text{(eq. 6)}$$

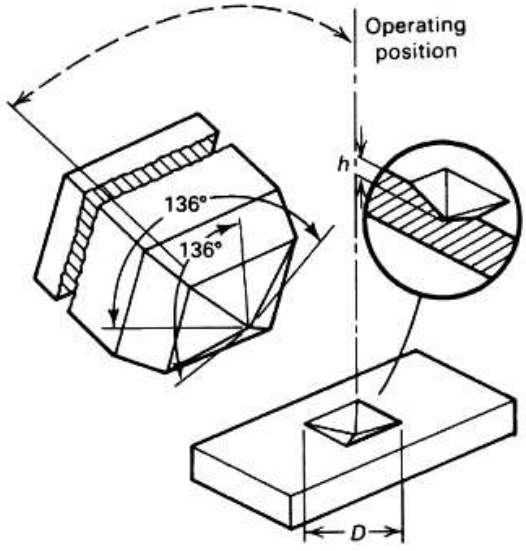

Figure 52 Diamond pyramid indenter used for the Vickers hardness test and resulting indentation in the sample. [43]

Vickers hardness test has wide variety of loads that can be selected. Table 17 presents the different test forces for metallic materials presented by their designations. In this thesis, 5kg force was used.

Table 17 Ranges of Vickers test force. [6]

Range of test force *F*, N	Hardness symbol	Designation
F ≥ 49.03	≥ HV 5	Vickers hardness test
1.961 ≤ F < 49.03	HV 0.2 to < HV 5	Low-force Vickers hardness test
0.098 07 ≤ F < 1.961	HV 0.01 to < HV 0.2	Vickers microhardness test

4.4.4 Tensile test

Tensile test is one of the most commonly used methods to find information about the mechanical properties. It is used to study the correlation of stress and elongation, and it gives values for yield strength ($R_{p0.2}$), tensile strength (R_m), reduction of area (Z%) and elongation (A%). [5] Test was executed according to the standard EN-ISO 6892-1 Metallic materials – Tensile testing [36]. The basic idea is to pull the test bar until a fracture occurs and then measure the difference of gauge and final lengths. Steps of changes during tensile test are illustrated in Figure 53 [43]. Bars were machined as shown in Figure 54. Diameter of the test piece along the gauge length (dimension *d*) was 10mm, the original gauge length (L_o) was 50mm and pulling speed was 10mm/min. An adequate section for hardness testing was taken from the other end (Figure 55). [5, 36] All tests were performed at room temperature (23±5) °C.

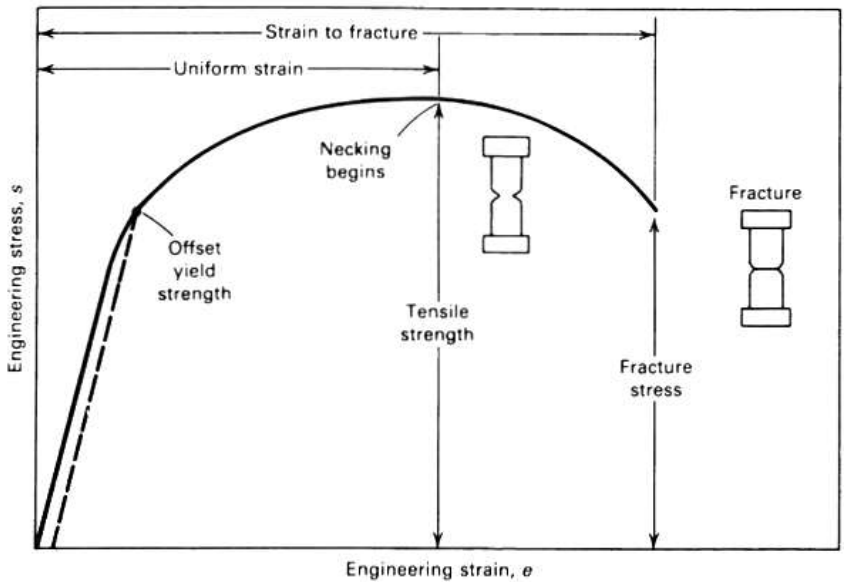

Figure 53 Engineering stress-strain curve illustrating the development during tensile test. [43]

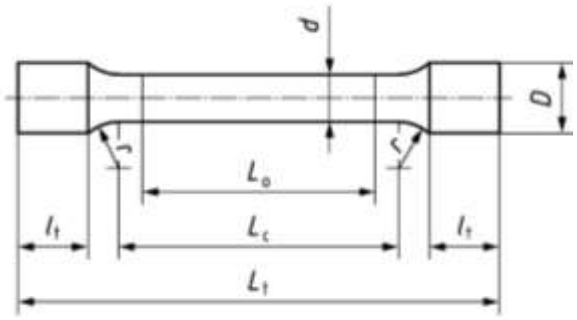

Figure 54 Dimensions of the tensile test bar. Now d=10mm, L_0=50mm and L_c=60mm. [24]

Figure 55 Tensile test bar and hardness test sample.

5 RESULTS AND DISCUSSION

This chapter presents the results of the tests conducted in this thesis. The results of austenitisation tests are explained, followed by austempering tests and finally the full austempering process. Each sub-section includes the results of microstructures and hardness, but the last part also presents tensile test results. Discussion is among the tables and figures, and in the end the reliability of these results is evaluated.

5.1 Results of austenitisation tests

5.1.1 Microstructures

Before we examine the real microstructure pictures taken with microscope, it is good to see what the surface of the casted samples was like after water quench. Figure 56 shows a sample of GJS-500-7 iron after austenitising at 860°C for one and a half hours. As can be seen, the surface rusts quickly in the water and some thin layers peeled off. Right after the sizzling hot pieces were immersed in water, some of the water around them evaporated and the surface was oxidised. One of the samples cracked due to internal stress caused by the fast temperature change.

Figure 56 Sample GJS-500-7 after austenitisation at 860°C.

The microstructure pictures were taken with microscope and the first samples were as-cast samples without any heat treatment. The etched pictures can be seen in Figure 57. The magnification is 50x, which means that picture is 50:1 compared to the original one.

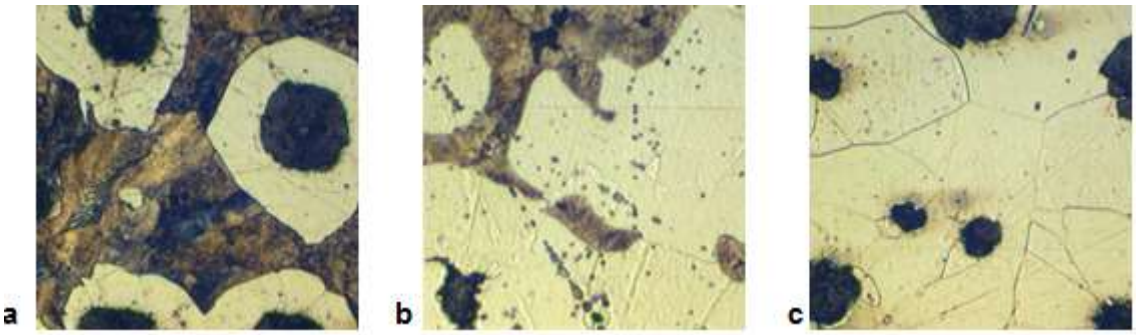

Figure 57 Microstructures of as-cast samples. a = GJS-500-7/2.09, b = GJS-500-14/3.42, c = GJS-600-10/4.09. Magnification 50x.

As can be seen in Figure 57a GJS-500-7 has clearly ferritic-pearlitic structure and therefore graphite nodules are surrounded by white area of ferrite and the matrix is naturally grey pearlite. In GJS-500-14 there are smaller areas of pearlite and GJS-600-10 has fully ferritic structure.

Microstructures of the first austenitised samples can be seen in Figure 58 and Figure 59. Figure 58 shows GJS-500-7/2.09 austenitised at 860°C, which is the normal austenitisation temperature for that type of iron and used as reference for the actual samples. Figure 59 shows samples austenitised at 920°C. Since these samples are quenched in water, the needles of these microstructures are martensite, which forms when austenite is cooled rapidly. Ausferritic matrix forms only when quenched in salt bath. Martensite plates in Figure 58 and Figure 59a are much smaller and thinner when compared to other materials. Figure 59b and Figure 59c have quite a similar structure, but the needles are slightly thicker in Figure 59c. Differences might be caused by the irregular segregation of silicon or by different cooling rates. Coarser structure usually possesses less toughness.

Figure 58 GJS-500-7/2.09 austenitised at 860°C.

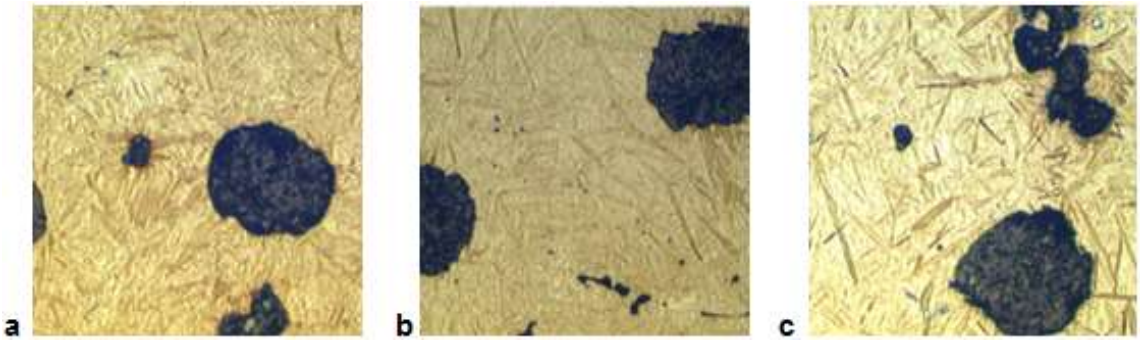

Figure 59 Microstructures of samples austenitised at 920°C. a = GJS-500-7/2.09, b = GJS-500-14/3.42, c = GJS-600-10/4.09.

Figure 60a and Figure 60Figure 59b show samples austenitised at 950°C and Figure 60cFigure 60d samples austenitised at 980°C. Left column shows GJS-500-14 and right one GJS-600-10. It seems that Figure 60b has the tightest packed needles, which can indicate higher strength and hardness. GJS-600-10 has wider needles than the other materials and also some clearer areas of martensite. Usually fine structure possesses higher toughness and generally better properties.

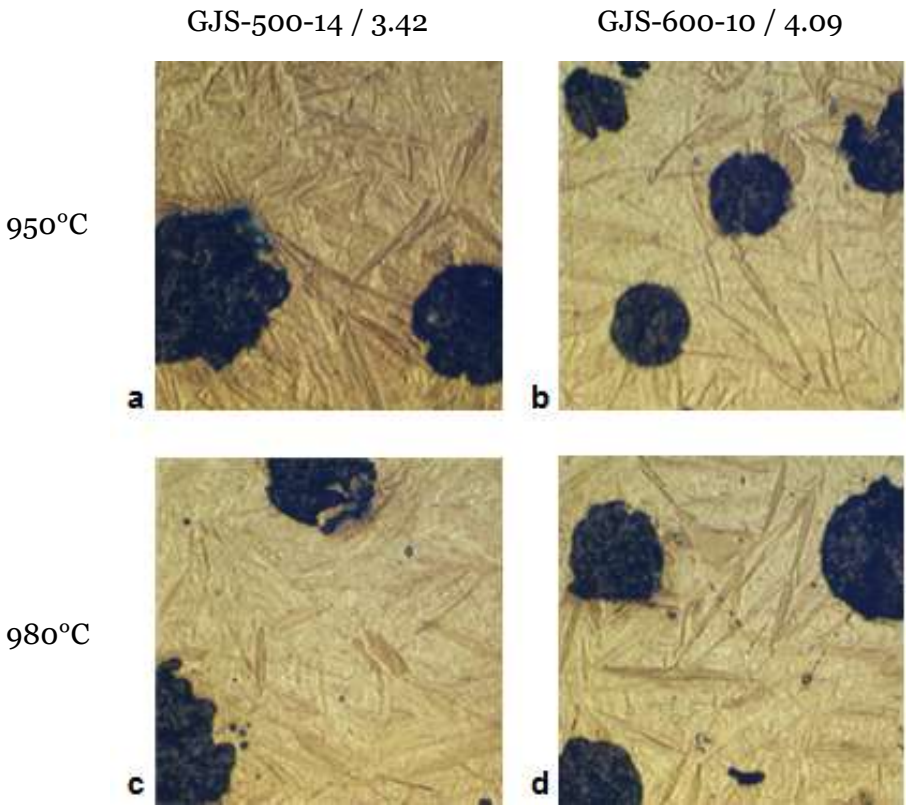

Figure 60 Microstructures of samples *a* and *b* austenitised at 950°C, *c* and *d* austenitised at 980°C. a,c = GJS-500-14/3.42, b,d = GJS-600-10/4.09.

5.1.2 Hardness tests

Standard as-cast ductile iron was compared to the austenitised samples. All were tested for both Brinell and Vickers hardnesses (Table 18 and Table 19), but the Brinell scale was not wide enough to measure hardness of the water quenched samples. Vickers was measured ten times and highest and lowest results left out, so that the result in the table is the average of eight measurements. Only one measurement with Brinell could be done due to the dimensions of the sample, but still the results confirm the differences between the materials.

Table 18 Hardness of as-cast irons.

Samples	Brinell hardness (HB)	Vickers hardness (HV5)	Standard deviation of Vickers
GJS-500-7/2.09	232	243.47	7.07
GJS-500-14/3.42	181	201.49	4.06
GJS-600-10/4.09	199	220.45	3.56

Table 19 Hardness after austenitising.

Samples	Austenitisation temperature (°C)	Vickers hardness (HV5)	Standard deviation of Vickers
GJS-500-7/2.09	860	775.00	36.89
GJS-500-7/2.09	920	760.16	21.82
GJS-500-14/3.42	920	705.25	37.43
GJS-500-14/3.42	950	720.92	38.72
GJS-500-14/3.42	980	703.20	41.04
GJS-600-10/4.09	920	717.08	24.93
GJS-600-10/4.09	950	716.73	30.56
GJS-600-10/4.09	980	723.57	23.55

Vickers machine gave the standard deviation and based on those results the standard error was calculated with equation 7,

$$S = \frac{s}{\sqrt{n}} \qquad \text{(eq. 7)}$$

where S is standard error, s is standard deviation and n is the size of the sample (y_1, ..., y_n). All results are shown in Figure 61, where error bars are defined by standard error. This figure shows that hardness has more than tripled in austenitisation and the material has hardened throughout the entire sample.

With materials GJS-500-14 and GJS-600-10 the results are very similar among different austenitisation temperatures, while all results vary in between 700-725 HV, but GJS-500-7 reaches 760-775 HV. These results were in the expected range. GJS-500-14's highest hardness value 721 HV was after 950°C austenitisation, which could already be seen from the fine needle structure in Figure 60a.

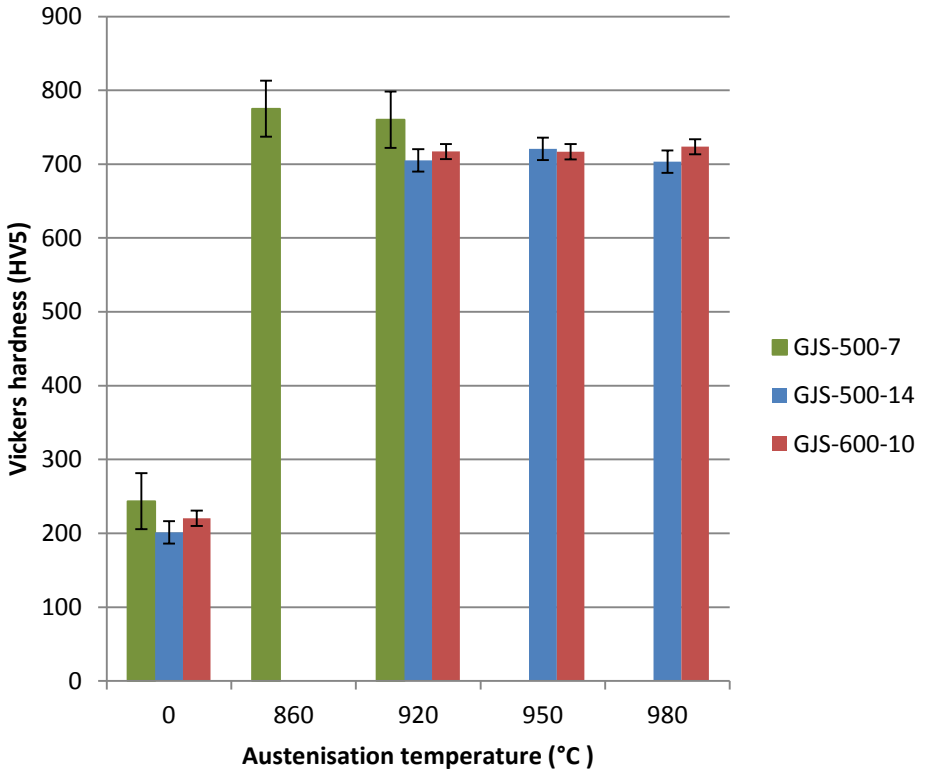

Figure 61 Vickers hardness results of as-cast samples and after austenitisations.

Temperature 950°C is selected for further austenitisations for materials GJS-500-14 and GJS-600-10 and temperature 860°C for GJS-500-7, while these are the lowest workable temperatures and with these the materials gained good hardness values. Also 920°C seems to be high enough for the materials with higher silicon content, but it is close to the theoretical border and therefore 950°C was a safer choice. Practical aspects must also be considered, while higher temperature (980°C) might cause undesired dimensional changes for some products and naturally higher heating also consumes more energy.

5.2 Results of austempering tests

5.2.1 Microstructures

Figure 62 shows a sample of GJS-600-10 iron after austenitising at 950°C and austempering at 350°C for half an hour. The casted surface is cracked but sawing surfaces remain unharmed.

Figure 62 Sample's cracked surface after 950°C austenitising and 350°C austempering.

Figure 63 on page 75 presents the microstructures of 290°C austempered samples. At the first glance, all pictures look similar with graphite nodules and grey and white matrix with randomly formed needles. However, there are small differences that can be noticed with a closer inspection. With the samples of half an hour, GJS-500-7 has plates of fine needles when in other materials the needle structure is coarser. At the one hour and 1.5 hours in the samples of GJS-500-14 there is a thin lighter layer of ferrite around the nodules, but not in all figures. This layer is so thin that it hardly has any effect on the properties. Instead, the smaller nodularity and nodule count of two hours' GJS-500-14 and all GJS-600-10 might have effect on the hardness.

Figure 64 on page 76 shows the microstructures of samples austempered at 310°C. More visible differences between the samples can be seen compared to the previous 290°C ones. There is a clear thicker light ferritic halo around nodules in the samples of GJS-500-14 (0.5h) and GJS-600-10 (0.5–1.5h), which indicates that the carbon content of austenite remains low due to higher silicon content around the nodules, and therefore ferrite appears. Luckily, this ferritic halo does not have remarkable effect on the mechanical properties, as

discovered later in this thesis. Another notable difference is with GJS-500-14 needle structure in one hour sample, where there are darker needle plates among the normal needle structure. This might be the result of a different kind of etching but also lower nodule count can lead to larger spacing between the nodules, therefore larger regions of segregation and finally to incomplete transformation with low carbon austenite or even martensite. [23]

The microstructures after **350°C** austempering treatment are in Figure 65 on page 77. Strong obervations are hard to make while the degree of etching seems to be slightly different in the pictures. Still the GJS-500-14 has more rough needle structure comparred to GJS-600-10 with fine needles. With GJS-600-10 the most obvious characteristic affecting the properties is the small nodule count and low nodularity.

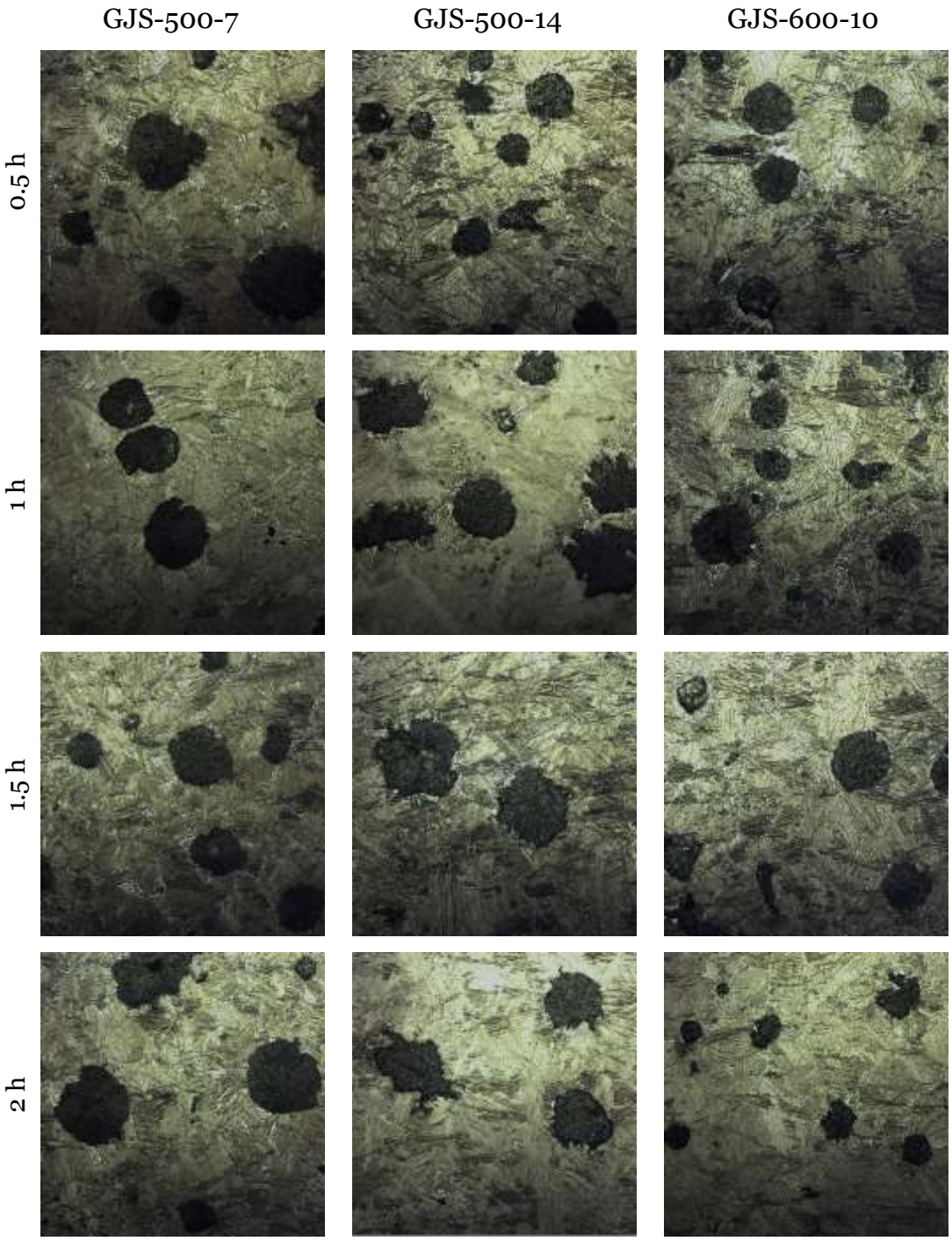

Figure 63 Austempering at 290°C. Same material in each columns. Different times in different rows, starting from 30 min (top row) and continuing 1 h, 1.5 h to 2 hours (bottom).Magnification 50x.

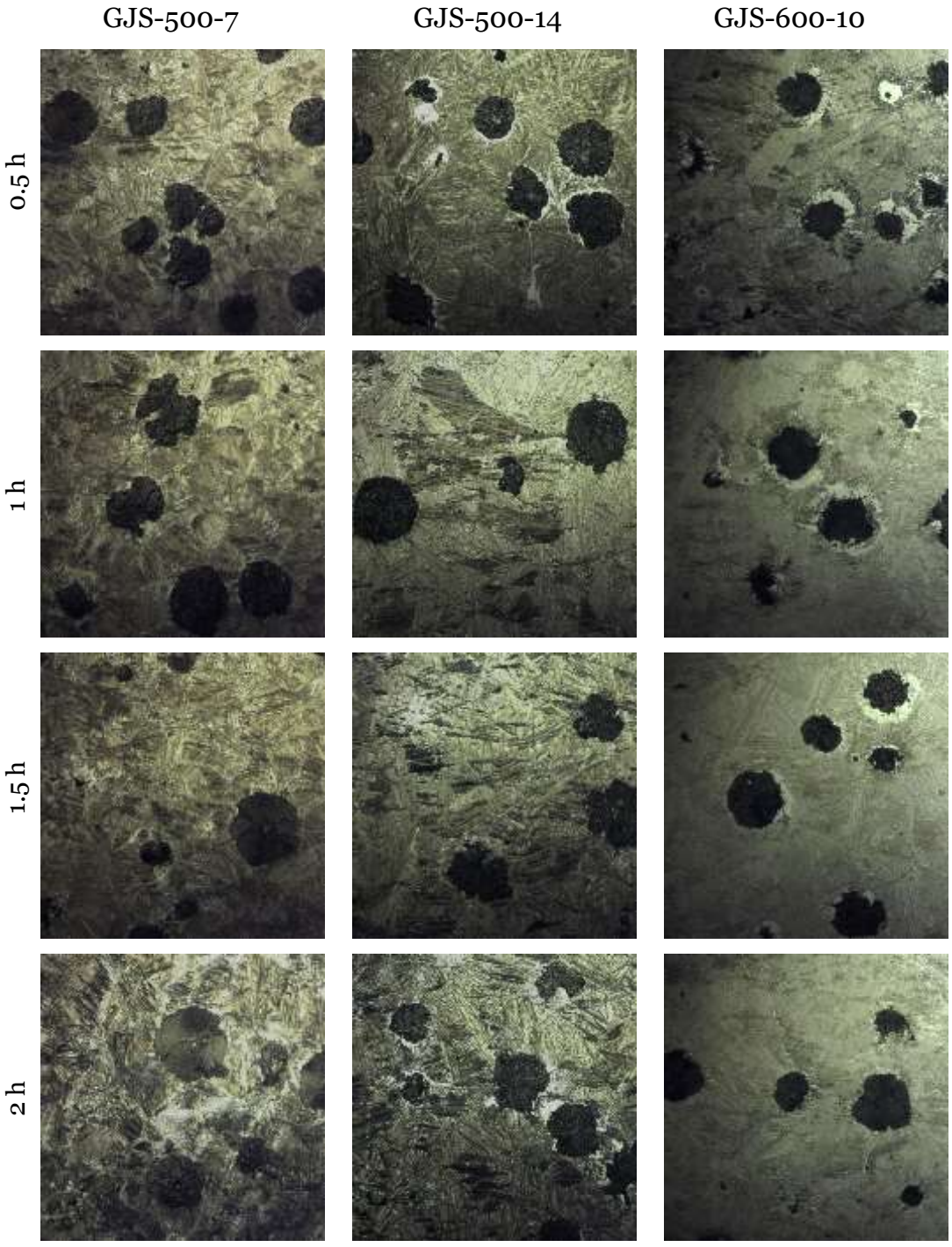

Figure 64 Austempering at 310°C. Same material in each column. Different times in different rows, starting from 30 min (top row) and continuing 1 h, 1.5 h to 2 hours (bottom). Magnification 50x.

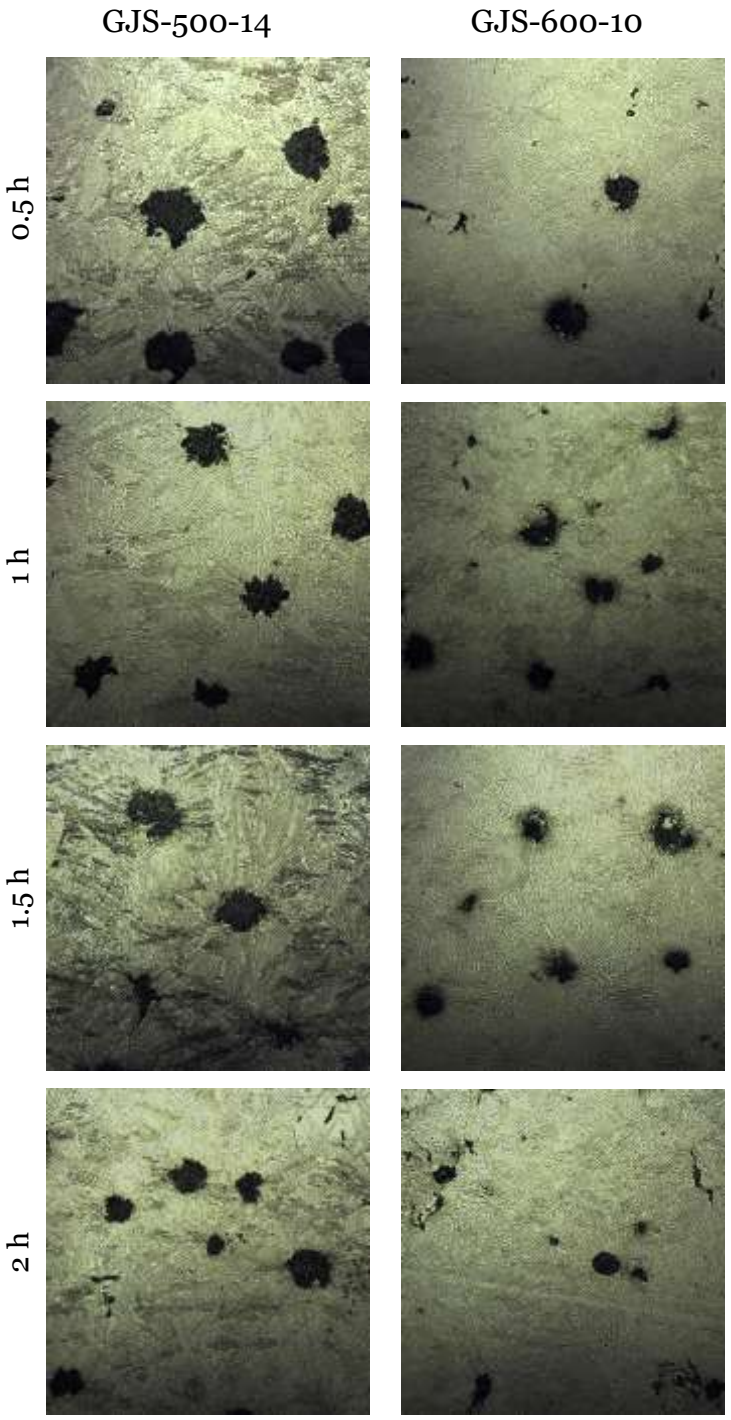

Figure 65 Austempering at 350°C. Same material in each column. Different times in different rows, starting from 30 min (top row) and continuing 1 h, 1.5 h to 2 hours (bottom). Magnification 50x.

5.2.2 Hardness tests

Brinell hardnesses are presented in Table 20 and Vickers hardnesses in Table 21, Table 22 and Table 23. Illustrations of the Vickers results with standard errors are in Figure 66, Figure 67 and Figure 68. Illustrations of Brinell results are in Appendix A and discussion about the reliability of Brinell hardness can be found in section 5.4.2.

Table 20 Brinell hardness (HB) of all austempered materials.

290°C	0.5h	1h	1.5h	2h
GJS-500-7	444	415	444	444
GJS-500-14	444	444	444	415
GJS-600-10	415	415	444	444
310°C	**0.5h**	**1h**	**1.5h**	**2h**
GJS-500-7	415	401	415	401
GJS-500-14	401	415	415	415
GJS-600-10	429	401	415	415
350°C	**0.5h**	**1h**	**1.5h**	**2h**
GJS-500-14	346	341	363	352
GJS-600-10	326	346	368	341

Table 20 shows that the Brinell hardness does not vary a lot among different materials at same austempering temperatures. With 290°C hardness values are the highest (415-444 HB) and with highest temperature 350°C they are the lowest (326-368 HB). The direction of these results is same as Vickers hardness values. Brinell tends to equalise the differences and Vickers separates materials better. When comparing Brinell hardness to the standardised grades, the ones austempered at 290°C reach the hardness requirements of GJS-1400-1, for 310°C the grade is GJS-1200-3 and for the ones at 350°C the grade is GJS-1050-6.

Table 21 Vickers hardness (HV5) of the materials austempered at 290°C.

Material	0.5h	1h	1.5h	2h	Standard deviation	Standard error
GJS-500-7	473.20	442.28	469.99	472.80	10.29	5.15
GJS-500-14	479.36	479.05	494.30	458.35	13.36	7.71
GJS-600-10	464.36	455.60	449.65	467.78	11.73	5.86

Standard deviation was calculated with equation 8 and standard error with equation 7.

$$s = \sqrt{\frac{\sum_{i=1}^{n}(x_i - \bar{x})^2}{n-1}} \qquad \text{(eq. 8)}$$

where s is standard deviation, n is the size of the sample (x_1, ..., x_n) and $\bar{x}$ is the mean of the values.

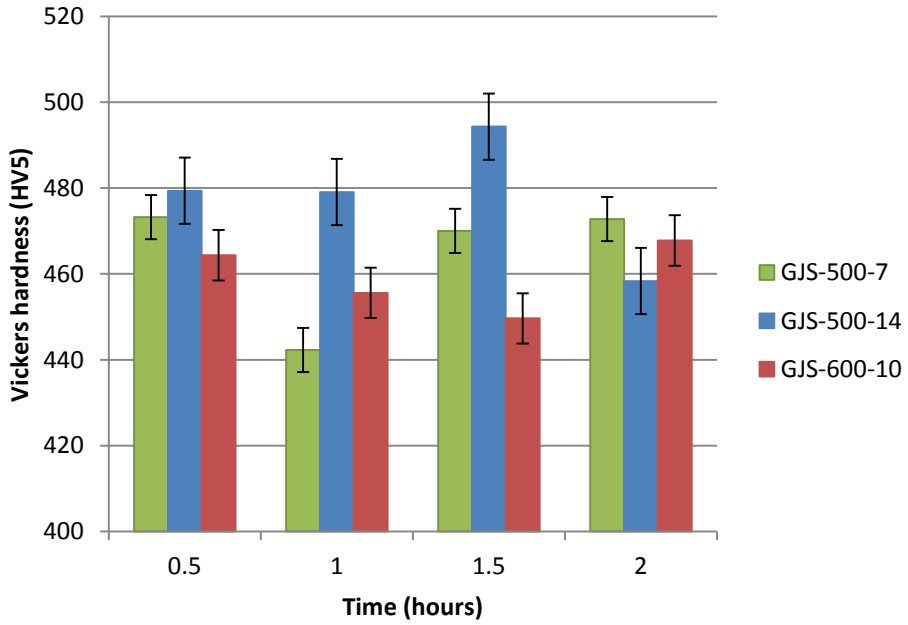

Figure 66 Vickers hardness of samples austempered at 290°C.

Hardnesses of the samples austempered at 310°C are in Table 22 and illustrated in Figure 67. Values range between 365 and 455 HV. With all the austempering times GJS-600-10 has the highest hardness values, but the difference to the next GJS-500-14 is only 8% at the highest. GJS-500-7 has the lowest hardness values, except after half an hour, when GJS-500-14 hardness is 20 HV lower. 310°C temperature might be too high for this material, therefore the shortest austempering time gives the best result. Also the weaker hardness value of GJS-500-14 after half an hour might result from the microstructure, since nodularity seems normal.

Table 22 Vickers hardness (HV5) of the materials austempered at 310°C.

Material	0.5h	1h	1.5h	2h	Standard deviation	Standard error
GJS-500-7	390.86	369.44	382.75	395.12	12.42	6.21
GJS-500-14	368.43	426.59	419.02	431.43	20.90	12.07
GJS-600-10	453.60	436.28	454.99	437.83	12.42	6.21

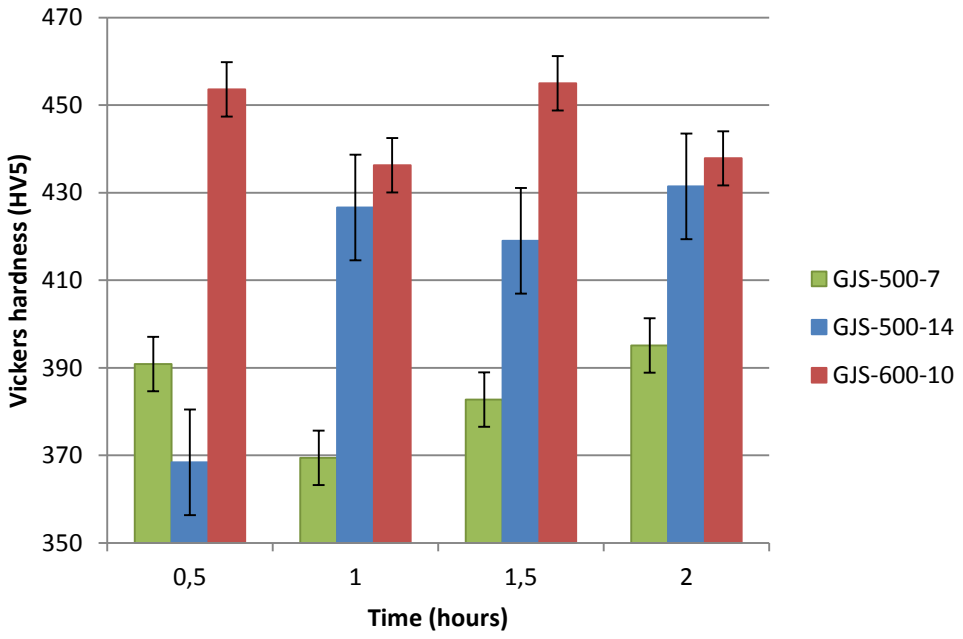

Figure 67 Vickers hardness of samples austempered at 310°C.

Hardness of the samples austempered at 350°C are presented in Table 23 and illustrated in Figure 68. Hardness of the samples vary between 360 and 415 HV. GJS-500-14 reaches its highest value after half an hour but GJS-600-10 requires one hour.

Table 23 Vickers hardness (HV5) of the materials austempered at 350°C.

Material	0.5h	1h	1.5h	2h	Standard deviation	Standard error
GJS-500-14	411.68	393.35	389.25	396.78	16.24	9.38
GJS-600-10	364.97	412.63	410.04	380.69	16.34	8.17

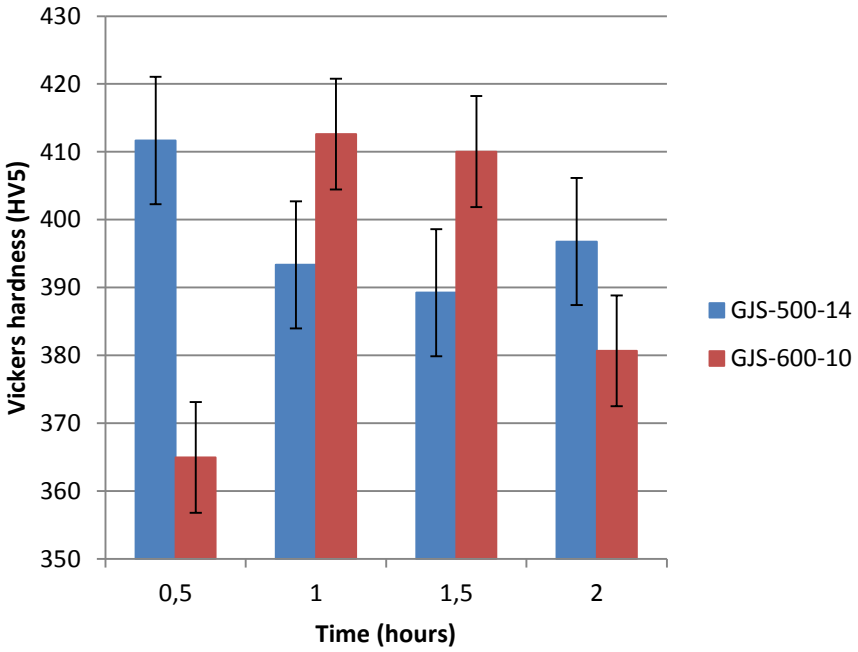

Figure 68 Vickers hardness of samples austempered at 350°C.

Based on these results the temperature 310°C and the duration of one hour were chosen for further tests with tensile bars. Decision was partially based on the good microstructures with enough needles. The Brinell hardness values (400–430 HB) also reached the hardness requirements of GJS-1200-3 (340–420 HB), which could be an example of the desired properties for the end result of this thesis. The ferritic halos were interesting, since they did not really affect the hardness negatively.

5.3 Results of full austempering process

5.3.1 Microstructures

Figure 69 show the microstructures of each tensile bar sample. Same materials are placed on the same row, since all had at least three separate samples. All were first austenitised at 860°C or 950°C and then austempered at 310°C for 60 minutes.

Overall the structures are quite variable, as there are different etching rates and even chunky graphite. GJS-500-7 has some impurities on the sample A and B is similar with less impurities. Sample C is darker and unlike previous samples has more plates than fine needles. Nodule count of sample C is much better than the others, but maybe the impurities misrepresented the results.

GJS-500-14 has both good and bad tensile bar samples. Sample A represents fine and desired microstructure, but graphite in samples B and C is in chunky form with lighter areas and no needles around it. Reason for chunky graphite is most likely that the good sample A was taken from the outermost layer of the Y-block, while the B and C were from the second layer. When the cast solidified, outermost layer solidified first and the middle part more slowly, and therefore the possibility for chunky graphite was larger. This graphite form can alter the mechanical properties.

With GJS-600-10 it is important to remember, that the sample A was only 0.5 hours in the salt bath. This is the reason why it is from now on marked with sign * to separate it from the others, which are austempered for 1 hour. All three samples have the darkest colouring of tensile bar samples due to etching or light exposure when taking the pictures. Also thin ferritic halo can be seen around some graphite nodules, similar to the halos seen at the previous austempering results of GJS-600-10 samples Figure 64. The matrix around these present pictures is still full of needles and therefore the lighter areas might not have such tangible effect on the other results.

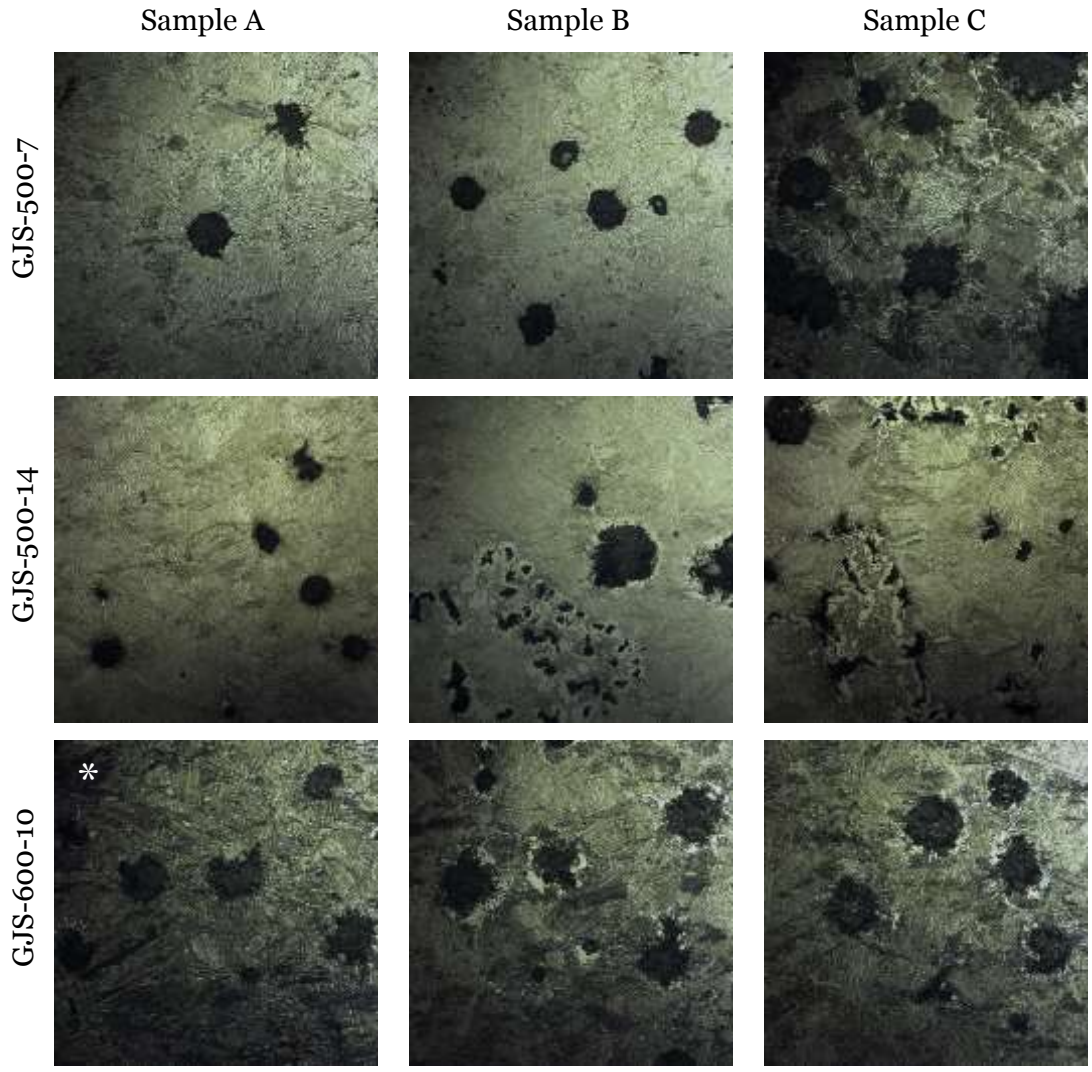

Figure 69 All samples austempered at 310°C for 60 minutes. All GJS-500-7 were austenitised at 860°C and other materials at 950°C. Each row represents same material but separate samples. Samples are named A, B and C starting from the left.

Since there was chunky graphite in GJS-500-14 samples B and C, additional two tensile bars were tested with the same 950°C austenitising and 310°C austempering heat treatment as the previous bars. Microstructures of these two are presented in Figure 70. The matrix is much better and closer to the one which sample A has. The microstructure is uniform and there are needles all around. Also nodule count and nodularity are at desired level. Only some darker needle areas exist, but it is not clear whether those are some undesired structure or not.

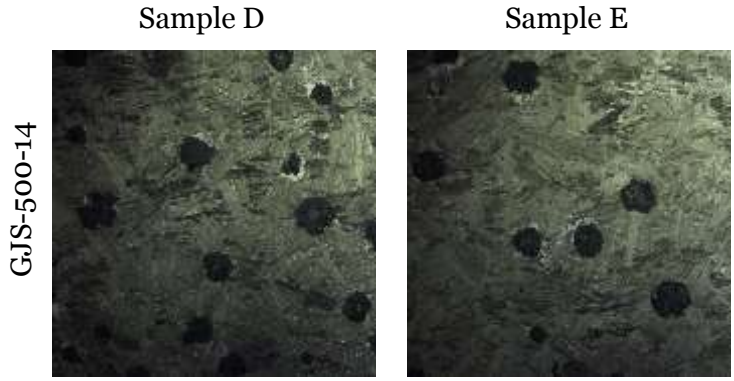

Figure 70 Additional tensile bars of GJS-500-14 austempered at 310°C for 60 minutes.

5.3.2 Hardness tests

Hardnesses of tensile bars are presented in Table 24 and illustrated in Figure 71 and Appendix B. Only with material GJS-600-10 the different hardness results are concordant but for GJS-500-7 and GJS-500-14 results vary a lot. For example GJS-500-14 sample B, Vickers gives the highest value of the group, when Brinell hardness is the lowest. Perhaps Vickers gives more local results while Brinell tells more about the overall hardness.

Table 24 Brinell and Vickers hardness of tensile bars.

Sample	Brinell hardness (HB)	Vickers hardness (HV5)
GJS-500-7/A	336	376
GJS-500-7/B	316	349
GJS-500-7/C	341	348
GJS-500-14/A	415	440
GJS-500-14/B	401	468
GJS-500-14/C	415	448
GJS-500-14/D	415	429
GJS-500-14/E	415	453
GJS-600-10/A*	415	460
GJS-600-10/B	401	441
GJS-600-10/C	429	474

Reliability of Vickers hardness is higher due to greater amount of measurements, therefore those are evaluated more closely. For GJS-500-7 Vickers hardness range is 348–376 HV, while the other materials reach 429–474 HV. This means more than 20% higher hardness for the solid solution strengthened grades. Chunky graphite in GJS-500-14 seems not to have great negative impact on hardness, while the results of sample B and C are same and even better than hardness of the ones with normal graphite. This was also found out by Larker, who says that "*chunky graphite shape may reduce fracture elongation and fracture toughness by up to 50% and reduce tensile and fatigue strength by 20-25%, while yield strength and hardness are hardly affected at all.*" [34] GJS-600-10 has the highest hardness of all, and it also has good nodularity.

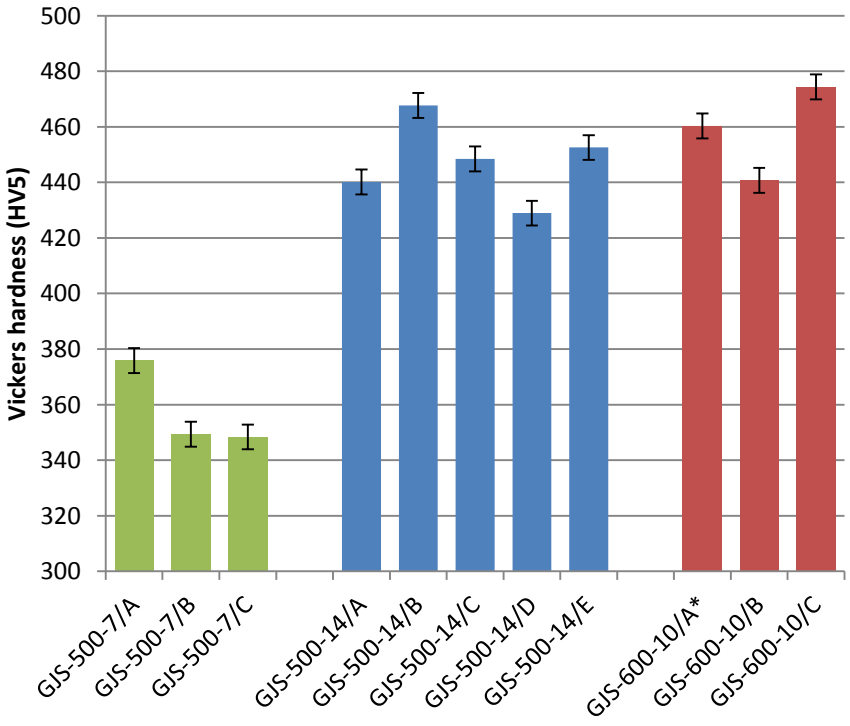

Figure 71 Vickers hardness of tensile bars.

5.3.3 Tensile strength test

Tensile strength test gives both yield strength and tensile strength, as well as the elongation of the test bar. Results are presented in Table 25 and illustrated in Figure 72, Figure 73 and Figure 74. Sample C of the material GJS-500-14 fractured unexpectedly during the tensile test, thus there are no strength values available. The elongation was evaluated to be very low due to the sudden fracture, only around 1%.

Table 25 Results of yield strength, tensile strength and elongation of the tensile bars.

Sample	Yield strength $R_{po,2}$ (MPa)	Tensile strength R_m (MPa)	Elongation A (%)
GJS-500-7/A	739	1073	9.7
GJS-500-7/B	788	1042	2.6
GJS-500-7/C	787	1072	6.1
GJS-500-14/A	1013	1321	5.2
GJS-500-14/B	907	1067	1.4
GJS-500-14/C	-	-	*~1*
GJS-500-14/D	1005	1388	8.1
GJS-500-14/E	983	1383	7.3
GJS-600-10/A*	887	1295	2.4
GJS-600-10/B	933	1390	5.9
GJS-600-10/C	920	1287	2.0

As can be seen in Figure 72, GJS-500-14 gains highest yield strength values (907–1013 MPa), while GJS-600-10 is in the second place (887–933 MPa) and GJS-500-7 has the lowest values (739–788 MPa). It is interesting to notice the high yield value of GJS-500-7 sample B, even when it does not have as good elongation as samples A and C. This shows that the elastic properties of this material are in order. Yet it falls behind when compared to solid solution strengthened materials by 15 to 20%.

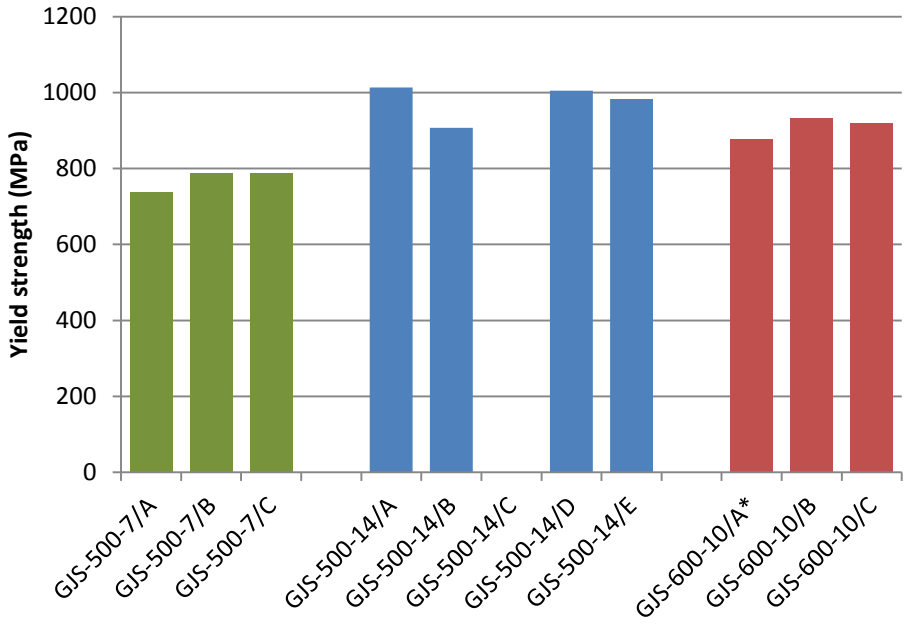

Figure 72 Yield strength $R_{p0.2}$ of the tensile bars.

Similar kinds of observations can be done about tensile strength in Figure 73. GJS-500-14 has highest tensile strength values with average 1364 MPa, when chunky graphite sample B was left out from the calculation. GJS-600-10 does not fall much behind with the average of 1324 MPa, but tensile strength of GJS-500-7 is approximately 300 MPa lower than the other grades. Naturally higher strength decreases the elongation.

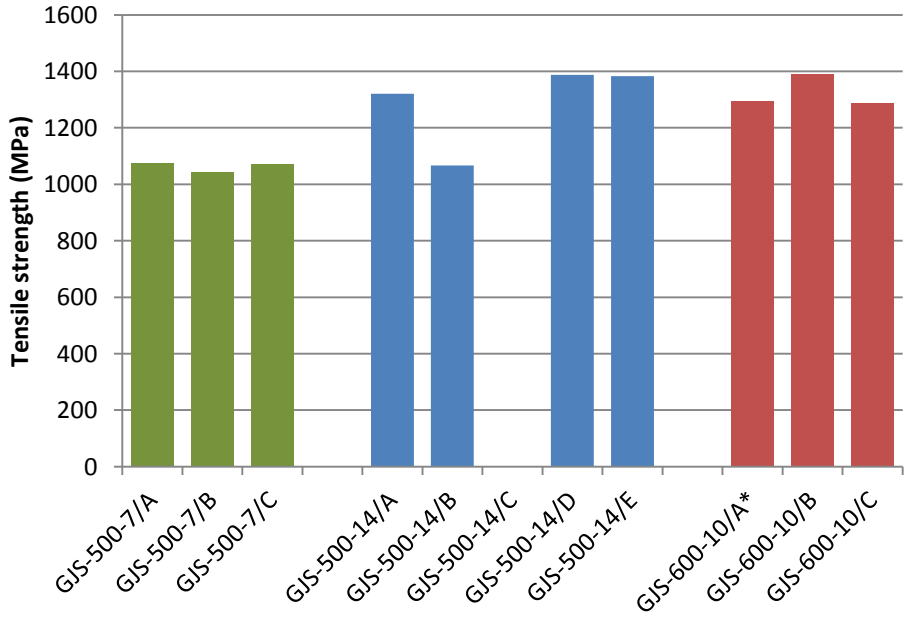

Figure 73 Tensile strength R_m of the tensile bars.

Lastly, elongations of the tensile bars are presented in Figure 74. Results vary a lot, which means that small details in the microstructure have significant effect on the deformation. GJS-500-7 has excellent elongations 6.1% and 9.7%, but then there is clearly something wrong with the sample B since it has only 2.6%. For GJS-500-14 it was clear by the microstructure pictures that samples B and C have chunky graphite and therefore their elongations are lower. The successful samples have elongation in the range of 6.1% to 8.1%. Sample B of GJS-600-10 has best elongation with 5.9%, but others remain at the level of 2–2.4%.

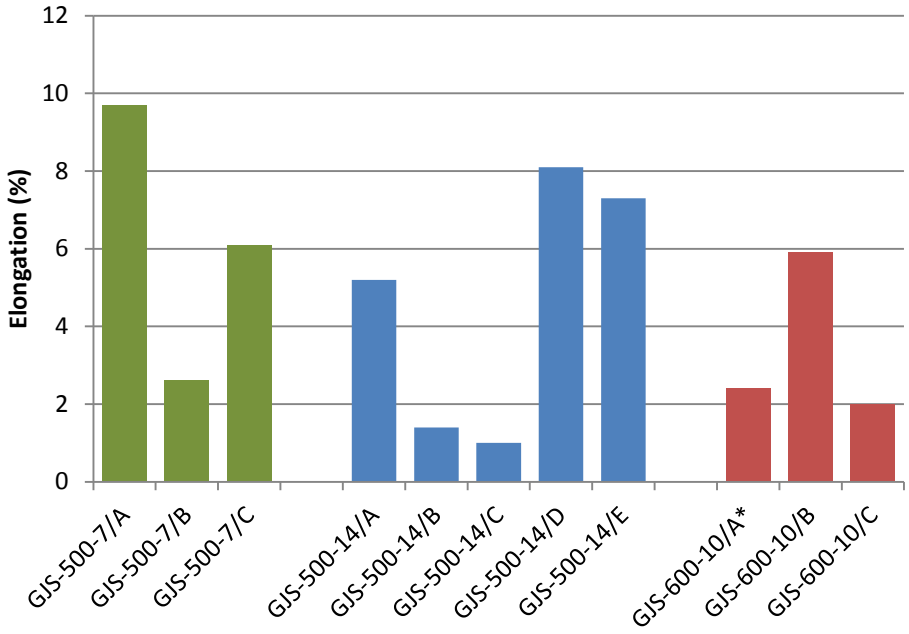

Figure 74 Elongation of the tensile bars.

5.3.4 Discussion and comparison of the results

These materials with a modified austempering heat treatment provide both positive and negative results. With tailored heat treatment GJS-500-14 gained approximately 30% better yield and tensile strength compared to GJS-500-7, but elongation was 13% lower. Instead, heat treated GJS-600-10 gained 22% better yield strength and 30% better tensile strength with 25% lower elongation. Hardness increased with both materials 20% compared to GJS-500-7.

On the other hand, these studied solid solution strengthened grades can be compared to conventional standardised ADI grades shown on page 26. Then GJS-500-7 can be referred to as standardised ADI grade GJS-1050-6 by its properties and GJS-500-14 fulfils the requirements of GJS-1200-3 easily. For both materials, elongation is at least 50% better compared to the standardised grade. GJS-600-10 almost reaches the properties of GJS-1200-3, but the uncertainty of the general elongation requires more research.

Nodularity did not play a major role with the mechanical results, but it could have been better if all the samples were casted as bars with diameter less than 30mm. Now many samples were cut from Y-blocks even as thick as 50 mm, and this might cause lower nodularity and nodule count rates and therefore affect the properties harmfully. Generally, it can be said that hardenability was high enough for these samples.

When comparing the best tensile test results of each material group, differences between materials can be noticed. GJS-500-7 sample A (Figure 75) does not have ferritic halo around the graphite nodules, but there are more areas with lighter colours (austenite) between the nodules. Austempering was successful and elongation better, but strength was not as high as in the other materials. Comparison between GJS-500-14 sample D (Figure 76) and GJS-600-10 sample B (Figure 77) is harder to make. Main difference and reason for poor elongation can be found from nodularity, since of GJS-500-14/D nodularity is 94% and nodule count 350 pcs/mm^2 and of GJS-600-10/B notably lower with 72% and 196 pcs/mm^2. This has negative effect on the mechanical properties, which are gathered to Table 26.

.

Figure 75 GJS-500-7 sample A.

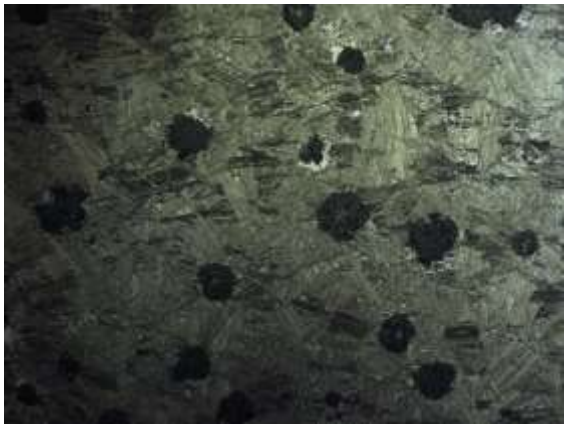

Figure 76 GJS-500-14 sample D.

Figure 77 GJS-600-10 sample B.

Table 26 Best properties of each material and GJS-600-10 sample A for comparison.

Sample	Yield strength $R_{po,2}$ (MPa)	Tensile strength R_m (MPa)	Elongation A (%)	Brinell hardness (HB)	Vickers hardness (HV5)
GJS-500-7/A	739	1073	9.7	336	376
GJS-500-14/D	1005	1388	8.1	415	429
GJS-600-10/A*	887	1295	2.4	415	460
GJS-600-10/B	933	1390	5.9	401	441

Moreover, when examining GJS-600-10 sample A, which was 30 minutes in salt bath, and sample B of one hour salt bath, it can be seen that the surface of the first one is much darker and there are less areas with light brown colour. If the etchings had the same effect, it can be presumed that with shorter salt bath time there must be more unstable austenite which has transformed into martensite at room temperature. Another option is that transformation occurred during tensile strength test. Martensite influences the properties negatively, by for example by reducing elongation.

It could be pondered if longer austempering time or higher temperature would have been better for GJS-600-10, which it had silicon content clearly over 4.0%. While silicon does delay the start of bainite formation, this material might have only reached the microstructural stage E-F (transformed to austenite) in Figure 45, while F-G (austenite enriched with carbon and becoming stable) would be the optimal. Type E-F can still transform to martensite by cooling to room temperature or by stress, and cause the lower elongation of GJS-600-10 sample A. More tests are required to find out how these are connected.

Based on all these results it can be said that there is potential for GJS-500-7 to fulfil the properties of GJS-1050-6, when austenitised at 860°C and austempered at 310° for one hour. Instead, GJS-500-14 and GJS-600-10 with this chemical composition and wall thickness can gain the properties of GJS-1200-3, when austenitised at 950°C, austempered at 310°C for one hour and the nodularity is on the required level. When comparing heat treated tested

materials with standardised solid solution grades, it can be seen that yield strength, tensile strength and hardness have doubled but elongation is only half of the original. These comparisons indicate that with higher silicon content higher strength properties can be reached, but elongation remains lower. It depends on the component and its purpose, which properties are more important.

5.4 Reliability of the results

5.4.1 Before and during the heat treatment

Heat treatment cannot affect the alloying of original grade or casting process. If there are some defects, they will not disappear during the process even if the microstructure changes. The given castings and their production impact the results, and in this study especially the composition, which naturally cannot be completely same with all pieces. Some grades of same iron came from different foundries and therefore the amounts of chemical elements differ slightly.

Sawing has its own accuracy, which causes the samples' shape to be different within the range of few millimeters. The shape of the original casting, whether it is a block or a bar, causes some differences on how the heat is conducted to the sample. Also the position of y-block, where the sample has been taken from, might affect for example the nodularity and therefore the end results.

During the heat treatment, each step and the handling of the sample affect the final result. How fast the samples are moved from one stage to another is critical, especially between furnace and salt bath. Also opening the hatch of the furnace always causes the temperature to drop dozens of degrees for a few minutes until it is again stabilised to the desired level. In this thesis, the heat treatment times were long enough and this did not have major effect on the result.

5.4.2 Microstructures

Pictures of the microstructures are not always easy to interpret, because the lattice structures are not always evident. Also the quality of grinding and possible scratches influence the clarity of the pictures. The microscope itself influences the pictures' quality by exposure, colours and accuracy of focusing, but some errors might have also caused by naming and marking the scaling incorrectly or by mixing the pictures. At all events, the precision has been one of the main priorities when handling the samples.

Nevertheless, etching is the main problem source with microstructure pictures. It affects greatly on the darkness and visibility of the structures. Etching times might have varied approximately 0.5 seconds which already causes evident differences in the outcome.

5.4.2 Hardness tests

Both Brinell and Vickers hardness tests have similar error sources. Both the surface quality and the measurement of the indentation must be precise to reach reliable result.

The quality of the surface has an effect on the final numerical value. It has to be well prepared to enable examining the indentation carefully but also to get a symmetrical dent. If the surface has an angle, the shape will lengthen from another side. Especially with Vickers test, the tips of the indentation must be accurate to get right values.

Most serious disadvantages of the Brinell method is the fact that the indentation is measured optically, which includes the risk for measuring errors. Therefore 0,05mm difference, the accuracy of the microscope's scale, could result of having even 15 HB difference. With bigger indentations the error is smaller, only around 5 HB. Modern, automatic image evaluation computer systems would reduce these errors significantly, as it did with Vickers hardness.

5.4.3 Tensile test

Before the tensile test, some errors can already be caused by the machining of the bar to the desired shape. Thickness can be slightly different and some tiny defaults in machining can cause the bar to fracture from thinnest part instead of the originally weakest point of the bar.

Tensile strength test itself was conducted according to the standard and performed by tensile test machine. Still there were few steps conducted manually, which might cause some errors to the final results. First of all, the bar can be attached to the machine with a small angle, which can cause the force to affect the bar unevenly. Secondly, there must be an educated guess of the elongation to fix the pulling force to right level. At certain point the meter observing sensitive elongation must be removed and then bar fractures. If the guess is not in the right range and bar fractures too early, complete tensile results cannot be measured. This happened with GJS-500-14 sample C.

Regardless, the main source of unreliability of the results is the amount of samples. There were only three samples of each grade, which naturally is too low amount to get reliable and generalisable results. Also the errors in nodularisation, like chunky graphite, were unfortunate and alter the overall impression of the material's properties.

6 CONCLUSION

The aim of this thesis was to find out how the properties change when tailored ADI heat treatment is applied to grades with unusually large amount of solicon. According to the theory, there are three identified ways how silicon affects the austempering heat treatment.

First, with higher silicon content the austenitising temperature must be higher, since silicon raises the upper critical temperature +50°C per percent of silicon and the whole matrix must be in austenite form before quenching. Second, quenching is affected when silicon pushes the area of pearlite formation to the right, then it is more unlikely pearlite to form and this improves hardenability. Third, austempering is influenced by widening the process window, because silicon accelerates ferrite growth during nucleation and delays formation of bainite.

The temperatures and times of the experimental part was planned and conducted according to these findings. The first austenitising test confirmed that 950°C was good austenitising temperature for the solid solution strengthened materials, but for reference grade GJS-500-7 it was too high and following tests with this material was conducted at austenitising temperature 860°C. In the second stage different austempering times and temperatures were tested, and due to fine needle structure and suitable hardness range temperature 310°C with one hour austempering time was selected for further investigations.

The third and last part of this thesis consisted of the tensile strength tests. Samples were heat treated as 25mm bars and austempered at 310°C for one hour. Then samples were machined to thinner tensile bar shape and tensile tests were conducted according to the standard. With tailored heat treatment GJS-500-14 gained approximately 30% better yield and tensile strength compared to GJS-500-7, but elongation was 13% lower. Instead, heat treated GJS-600-10 gained 22% better yield strength and 30% better tensile strength with 25%

lower elongation. Hardness increased with both materials 20% compared to GJS-500-7.

In addition, these new materials with tailored heat treatment can be compared to standardised ADI grades. The results showed that with these heat treatments GJS-500-7 gained properties of standardised ADI grade GJS-1050-6. For GJS-500-14 and GJS-600-10 the closest reference was the GJS-1200-3, but most of the properties were even exceeded. Especially elongation was substantially better, even double, with the same strength values. There is potential for a novel ADI grade with example values GJS-1300-950-7. These kinds of properties allow designing components with thinner wall thickness which causes weight savings.

There are plenty of topics for further research. There should be research with more samples, different wall thicknesses and different silicon contents to find out the generalisable properties of each grade. Also closer look can be taken on different austempering times and especially temperatures, since the optimal combination should be found for both energy and cost saving reasons. Furthermore, the microstructures can be examined with other methods to be certain of the matrices formed. More work and careful processing is needed to improve nodularity and nodule count of solid solution strengthened grades. Naturally these materials must be later tested with real components and applications to see how these behave during casting and what kind of stress they bear in the shape of a component.

REFERENCES

[1] Sahoo, S. K. A *Study on the effect of austempering temperature, time and copper addition on the mechanical properties of austempered ductile iron*. Rourkela, National Institute of Technology, Department of Metallurgical and Materials Engieering. India 2012.

[2] *EN-1563. Founding Spheroidal Graphite Cast Iron*. Paris, France 2012. European Committee for Standardization.

[3] Duit, B., Degirmenci, S., Şirin, B. EN 1563 – *New generation ductile irons (solid solution strengthened ductile irons)*. 7. International Congress of Casting. Ankiros, Turkey, September 2014. [referred 19.12.2014]
https://ankirosfoundrycongresstr.files.wordpress.com/2014/09/manuscript24.pdf

[4] Rundman, K. B. "*It's About Austenite and Carbon, Mate" -A Story of the Physical Metallurgy of ADI - Part II*. Michigan Technological University.

[5] Valuatlas. *Cast Word* (definitions). Finland 2014. [reference 4.7.2014]
http://www.valuatlas.fi/

[6] Metalliteollisuuden keskusliitto, MET. *Raaka-aine käsikirja 2: Valuraudat ja valuteräkset*. 2nd ed. Metalliteollisuuden Kustannus Oy, 2001. ISBN 951-817-757-0.

[7] Suomen Valimotekniikan Yhdistys ry. *Valimoviesti 1/2014 ja 2/2014*. Oulu, Finland.

[8] AFS. *47th Census of World Casting Production*.

[9] Resources for students studying Design and Technology. *Sand Casting*. [referred 25.11.2014] http://dtresource.com/index.html

[10] ASM Handbook, Vol 15, *Casting*. The Materials Information Society. USA 1996. ISBN 0-87170-007-7.p. 63 and p. 648.

[11] Autere, E. & Ingman, Y. *Valimotekniikka 1*. Vol. 4. Helsinki, Finland. 1982. ISBN 951-793-538-2.

[12] Foundry Lecixon (definitions) [reference 28.10.2014]
http://www.giessereilexikon.com/en/foundry-lexicon

[13] Componenta, *Valajat koulutusmateriaali - Metallurgian perusteet*.

[14] *Encyclopedia of Materials: Science and Technology*. Vol 1-11. 2001. ISBN 978-0-08-052358-3 (electronic).

[15] Ductile Iron Society. Ductile Iron Data, Section 2, *Introduction* and Section 4, *Austempered Ductile Iron*. Revised by J. R. Keough (August 1998). USA, 2013. [reference 15.10.2014] http://www.ductile.org/

[16] Kivivuori, S., Härkönen, S. Lämpökäsittelyoppi. Teknologiateollisuus. Finland 2004. ISBN 951-817-849-6.

[17] SFS-EN ISO 945-1:2008/Cor 1:2010. *Microstructure of cast irons. Part 1: Graphite classification by visual analysis.* Helsinki, Finland 2010. Finnish Standards Association, SFS.

[18] Dorazil, E. *High Strength austempered ductile cast iron*. England 1991. Publishing House of the Czechoslovak Academy of Sciences.

[19] ASM Handbook, Vol 4, *Heat Treatment*. The Materials Information Society. USA 1995. ISBN 0-87170-379-3. p. 152-163, p. 665-708

[20] American Society for Metals. *Heat Treating, Metals Handbook*, Ninth Edition, Volume 4. Chapter Heat Treating of Cast Irons. p. 525-558. United States of America. 1981. ISBN 0-87170-010-7.

[21] Kovacs, B. V. *Alloying elements and heat treatment of ADI*. Kosmar Enterprises. Michigan, USA. Helsinki ADI Conference 1994.

[22] Bayare, H, & Elliot, R. *Thermal and mechanical stability of austenite in High Mn ADI*. Manchester Materials Science Centre. United Kingdom 2000. 20th ASM Heat Treating Society Conference.

[23] Hayrynen, K. L. *The Production of Austempered Ductile Iron (ADI)*. Michigan, USA 2002. 2002 World Conference on ADI. [referred 19.12.2014]

[24] EN 1564 - ADI. *Founding - Ausferritic spheroidal graphite cast irons*. European Committee for Standardization.

[25] Key to Metals. *Metals Knowlegde: The Strengthening of Iron and Steel.* 2003. [referred 9.12.2014]
http://www.keytometals.com/page.aspx?ID=CheckArticle&site=kts&NM=107

[26] Shah, K. P. *The Hand Book on Mechanical Maintenance. Classification of Alloys*. India. [referred 10.12.2014] http://practicalmaintenance.net/?p=1176

[27] Björkegren, L-E., and Hamberg, K. *Ductile iron with better machinability compared to conventional grades*. Foudryman. Sweden, December 1998. p. 386-391.

[28] Piaskowski, J. *Tech Spotlight – Ductile iron containing ~3.9% silicon*. Foundry Research Institute, Advanced Materials & Process, February 2003. Poland.

[29] ASTM A897/A897M-03, *Standard Specification for Austempered Ductile Iron Castings*. ASTM International. USA 2003. DOI: 10.1520/A0897_A0897M-03.

[30] Charoencilaisiri, S., Stefancescu, D. M, Ruxanda, R. & Piwonka, T. S. *Thin wall compacted graphite iron castings*. American Foundry Society. USA 2001.

[31] Inquus, Inc. OpenStudy service. [reference 22.10.2014] http://openstudy.com/

[32] Zimba, J. *Transformation kinetics during the austempering of ductile iron and practical implications*. University of Zimbabwe. Zimbabwe, 2000.

[33] Meehanite. *Guidelines for designing and machining meehanite ADI castings*.

[34] Larker, R. *Solution strengthened ferritic ductile iron ISO 1083/JS/500-10 provides superior consistent properties in hydraulic rotators*. Sweden 2009. Overseas Foundry. Article ID: 1672-6421(2009)04-343-09.

[35] ASTM A518/A518M-99(2008), *Standard Specification for Corrosion-Resistant High-Silicon Iron Castings*. ASTM International. USA 2008. DOI: 10.1520/A0518_ A0518M-99R08.

[36] Lincoln J. A. *Proc. of 1st International Conference on Austempered Ductile Iron*. April 1984, Chicago. p.167

[37] American Foundry Society. *Iron Castings Engineering Handbook*. USA 2003. p. 271-307. ISBN 0-87433-260-5.

[38] FactSage – Integrated Thermodynamic Databank System. 2010. [reference 17.10.2014] http://www.crct.polymtl.ca/factsage/fs_general.php

[39] Componenta, quality department. *Process instructions of ADI*. Finland 2008.

[40] Stuers –Products. Grinding & Polishing. 2014. [reference 4.9.2014] http://www.struers.com/default.asp?top_id=3&main_id=10&sub_id=15&doc_id=204

[41] ImageJ. July, 2014. [reference 17.10.2014] http://imagej.net/Welcome

[42] ISO 6506-1: *Metallic materials. Brinell hardness test. Part 1: Test method*.

[43] ASM Handbook, Vol 8, *Mechanical Testing*. The Materials Information Society. USA 1995. ISBN 0-87170-007-7.

[44] ISO 6507-1:2005 (en). *Metallic materials, Vickers hardness test, Part 1: Test method*.

APPENDICES

Appendix A: Illustrations of Brinell hardness results of austempering.

Appendix B: Brinell hardness of tensile bars

APPENDIX A: Illustrations of Brinell hardness results of austempering

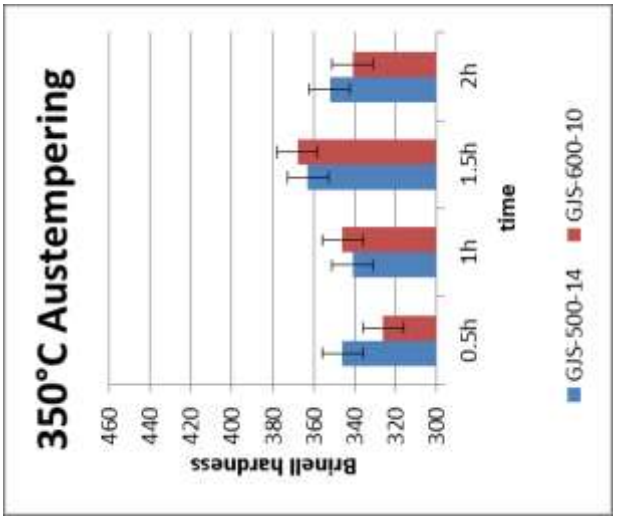

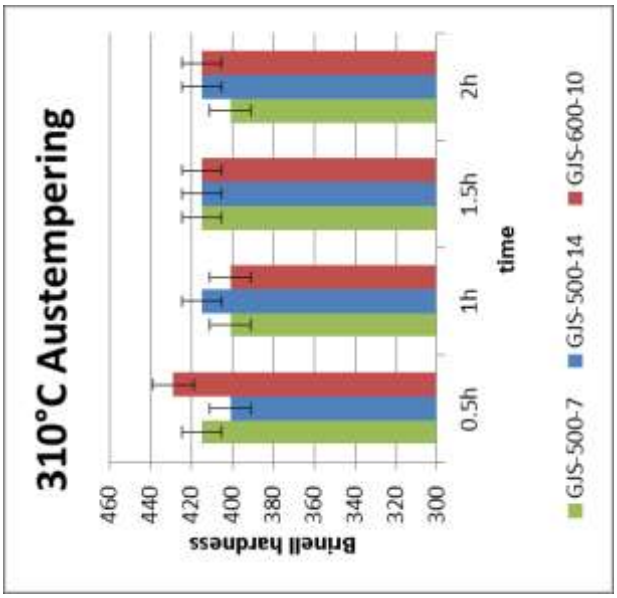

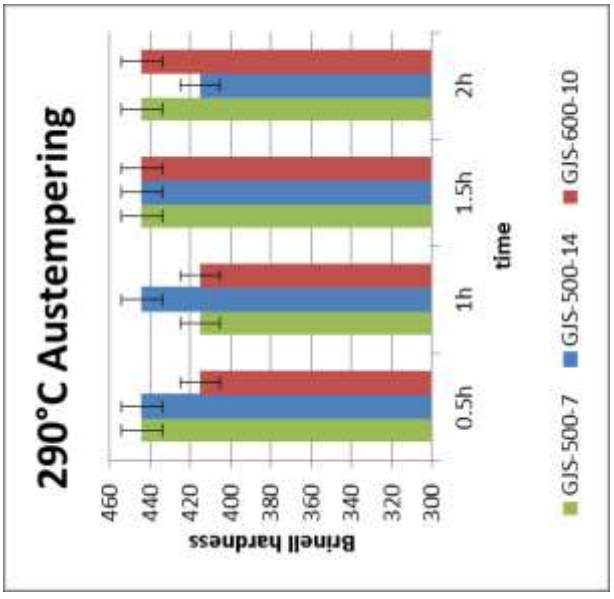

APPENDIX B: Brinell hardness of tensile bars